SEXUAL DIMORPHISMS IN THE ADIPOSE BIOLOGY OF VASOACTIVE INTESTINAL

PEPTIDE DEFICIENT MICE

A Thesis
Submitted to the Graduate Faculty
of the
North Dakota State University
of Agriculture and Applied Science

By

Emma Hawley

In Partial Fulfillment of the Requirements
for the Degree of
MASTER OF SCIENCE

Major Department:
Microbiological Sciences

May 2022

Fargo, North Dakota

North Dakota State University
Graduate School

Title

SEXUAL DIMORPHISMS IN THE ADIPOSE BIOLOGY OF VASOACTIVE INTESTINAL PEPTIDE DEFICIENT MICE

By

Emma Hawley

The Supervisory Committee certifies that this ***disquisition*** complies with North Dakota

State University's regulations and meets the accepted standards for the degree of

MASTER OF SCIENCE

SUPERVISORY COMMITTEE:

Dr. Glenn Dorsam

Chair

Dr. Samiran Banerjee

Dr. Birgit Pruess

Dr. John Wilkinson

Dr. Kendall Swanson

Dr. Jiha Kim

Approved:

06/03/2022	Dr. John McEvoy
Date	Department Chair

ABSTRACT

Both VIP and PACAP deficient mice display impaired fat storage, but only the molecular adipose characteristics of PACAP KO mice are known. While mice deficient in these peptides are lean, supplementation could promote weight gain in livestock after establishing tissue distribution. We investigated both sides of this 'metabolic coin' by measuring serum metabolites, adipocyte area, and pscWAT gene expression in VIP deficient mice and screening 15 ruminant tissues for VIP, PACAP, and their receptors using RT-qPCR. We found male VIP deficient mice displayed hypertrophic adipocytes, low serum FFAs, and suppressed relative mRNA expression of TMEM26. In ruminants, VIP and PACAP showed similar expression patterns, whereas their receptors had divergent tissue distributions. We conclude that VIP deficiency affects the investigated adipose characteristics in male but not female mice. Additionally, we predict that VIP supplementation in ruminants would promote weight gain since its mRNA distribution is similar to mice.

DEDICATION

I would like to dedicate this paper to those who taught me lessons necessary to overcoming the

challenges of the past two years.

To my parents, Saima and Darin. For providing me with opportunity and motivation. At a young

age, you convinced me that anything is possible with hard work and dedication. I attribute my

completion of this thesis to both of your guidance.

To Noah. For being my rock and teaching me how to get through the most stressful moments.

To rock climbing friends. For showing me that good things don't come easy, whether that's a

master's degree or overhung boulder routes.

And to all those who I have had the pleasure of meeting at NDSU. For allowing me to be a part

of a scientific community filled with intelligent minds and witty personalities.

"The more you read, the more things you will know. The more you learn, the more places

you'll go" - Dr. Suess

TABLE OF CONTENTS

LIST OF TABLES

LIST OF FIGURES

LIST OF ABBREVIATIONS

AA...Amino Acid

APs...Adipocyte Precursors

ATP...Adenosine Triphosphate

BAT...Brown Adipose Tissue

cAMP...Cyclic Adenosine Monophosphate

CDC ....Center for Disease Control

CKMT..Creatine Kinase Mitochondrial

CIDEA ....Cell Death Inducing DFFA Like Effector A

dWAT ....Dorsolumbar White Adipose Tissue

FFA ....Free Fatty Acid

GHRH ....Growth Hormone Releasing Hormone

GIP ....Gastric Inhibitory Peptide

GLP1 ....Glucagon Like Peptide 1

GLP2 ....Glucagon Like Peptide 2

iWAT ....Inguinal White Adipose Tissue

Kd..Dissociation Constant

KO...Knock Out

min ....Minute

nM...NanoMolar

PAC1..PACAP Receptor 1

PACAP...Pituitary Adenylate Cyclase-Activating Polypeptide

PCR...Polymerase Chain Reaction

1. REVIEWING THE ROLES OF VIP AND PACAP SIGNALING IN ADIPOSE AND WHOLE-BODY METABOLISM

1.1. Abstract

Fat depots are now widely accepted as a metabolic organ with tissue consisting of various cell types including adipocytes that secrete hormones and cytokines. A new goal of metabolic research has been to better understand the pathways involved in maintaining healthy adipose function, which could help treat adipose related disease such as type II diabetes. The most identical members of the secretin family, VIP and PACAP, are known as the "sister peptides" and have comparable impacts on whole body metabolism. Studies involving both supplementation and genetic deletion of these peptides show important functions in lipolysis, body growth, GI function, Feeding Behavior, and adipocyte biology. In this review we compare some of the known role of VIP and PACAP in adipose and whole-body metabolism.

1.2. Background

The VIP/PACAP superfamily contains a group of peptides who presumedly emerged from an exon duplication and two tetraploidization events of a common PACAP-like ancestor gene (Cardoso et al., 2020). Members of this family include PACAP, VIP, PACAP-related peptide (PRP), peptide histidine valine (PHV), peptide histidine methionine (PHM), growth hormone releasing hormone (GHRH) and secretin (Cardoso et al., 2020). Support for the tetraploidization hypothesis is displayed in the highly conserved sequence homology of PACAP among both vertebrates and invertebrates (Pirger, 2016). Both VIP and PACAP are highly conserved amongst vertebrate, where PACAP-27 is fully conserved in all classes expect for the chicken and VIP differs in chicken, guinea pig, fish, and amphibia (Langer, 2022). The amino acid sequence of PACAP-27 is identical in humans, salmon, and catfish, whereas VIP is only

87% conserved, thus supporting the idea that the superfamily's common ancestor gene was more "PACAP-like" (Sherwood, 2000). There also is evidence for the connection of this ancestral gene to another group of hormones with similar identity known as the glucagon-like peptides. Members of the family include glucagon, glucagon-like peptides (GLP1 and 2) and gastric inhibitory peptide (GIP) (Cardoso et al., 2020). Together, members of both the PACAP/VIP and glucagon-like families share close amino acid identity, with VIP & PACAP showing the highest similarity (68% AA identity) (**Table 1.1).**

Table 1.1. PACAP-VIP Superfamily AA Identity.

Peptide	Sequence Accession#	NH3$^+$ - AA Sequence - COO$^-$	Identity to PACAP	Identity to VIP
PACAP-38	P18509 | 132-169	HSDGIFTDSYSRYRKQMAVKKYLAAVLGKRY KQRVKNK **	100%	68%
PACAP-27	P18509 | 132-158	HSDGIFTDSYSRYRKQMAVKKYLAAVL**	100%	68%
VIP	P01282 | 125-152	HSDAVFTDNYTRLRKQMAVKKYLNSILN **	68%	100%
PHV	P01282 | 81-122	HADGVFTSDFSKLLGQLSAKKYLESLMGKRVS SNISEDPVPV	40%	43%
GLP1	P01275 | 98-128	HAEGTFTSDVSSYLEGQAAKEFIAWLVKGRG**	33%	18%
Glucagon	P01275 | 53-81	HSQGTFTSDYSKYLDSRRAQDFVQWLMNT	30%	32%
GHRH	P01286 | 32-75	YADAIFTNSYRKVLGQLSARKLLQDIMSRQQG ESNQERGARARL**	24%	32%
PHM	P01282 | 81-107	HADGVFTSDFSKLLGQLSAKKYLESLM**	22%	43%
Secretin	P09683 | 28-54	HSDGTFTSELSRLREGARLQRLLQGLV**	22%	29%
GLP2	P01275 | 146-178	HADGSFSDEMNTILDNLAARDFINWLIQTKITD	22%	21%
GIP	P09681 | 52-93	YAEGTFISDYSIAMDKIHQQDFVNWLLAQKGK KNDWKHNITQ	16%	0%
PRP	P18509 | 82-129	DVAHGILNEAYRKVLDQLSAGKHLQSLVARGV GGSLGGGAGDDAEPLS	0%	0%

Peptide identity was determined using NCBI multiple alignment tool: Identity = # of similar AA/AA in VIP or PACAP x 100. ** Indicates C Terminal Amidation. Sequences acquired from uniprot.org (Bateman, 2021).

Because VIP and PACAP share the highest percent identity, it is not surprising that they can bind to the same receptors (Hirabayashi, 2018), and it is important to consider both peptides

in studies regarding their functionality. VIP was first isolated from porcine small intestines and identified as a 28 amino acid neuropeptide (Said & Mutt, 1970). The C-terminus of VIP is amidated, thus neutralizing the carboxy-terminus and increasing the peptide's stability and allowing it to evade enzymatic degradation by peptidases (Fahrenkrug, 1989). VIP mRNA expression is highest along the intestinal tract (Fagerberg, 2014), where it is likely delivered by neurons and immune cells (Delgado, 2011). VIP^{+} neurons (VIPergic) are also present in the central nervous system, primarily the hippocampus region, suggesting this neuropeptide is a key player in the gut-brain axis (Cunha-Reis, 2020).

VIP's 'sister peptide', PACAP, was first recovered from the ovine hypothalamus where it exists in two isoforms of different amino acid length: 27 and 38 (Miyata et al., 1990). PACAP is secreted throughout the central nervous system, with traces in the intestine (Hannibal, 1997)(Fagerberg, 2014). One reason that VIP and PACAP are considered "sister" peptides is that they both bind a pair of class B G-protein-coupled receptors (GPCRs), called VPAC1 and VPAC2 with equal affinity (Harmar, 2012). PACAP also binds a third receptor known as PAC1, another Class B GPCR, with 1000 times greater affinity than VIP (Hirabayashi, 2018) (**Figure 1.1**).
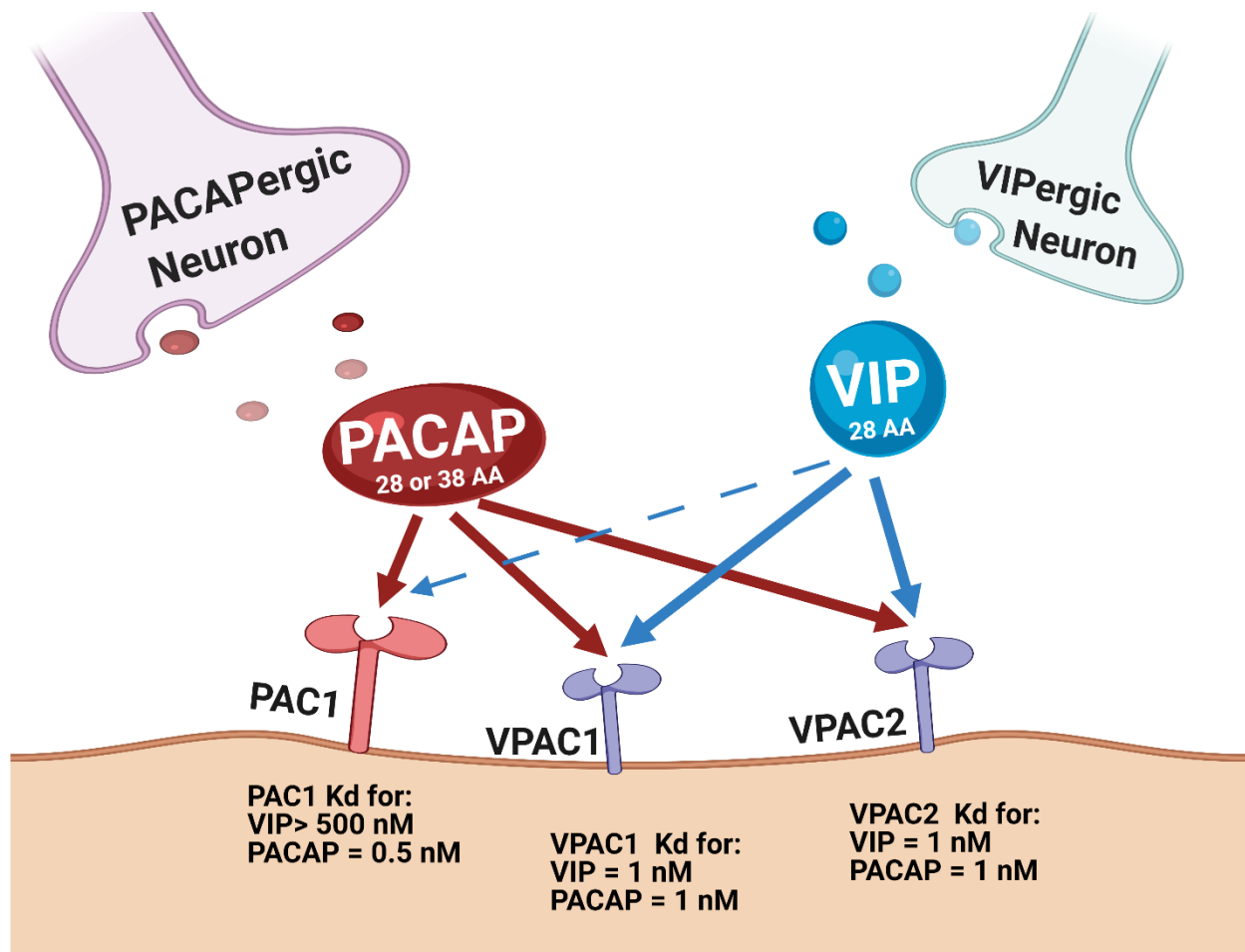
Figure 1.1. VIP & PACAP Cell Signaling Mechanism and Receptor Binding Affinities. Adapted from (Hirabayashi, 2018). Kd = dissociation constant. nM = nanomolar.

1.3. VIP and PACAP's Role in Whole Body Metabolism

1.3.1. Lipolytic Properties of VIP and PACAP

Lipolysis is defined as the breakdown of stored lipids into three fatty acids and glycerol, which are metabolites that can be used for energy throughout the body (Duncan et al., 2007). Adipocyte lipolysis is sensitive to the exposure of VIP and other superfamily members. In 1973, only three years after the initial isolation of VIP, epididymal white adipose tissue (eWAT) of male rats was used to identify the neuropeptide's ability to induce cAMP production (Desbuquois et al., 1973). Briefly, 100 nM VIP induced a 4.8-fold increase in cAMP production as well as a 170-fold increase in the release of free fatty acids (FFAs) from cultured adipocytes.

4

Additionally, VIP elevated cAMP and FFAs more than glucagon, secretin, or peptide histidine isoleucine (murine equivalent of PHM) in adipocytes (Desbuquois et al., 1973). The same cAMP response, however, was not conserved in pancreatocytes or hepatocytes, where cAMP production is more sensitive to secretin and glucagon (BATAILLE et al., 1974) (Gardner et al., 1976). The lipolytic function of VIP is unreported outside of mammalian subjects, however a VIP-like peptide found in the *C. elegans* nematode is essential for fat mobilization (Temmerman et al., 2012).

PACAP induces lipolysis, by causing a 6-fold increase in glycerol release from cultured rat adipocytes (Åkesson et al., 2003), although FFA release has not been described in the literature. Interestingly, this lipolytic function is completely abolished in the presence of insulin by a mechanism suggested to involve phosphatidyl inositol 3-kinase and the phosphorylation of protein kinase B (Åkesson et al., 2003). Central administration of either VIP or PACAP into chicks increases plasma FFAs, suggesting a common receptor mediates lipolysis (Tachibana 2007). Agonism of the receptors shared by these two hormones show that VPAC2, but not VPAC1 or PAC1, elicit lipolytic effects, suggesting that PACAP and VIP induce lipolysis through the common receptor VPAC2 (Åkesson et al., 2005).

1.3.2. Body Dysmorphia in VIP & PACAP KO mice

One of the first observations made using VIP KO mice was their low body weight in comparison to WT littermates (Girard, 2006). Further, their body composition is also altered: low body fat and high lean mass are maintained during the first 25 weeks of age in male VIP KOs (Vu et al., 2015). The complete distribution of lean mass is unknown, although KOs are shown to have a larger pancreas, colon and small intestine weight when represented as percent of body weight (Lelievre, 2007). PACAP KO mice also exhibit lower body weights with decreased

visceral and subcutaneous fat mass (Tomimoto et al., 2008). In attempt to better understand the mechanisms impacting their body dysmorphia, many labs have focused investigating changes in the GI tract, neural tissue and adipose of VIP and PACAP deficient mice. Expression of the VPAC1, VPAC2 and PAC1 receptors in all three of these organs lends support to the hypothesis that VIP and PACAP work in concert to maintain the gut-brain-adipose axis.

1.3.3. Gastrointestinal Functions Mediated by VIP & PACAP

A primal function of the gastrointestinal (GI) tract is nutrient absorption, which is mediated by many factors, including a microbial composition that affects nutrient availability and hormonal crosstalk between the brain and adipose tissue (May, 2021). Metabolically unhealthy obese individuals have decreased microbial alpha-diversity when compared to obese subjects without characteristics of metabolic disease such as T2D, hypertension, dyslipidemia, or increased waist circumference (Kim, 2020). Similarly, the VIP KO mice harbor decreased alpha-diversity of fecal microbiota with a net depletion in the *Firmicutes → Clostridiales* lineage as well as an enrichment of the *Proteobacteria* and *Bacteroidetes* phyla in both male and female mice (Bains, 2019). This study also reports a significant increase in the *Bacteroides* genus, which are gram negative bacteria that contribute to elevated lipopolysaccharide induced inflammation and are associated with irritable bowel disease (IBD) (Bloom, 2011). Comparably, both male and female PACAP KO mice have a slight increase in *Bacteroides,* however also display depleted *Bifidobacterium* (Heimesaat, 2017). A decreased abundance of *Bifidobacterium* is associated with irritable bowel disease and celiac disease, thus PACAP KO mice may also be models of these inflammatory disorders (Nadal et al, 2007). The VIP pathway has been extensively reviewed for IBD (Abad, 2018) and PACAP KO mice develop higher colonic inflammation following dextran sodium sulfate challenge, making them susceptible to GI disorders (Nemetz,

2007). Delayed growth and poor appetite are associated with IBD, however causes of the disease are unclear (Wong, 2021). Since both VIP and PACAP KO mice harbor body dysmorphia and distinct microbial dysbiosis, these neuropeptides may be important for a maintaining the gut-brain-adipose axis.

1.3.4. Neuropeptide Control Over Energy Expenditure/Food Intake

To explain why VIP or PACAP deficiency results in a lean phenotype, experiments to investigate energy expenditure and food intake have been conducted. Surprisingly, PACAP deficiency causes no change in resting energy expenditure compared to wildtype littermates at thermoneutrality in either sex (Diané, 2014). With norepinephrine administration, however, they are unable to increase resting metabolic rate (Diané, 2014). On the other hand, intracerebroventricular administration of PACAP induced hyperthermia, whereas the same method of delivery with VIP shows no effect on body temperature in mice (Masuo, 1995). Central delivery of PACAP increases, and VIP decreases, resting energy expenditure in chicks suggesting that body temperature may be a PACAP-mediated event conserved across species (Tachibana 2007). PACAP induced hyperthermia is directed through the PAC1 receptor on the ventromedial nucleus of the hypothalamus, explaining why VIP appears to be a less potent regulator of hypothalamic directed thermogenesis (Chang, 2020). The experiments conducted thus far show that PACAP regulates body temperature through mechanisms which also influence energy expenditure, however VIP decreases body temperature through mechanisms that are unexplained by changes in energy expenditure. The question that emerges is whether these hormones impact feeding behavior, which could also explain the body dysmorphia that is observed in KO mice.

Feeding patterns of the VIP deficient mice are different to that of wild type mice, which can be explained by the presence of VPAC2 receptors on retina and regions of the brain controlling circadian rhythm (Bechtold, 2008). Both VIP and VPAC2 KO mice exhibit a circadian dysfunction, which results in disrupted habits of food intake. Consistent amongst the literature is the observation that VIP deficient mice consume more food during the light phase than their wild-type littermates, however there is disagreement regarding the changes in total food intake. In one study during a 12 hour light/dark cycle, wild type mice consumed more food between 12pm-6pm (dark phase), whereas VIP and VPAC2 deficient mice consumed the largest percentage of their food between 6am-12pm(light phase) (Bechtold, 2008). Despite this shift in feeding behavior, the cumulative food intake observed in this study was the same between all mice when calculated as g of food/gram body weight. Similarly, another study found that VIP deficient mice consumed less food during the dark phase than their wildtype littermates, however VIP KO mice ate a cumulative of 15% less food (Vu, 2015). One explanation for the inconsistent conclusions about food intake between studies could be whether food intake is normalized to mouse body weight.

Similarly, male PACAP KO mice display a shift from nocturnal to daytime feeding behavior (Nguyen, 2020), however neither male nor female PACAP KO mice have changes in food intake when displayed as percentage of food eat/average body weight (Sherwood, 2007) (Adams, 2007). Because PAC1 receptors are expressed in regions of the brain controlling appetite, PAC1 agonists/antagonists have been explored as therapeutics to control eating behavior. The anorexigenic effects of PACAP administration has been studied in mice, rats and goldfish, whereas hypophagia is absent in mice lacking the receptor PAC1 (Sureshkumar, 2021). Both peripheral and intracerebroventricular PACAP delivery result in decreased feeding

8

behaviors, whereas these affects are absent in the PAC1 KO mice (Vu, 2015). Both VPAC2 and

PAC1 are expressed on proopiomelanocortin (POMC) neurons, regions of the CNS controlling

feeding behavior, only PAC1 is present on agouti related peptide (AgRP) neurons, which could

explain why intracerebroventricular VIP is unable to produce the same hypophagia effects

(Mounien, 2008).

The investigations regarding PACAP & VIP's role in energy expenditure and food intake

point to PACAP/PAC1 mediated control over body temperature and feeding behaviors. This

claim is supported by the necessity of raising PACAP KO mouse pups in warm conditions to

prevent premature death from hypothermia (Adams, 2007). PAC1 enriched areas of the brain

have been shown to mediate feeding and thermogenesis through the hypothalamic ventromedial

nuclei, which is a region of the brain influencing energy homeostasis (Sureshkumar, 2021).

There is also support for VPAC2 mediated eating behavior, since VPAC2 KO mice experience a

decrease in food intake (Asnicar, 2002), while VPAC1 KOs do not exhibit this same phenotype

(Sanford, 2022).

1.4. Adipose is a Complex Tissue Impacted by VIP and PACAP Signaling

1.4.1. The Metabolic Organ Storing Fat in Our Body

Obesity is characterized by an accumulation of fat mass, which is now widely accepted as

a metabolic organ (Ottaviani, 2011). Adipose is an exceptionally plastic tissue with the ability to

modify its cellular composition in response to hormonal changes within the mammalian host

(Qian, 2021). Lipids, often referred to as fats, are a hydrophobic biomolecule stored in

specialized mammalian fat cells known as adipocytes (Ottaviani, 2011). Adipocytes have a cell

phenotype uniquely specialized for the storage of lipids by utilizing organelles known as lipid

droplets, which can fill a large portion of the cell's volume (Fujimoto & Parton, 2011). Lipid

droplets vary in size as they grow and shrink because of the organism's metabolic demands (Yu, 2016).

Adipocytes reside in a matrix known as the stromal vascular fraction (SVF), which is composed of immune cells, preadipocytes, stem cells and secreted metabolites (Ramakrishnan, 2018). Adipose tissue is considered a metabolic organ since adipocytes secrete a plethora of adipokines (hormones and cytokines) to communicate the cell's functional status to peripheral tissues in the body (Kong, 2019). For instance, high levels of leptin in the blood are associated with hypertrophic adipocytes in the case of diet induced obesity (Skurk, 2007). Since leptin receptors in the brain impact eating behavior, leptin has been described as an important adipokine for communicating satiety between adipocytes and the central nervous system (Kwon, 2016). Another factor that influences adipokine secretion is the type of adipocyte from which they are being released. Three diverse types of adipocytes have been identified in males as white, brown, and beige, whereas females can also obtain a fourth cell type known as pink adipocytes (Giordano, 2014).
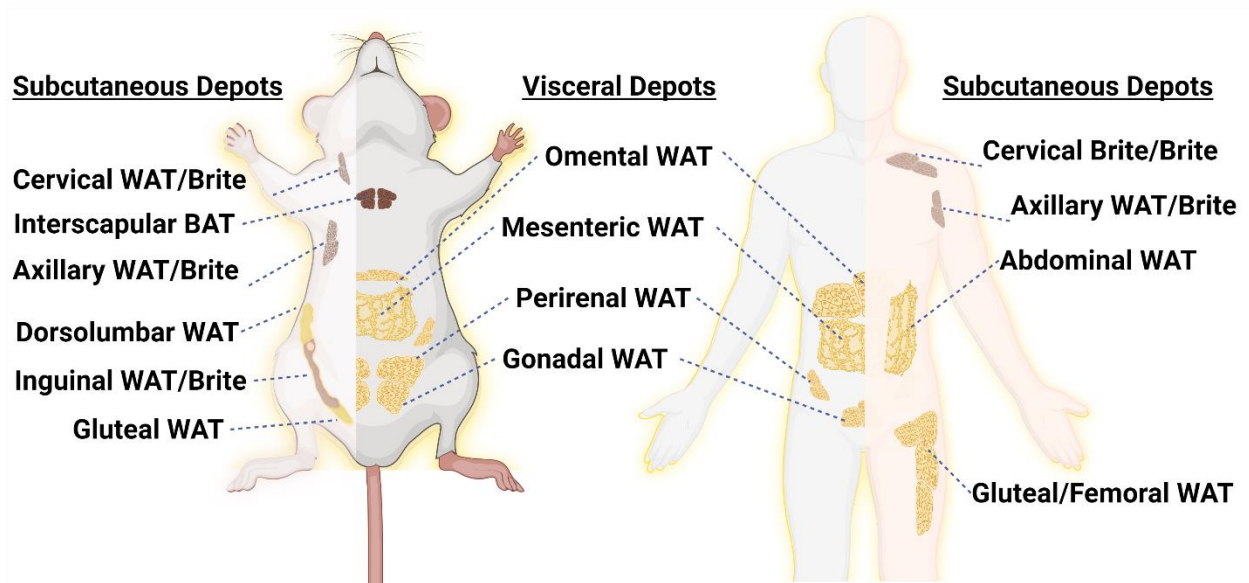
Figure 1.2. Locations of Major WAT, BAT, and Brite Depots in Mice and Humans. Adapted from (Chusyd, 2016).

1.4.2. White Adipocytes

Structurally, WAT cells are unilocular, meaning they contain a single lipid droplet that can take up most of the cell's mass (Fujimoto & Parton, 2011). An important function of WAT is lipid storage, but they are also capable of breaking down fat stores (lipolysis) and secreting adipokines (Skurk, 2007). WAT depots can be located inside the peritoneal cavity (visceral WAT) or between the skin and outer abdominal wall (subcutaneous WAT) (Smith, 2019). Both mice and humans have comparable visceral depots (e.g. omentum, gonadal, mesentery, and perirenal), however the anatomical location of their subcutaneous depots are more variable (Chusyd, 2016) (**Figure 1.2**). Leptin is a WAT adipokine which binds to neuronal receptors located in the mediobasal part of the hypothalamus to convey signals of satiety and decreasing food intake (Kwon, 2016). With larger amounts of WAT in obesity comes hyperleptinemia, which can result in leptin resistance and reduce the adipokine's efficacy at regulating food intake (Morris, 2009).

1.4.3. Brown Adipocytes

It is postulated that brown adipose tissue (BAT) evolved thermogenic capability to allow organisms to adapt to cold environments (Jung, 2018). BAT is unique from WAT in structure and function, allowing it to burn energy for heat, rather than storing excess lipids (Mae, 2021). The process of releasing heat energy is carried out by uncoupling protein 1 (UCP1), which is embedded into the mitochondrial membrane where it uncouples ATP synthase activity (Ricquier, 2000). The proton gradient, which drives ATP synthesis is released when UCP1 pumps protons back into the mitochondrial matrix and releases the energy in the form of heat rather than ATP synthesis (Ramsden, 2012)(**Figure 1.3**). Brown adipocytes have a multilocular appearance (multiple small lipid droplets), which provides more surface area for frequent access to the lipid

stores that can fuel thermogenesis (Nishimoto, 2017). Smaller lipid droplets also allow for brown

adipocytes to fill up free cytoplasmic space with mitochondria that contain UCP1, increasing the

thermogenic capacity of the cell (Ricquier, 2000). The interscapular BAT region contains the

largest depot in mice, and is often used for research, however only human infants are known to

obtain BAT in that region, suggesting that BAT plays a greater role in the physiology of adult

mice than adult humans (Sacks & Symonds, 2013). Further, regions considered to be "brown" in

adult humans resemble the gene expression profile of beige adipocytes in mice (Spiegelman,

2013). These beige/BAT depots in humans constitutes about 4.3% of total human body as their

primary function is to burn fat for thermal energy (Leitner 2017).
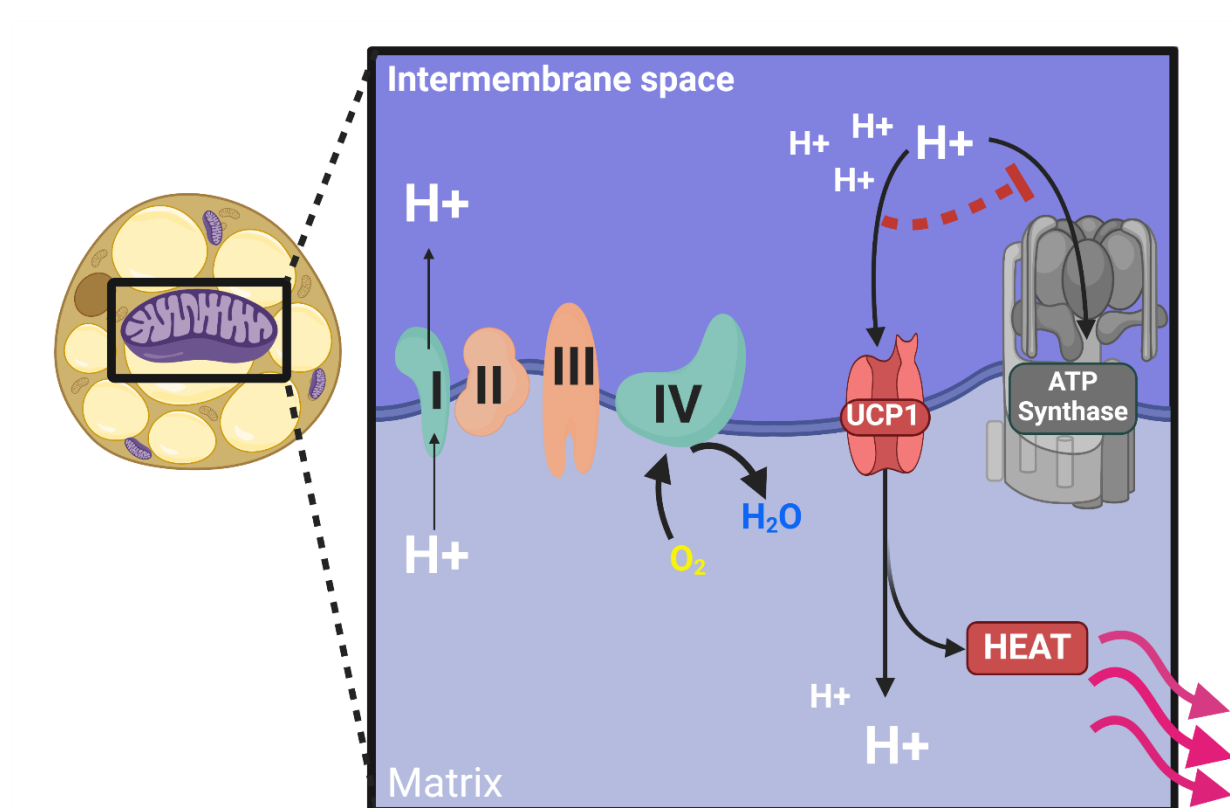
Figure 1.3. UCP1-Mediated Non-Shivering Thermogenesis.
Image Adapted from (Ramsden, 2012).

1.4.4. Beige Adipocytes

Beige cells are a type of adipocyte that function like white adipocytes until activated for heat production where they become multilocular, increase mitochondrial biosynthesis and begin to resemble brown adipocytes (Jung, 2018). Inactive beige adipocytes are often referred to as "beige preadipocytes", who reside in WAT depots until programmed for heat production by a stimulator molecule such as norepinephrine (Spiegelman, 2013). Sympathetic innervation of WAT is the main source of norepinephrine (NE), however sympathetic neuron-associated macrophages (SAMs) may impact this supply (Nguyen, 2011). It is unclear how SAMs influence NE molecules, in which some research groups have found them to secrete NE and others show degradation of NE secreted by sympathetic neurons (Pirzgalska, 2018). Still, SAMs play a central role in adipose thermogenesis as modifying genes utilized by these macrophages affects adipose innervation and lipolysis capacity (Pirzgalska, 2018).

Classical NE activation of beige preadipocytes is a process also called "beiging", whereby beige preadipocytes in WAT tissue become active "brown in white adipose tissue" or "brite" cells (Spiegelman, 2013). In the presence of cold exposure and/or sympathetic arousal, beige preadipocytes become activated and undergoes the structural modifications of 1) increased mitochondrial biosynthesis 2) lipolysis and 3) UCP1 expression (Mae, 2021). These changes increase the thermogenic functionality of an adipocyte, increasing heat production in cold environments (Mae, 2021).

1.4.5. Pink Adipocytes

Pink adipocytes are a fourth type of adipose cell which have been observed in female mammary tissue for lactation (Giordano, 2014). During pregnancy, subcutaneous WAT (scWAT) in mammary tissue can transdifferentiate into pink adipocytes, which contain a smaller

lipid droplet and milk secreting granules (Giordano, 2014). It is unclear whether pink and beige adipocytes arise from the trans-differentiation of pre-existing white cells or if new cells are recruited through de novo adipogenesis (Cinti, 2018). With evidence supporting both possibilities, adipose 'beiging' and 'pinking' likely stem from dual-conversion of both de novo cells as well as white-turned-beige/pink cells. Additionally, an experiment tracking white and pink cell markers found that pink adipocytes could even transdifferentiate back to white adipocytes after the pregnancy and lactation period had ended (Morroni, 2004).

1.4.6. Lineages and Differentiation of Adipocytes

As described, four types of adipocytes are recognized in mammals as brown, white, beige or pink classification. Because only brown, white and beige cells are present in both males and non-lactating females, these three will be the main focus of the remainder of this review. Interestingly, these three cells do not all arise from the same precursor lineages (Jung, 2018). Both beige and white adipocytes arise from a common adipose progenitor lineage, although it is still unclear whether beige adipocytes diverge during early differentiation or transdifferentiate from existing mature white adipocytes (Ikeda, 2018). The differentiation of beige adipocytes is promoted by the nuclear receptor known as peroxisomal proliferation factor gamma (PPARγ) often referred to as the master regulator of adipogenesis (Ma, 2018). Brown adipocytes are more closely related to muscle cells, as both arise from Myf5$^+$ progenitors (Nishimoto, 2017) (**Figure 1.4**). The shared lineage of muscle and BAT cells is unexpected, but explainable as muscle cells can also produce shivering thermogenesis from involuntary muscle contractions via myosin-mediated ATP hydrolysis and calcium transport (Periasamy, 2017).
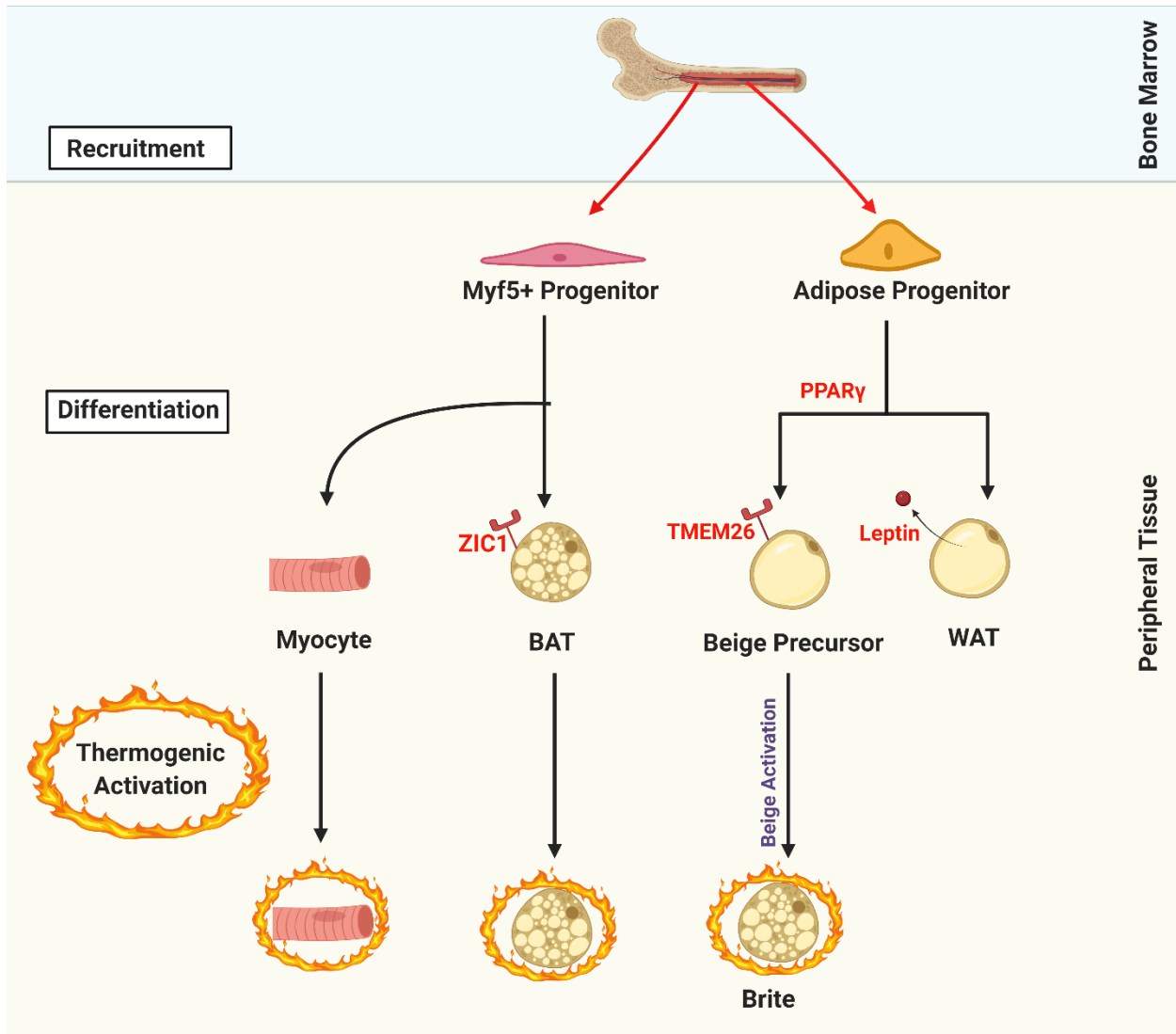
Figure 1.4. Differentiation and Activation of Muscle, WAT, BAT, and Brite cells.

1.4.7. VIP & PACAP Influence Adipose Biology

PAC1 expression is altered in all types of adipocytes under cold exposure, validating PACAP's observed importance in mammalian's thermogenic adaptation (Cline, 2018). This same study verified that VPAC1 and VPAC2 are also expressed in gonadal and inguinal fat pads of mice, which supports the observation in VPAC2 agonistic potential to induce lipolysis (Åkesson, 2005). Interestingly, this study also found that VPAC1 mRNA was upregulated in brown adipocytes post-maturation, suggesting an important role for VPAC1 in BAT biology.

15

Under cold exposure, the PACAP KO mice display impaired BAT thermogenesis, whereas their inguinal WAT region displays enhanced gene expression of the thermogenic protein known as uncoupling protein 1 (Diané, 2014). The thermogenic gene CIDEA and creatine metabolizing gene CKMT is dysregulated in the iWAT of female PACAP KO mice compared to wildtypes following a 3.5-week cold exposure, whereas males show changes in another gene related to creatine metabolism known as GATM (Filatov, 2021). The gonadal fat pad of PACAP KO mice is severely depleted, however the adipocyte cell size remains unchanged (Tomimoto, 2008). PACAP deficient mice have lower levels of serum leptin, which is likely the result of their decreased body fat (Adams, 2007). Interestingly, the lower fat profile of VIP deficient mice is accompanied by an increase in serum leptin, but it is unlikely that increased body fat could explain this observation based on the defect in fat storage in VIP KO mice (Vu, 2015). One explanation for this observation could be if the adipose depots were composed of larger white adipocytes, as leptin secretion is positively correlated with cell size (Skurk, 2007).

1.5. Conclusion

The 'sister peptides' VIP and PACAP are vital to many whole-body metabolic processes, as demonstrated by the adverse phenotypes resulting from their knockout mice. Body dysmorphia and changes gut microbial structures are observed in the absence of either peptide. Additionally, both VIP and PACAP KO mice experience abnormal circadian rhythm paired with different feeding behaviors, but PACAP appears to be more important in the central nervous system's mediation of thermogenesis. Additionally, PACAP KO mice display impaired brown adipose function, although the adipose tissue of VIP deficient mice has not been investigated at the molecular level.

1.6. References

Abad, C., & Tan, Y.-V. (2018). Immunomodulatory roles of pacap and VIP: Lessons from knockout mice. *Journal of Molecular Neuroscience*, *66*(1), 102–113. https://doi.org/10.1007/s12031-018-1150-y

Åkesson Lina, Ahrén Bo, Manganiello, V. C., Holst, L. S., Edgren, G., & Degerman, E. (2003). Dual effects of pituitary adenylate cyclase-activating polypeptide and isoproterenol on lipid metabolism and signaling in primary rat adipocytes. *Endocrinology*, *144*(12), 5293–5299. https://doi.org/10.1210/en.2003-0364

Åkesson, L., Ahrén, B., Edgren, G., & Degerman, E. (2005). VPAC2-R mediates the lipolytic effects of pituitary adenylate cyclase-activating polypeptide/vasoactive intestinal polypeptide in primary rat adipocytes. *Endocrinology*, *146*(2), 744–750. https://doi.org/10.1210/en.2004-0504

Asnicar, M. A., Köster, A., Heiman, M. L., Tinsley, F., Smith, D. P., Galbreath, E., Fox, N., Ma, Y. L., Blum, W. F., & Hsiung, H. M. (2002). Vasoactive intestinal polypeptide/pituitary adenylate cyclase-activating peptide receptor 2 deficiency in mice results in growth retardation and increased basal metabolic rate. *Endocrinology*, *143*(10), 3994–4006. https://doi.org/10.1210/en.2002-220354

Bataille, D., Freychet, P. & Rosselin, G (1974). Interactions of glucagon, gut glucagon, vasoactive intestinal polypeptide and secretin with liver and fat cell plasma membranes: Binding to specific sites and stimulation of adenylate cyclase1. *Endocrinology*, *95*(3), 713–721. https://doi.org/10.1210/endo-95-3-713

Bains, M., Laney, C., Wolfe, A. E., Orr, M., Waschek, J. A., Ericsson, A. C., & Dorsam, G. P. (2019). Vasoactive intestinal peptide deficiency is associated with altered gut microbiota communities in male and female C57BL/6 mice. *Frontiers in Microbiology*, *10*. https://doi.org/10.3389/fmicb.2019.02689

Bloom, S. M., Bijanki, V. N., Nava, G. M., Sun, L., Malvin, N. P., Donermeyer, D. L., Dunne, W. M., Allen, P. M., & Stappenbeck, T. S. (2011). Commensal bacteroides species induce colitis in host-genotype-specific fashion in a mouse model of inflammatory bowel disease. *Cell Host & Microbe*, *9*(5), 390–403. https://doi.org/10.1016/j.chom.2011.04.009

Bechtold, D. A., Brown, T. M., Luckman, S. M., & Piggins, H. D. (2008). Metabolic rhythm abnormalities in mice lacking VIP-VPAC2 signaling. *American Journal of Physiology-Regulatory, Integrative and Comparative Physiology*, *294*(2). https://doi.org/10.1152/ajpregu.00667.2007

Cardoso, J. C., Garcia, M. G., & Power, D. M. (2020). Tracing the origins of the pituitary adenylate-cyclase activating polypeptide (PACAP). *Frontiers in Neuroscience*, *14*. https://doi.org/10.3389/fnins.2020.00366

Cinti, S. (2018). Pink adipocytes. *Trends in Endocrinology & Metabolism*, *29*(9), 651–666. https://doi.org/10.1016/j.tem.2018.05.007

Chang, R., Hernandez, J., Gastelum, C., Guadagno, K., Perez, L., & Wagner, E. J. (2020). Pituitary adenylate cyclase-activating polypeptide excites Proopiomelanocortin neurons: Implications for the regulation of energy homeostasis. *Neuroendocrinology*, *111*(1-2), 45–69. https://doi.org/10.1159/000506367

Chusyd, D. E., Wang, D., Huffman, D. M., & Nagy, T. R. (2016). Relationships between rodent white adipose fat pads and human white adipose fat depots. *Frontiers in Nutrition*, *3*. https://doi.org/10.3389/fnut.2016.00010

Cline, D. L., Short, L. I., Forster, M. A., & Gray, S. L. (2018). Adipose tissue expression of PACAP, VIP, and their receptors in response to cold stress. *Journal of Molecular Neuroscience*, *68*(3), 427–438. https://doi.org/10.1007/s12031-018-1099-x

Cunha-Reis, D., & Caulino-Rocha, A. (2020). VIP modulation of hippocampal synaptic plasticity: A role for VIP receptors as therapeutic targets in cognitive decline and Mesial Temporal Lobe epilepsy. *Frontiers in Cellular Neuroscience*, *14*. https://doi.org/10.3389/fncel.2020.00153

Delgado, M., & Ganea, D. (2011). Vasoactive intestinal peptide: A neuropeptide with pleiotropic immune functions. *Amino Acids*, *45*(1), 25–39. https://doi.org/10.1007/s00726-011-1184-8

Desbuquois, B., Laudat, M. H., & Laudat, P. (1973). Vasoactive intestinal polypeptide and glucagon: Stimulation of adenylate cyclase activity via distinct receptors in liver and fat cell membranes. *Biochemical and Biophysical Research Communications*, *53*(4), 1187–1194. https://doi.org/10.1016/0006-291x(73)90590-1

Diané, A., Nikolic, N., Rudecki, A. P., King, S. M., Bowie, D. J., & Gray, S. L. (2014). Pacap is essential for the adaptive thermogenic response of brown adipose tissue to cold exposure. *Journal of Endocrinology*, *222*(3), 327–339. https://doi.org/10.1530/joe-14-0316

Duncan, R. E., Ahmadian, M., Jaworski, K., Sarkadi-Nagy, E., & Sul, H. S. (2007). Regulation of lipolysis in adipocytes. *Annual Review of Nutrition*, *27*(1), 79–101. https://doi.org/10.1146/annurev.nutr.27.061406.093734

Fagerberg, L., Hallström, B. M., Oksvold, P., Kampf, C., Djureinovic, D., Odeberg, J., Habuka, M., Tahmasebpoor, S., Danielsson, A., Edlund, K., Asplund, A., Sjöstedt, E., Lundberg, E., Szigyarto, C. A.-K., Skogs, M., Takanen, J. O., Berling, H., Tegel, H., Mulder, J., … Uhlén, M. (2014). Analysis of the human tissue-specific expression by genome-wide integration of transcriptomics and antibody-based proteomics. *Molecular & Cellular Proteomics*, *13*(2), 397–406. https://doi.org/10.1074/mcp.m113.035600

Fahrenkrug, J., Ottesen, B., & Palle, C. (1989). Non-amidated forms of VIP (glycine-extended VIP and VIP-free acid) have full bioactivity on smooth muscle. *Regulatory Peptides*, *26*(2), 155. https://doi.org/10.1016/0167-0115(89)90034-7

Filatov, E., Short, L. I., Forster, M. A., Harris, S. S., Schien, E. N., Hughes, M. C., Cline, D. L., Appleby, C. J., & Gray, S. L. (2021). Contribution of thermogenic mechanisms by male and female mice lacking pituitary adenylate cyclase-activating polypeptide in response to cold acclimation. *American Journal of Physiology-Endocrinology and Metabolism*, *320*(3). https://doi.org/10.1152/ajpendo.00205.2020

Fujimoto, T., & Parton, R. G. (2011). Not just fat: The structure and function of the lipid droplet. *Cold Spring Harbor Perspectives in Biology*, *3*(3). https://doi.org/10.1101/cshperspect.a004838

Gardner, J. D., Conlon, T. P., & Adams, T. D. (1976). Cyclic amp in pancreatic acinar cells: Effects of gastrointestinal hormones. *Gastroenterology*, *70*(1), 29–35. https://doi.org/10.1016/s0016-5085(76)80399-x

Giordano, A., Smorlesi, A., Frontini, A., Barbatelli, G., & Cinti, S. (2014). Mechanisms in endocrinology: White, Brown and pink adipocytes: The extraordinary plasticity of the adipose organ. *European Journal of Endocrinology*, *170*(5). https://doi.org/10.1530/eje-13-0945

Girard, B. A., Lelievre, V., Braas, K. M., Razinia, T., Vizzard, M. A., Ioffe, Y., Meskini, R. E., Ronnett, G. V., & Waschek, J. A. (2006). Noncompensation in peptide/receptor gene expression and distinct behavioral phenotypes in VIP- and pacap-deficient mice. *Journal of Neurochemistry*, *99*(2), 499–513. https://doi.org/10.1111/j.1471-4159.2006.04112.x

Hannibal, J., Ekblad, E., Mulder, H., Sundler, F., & Fahrenkrug, J. (1997). Pituitary adenylate cyclase activating polypeptide (PACAP) in the gastrointestinal tract of the rat: Distribution and effects of capsaicin or denervation. *Cell and Tissue Research*, *291*(1), 65–79. https://doi.org/10.1007/s004410050980

Harmar, A. J., Fahrenkrug, J., Gozes, I., Laburthe, M., May, V., Pisegna, J. R., Vaudry, D., Vaudry, H., Waschek, J. A., & Said, S. I. (2012). Pharmacology and functions of receptors for vasoactive intestinal peptide and pituitary adenylate cyclase-activating polypeptide: Iuphar Review 1. *British Journal of Pharmacology*, *166*(1), 4–17. https://doi.org/10.1111/j.1476-5381.2012.01871.x

Heimesaat, M. M., Reifenberger, G., Vicena, V., Illes, A., Horvath, G., Tamas, A., Fulop, B. D., Bereswill, S., & Reglodi, D. (2017). Intestinal microbiota changes in mice lacking pituitary adenylate cyclase activating polypeptide (PACAP) — bifidobacteria make the difference. *European Journal of Microbiology and Immunology*, *7*(3), 187–199. https://doi.org/10.1556/1886.2017.00021

Hirabayashi, T., Nakamachi, T., & Shioda, S. (2018). Discovery of pacap and its receptors in the brain. *The Journal of Headache and Pain*, *19*(1). https://doi.org/10.1186/s10194-018-0855-1

Ikeda, K., Maretich, P., & Kajimura, S. (2018). The common and distinct features of brown and beige adipocytes. *Trends in Endocrinology & Metabolism*, *29*(3), 191–200. https://doi.org/10.1016/j.tem.2018.01.001

Jung, S. M., Sanchez-Gurmaches, J., & Guertin, D. A. (2018). Brown adipose tissue development and metabolism. *Brown Adipose Tissue*, 3–36. https://doi.org/10.1007/164_2018_168

Kim, M.-H., Yun, K. E., Kim, J., Park, E., Chang, Y., Ryu, S., Kim, H.-L., & Kim, H.-N. (2020). Gut microbiota and metabolic health among overweight and obese individuals. *Scientific Reports*, *10*(1). https://doi.org/10.1038/s41598-020-76474-8

Kong, Y., Zhang, S., Wu, R., Su, X., Peng, D., Zhao, M., & Su, Y. (2019). New insights into different adipokines in linking the pathophysiology of obesity and psoriasis. *Lipids in Health and Disease*, *18*(1). https://doi.org/10.1186/s12944-019-1115-3

Kwon, O., Kim, K. W., & Kim, M.-S. (2016). Leptin signalling pathways in hypothalamic neurons. *Cellular and Molecular Life Sciences*, *73*(7), 1457–1477. https://doi.org/10.1007/s00018-016-2133-1

Langer, I., Jeandriens, J., Couvineau, A., Sanmukh, S., & Latek, D. (2022). Signal transduction by VIP and pacap receptors. *Biomedicines*, *10*(2), 406. https://doi.org/10.3390/biomedicines10020406

Ma, X., Wang, D., Zhao, W., & Xu, L. (2018). Deciphering the roles of PPARΓ in adipocytes via dynamic change of transcription complex. *Frontiers in Endocrinology*, *9*. https://doi.org/10.3389/fendo.2018.00473

Mae, J., Nagaya, K., Okamatsu-Ogura, Y., Tsubota, A., Matsuoka, S., Nio-Kobayashi, J., & Kimura, K. (2021). Adipocytes and stromal cells regulate brown adipogenesis through secretory factors during the postnatal white-to-brown conversion of adipose tissue in Syrian hamsters. *Frontiers in Cell and Developmental Biology*, *9*. https://doi.org/10.3389/fcell.2021.698692

Masuo, Y., Noguchi, J., Morita, S., & Matsumoto, Y. (1995). Effects of intracerebroventricular administration of pituitary adenylate cyclase-activating polypeptide (PACAP) on the motor activity and reserpine-induced hypothermia in murines. *Brain Research*, *700*(1-2), 219–226. https://doi.org/10.1016/0006-8993(95)00978-y

May, K. S., & den Hartigh, L. J. (2021). Modulation of adipocyte metabolism by microbial short-chain fatty acids. *Nutrients*, *13*(10), 3666. https://doi.org/10.3390/nu13103666

Miyata, A., Jiang, L., Dahl, R. D., Kitada, C., Kubo, K., Fujino, M., Minamino, N., & Arimura, A. (1990). Isolation of a neuropeptide corresponding to the N-terminal 27 residues of the pituitary adenylate cyclase activating polypeptide with 38 residues (PACAP38). *Biochemical and Biophysical Research Communications*, *170*(2), 643–648. https://doi.org/10.1016/0006-291x(90)92140-u

Morris, D. L., & Rui, L. (2009). Recent advances in understanding leptin signaling and leptin resistance. *American Journal of Physiology-Endocrinology and Metabolism*, *297*(6). https://doi.org/10.1152/ajpendo.00274.2009

Morroni, M., Giordano, A., Zingaretti, M. C., Boiani, R., De Matteis, R., Kahn, B. B., Nisoli, E., Tonello, C., Pisoschi, C., Luchetti, M. M., Marelli, M., & Cinti, S. (2004). Reversible transdifferentiation of secretory epithelial cells into adipocytes in the mammary gland. *Proceedings of the National Academy of Sciences*, *101*(48), 16801–16806. https://doi.org/10.1073/pnas.0407647101

Mounien, L., Do Rego, J.-C., Bizet, P., Boutelet, I., Gourcerol, G., Fournier, A., Brabet, P., Costentin, J., Vaudry, H., & Jégou, S. (2008). Pituitary adenylate cyclase-activating polypeptide inhibits food intake in mice through activation of the hypothalamic melanocortin system. *Neuropsychopharmacology*, *34*(2), 424–435. https://doi.org/10.1038/npp.2008.73

Nadal, I., Donant, E., Ribes-Koninckx, C., Calabuig, M., & Sanz, Y. (2007). Imbalance in the composition of the duodenal microbiota of children with coeliac disease. *Journal of Medical Microbiology*, *56*(12), 1669–1674. https://doi.org/10.1099/jmm.0.47410-0

Nemetz, N., Abad, C., Lawson, G., Nobuta, H., Chhith, S., Duong, L., Tse, G., Braun, J., & Waschek, J. A. (2007). Induction of colitis and rapid development of colorectal tumors in mice deficient in the neuropeptide PACAP. *International Journal of Cancer*, *122*(8), 1803–1809. https://doi.org/10.1002/ijc.23308

Nguyen, K. D., Qiu, Y., Cui, X., Goh, Y. P., Mwangi, J., David, T., Mukundan, L., Brombacher, F., Locksley, R. M., & Chawla, A. (2011). Alternatively activated macrophages produce catecholamines to sustain adaptive thermogenesis. *Nature*, *480*(7375), 104–108. https://doi.org/10.1038/nature10653

Nguyen, T. T., Kambe, Y., Kurihara, T., Nakamachi, T., Shintani, N., Hashimoto, H., & Miyata, A. (2020). Pituitary adenylate cyclase-activating polypeptide in the ventromedial hypothalamus is responsible for food intake behavior by modulating the expression of agouti-related peptide in mice. *Molecular Neurobiology*, *57*(4), 2101–2114. https://doi.org/10.1007/s12035-019-01864-7

Nishimoto, Y., & Tamori, Y. (2017). Cide family-mediated unique lipid droplet morphology in white adipose tissue and brown adipose tissue determines the adipocyte energy metabolism. *Journal of Atherosclerosis and Thrombosis*, *24*(10), 989–998. https://doi.org/10.5551/jat.rv17011

Ottaviani, E., Malagoli, D., & Franceschi, C. (2011). The evolution of the adipose tissue: A neglected enigma. *General and Comparative Endocrinology*, *174*(1), 1–4. https://doi.org/10.1016/j.ygcen.2011.06.018

Langer, I., Jeandriens, J., Couvineau, A., Sanmukh, S., & Latek, D. (2022). Signal transduction by VIP and pacap receptors. *Biomedicines*, *10*(2), 406. https://doi.org/10.3390/biomedicines10020406

Leitner, B. P., Huang, S., Brychta, R. J., Duckworth, C. J., Baskin, A. S., McGehee, S., Tal, I., Dieckmann, W., Gupta, G., Kolodny, G. M., Pacak, K., Herscovitch, P., Cypess, A. M., & Chen, K. Y. (2017). Mapping of human brown adipose tissue in lean and obese young men. *Proceedings of the National Academy of Sciences*, *114*(32), 8649–8654. https://doi.org/10.1073/pnas.1705287114

Lelievre, V., Favrais, G., Abad, C., Adle-Biassette, H., Lu, Y., Germano, P. M., Cheung-Lau, G., Pisegna, J. R., Gressens, P., Lawson, G., & Waschek, J. A. (2007). Gastrointestinal dysfunction in mice with a targeted mutation in the gene encoding vasoactive intestinal polypeptide: A model for the study of intestinal ileus and Hirschsprung's disease. *Peptides*, *28*(9), 1688–1699. https://doi.org/10.1016/j.peptides.2007.05.006

Periasamy, M., Herrera, J. L., & Reis, F. C. (2017). Skeletal muscle thermogenesis and its role in whole body energy metabolism. *Diabetes & Metabolism Journal*, *41*(5), 327. https://doi.org/10.4093/dmj.2017.41.5.327

Pirger, Z., Krajcs, N., & Kiss, T. (2016). Occurrence, distribution, and physiological function of pituitary adenylyl cyclase-activating polypeptide in invertebrate species. *Current Topics in Neurotoxicity*, 19–31. https://doi.org/10.1007/978-3-319-35135-3_2

Pirzgalska, R. M., & Domingos, A. I. (2018). Macrophages in obesity. *Cellular Immunology*, *330*, 183–187. https://doi.org/10.1016/j.cellimm.2018.04.014

Qian, S., Tang, Y., & Tang, Q.-Q. (2021). Adipose tissue plasticity and the pleiotropic roles of BMP signaling. *Journal of Biological Chemistry*, *296*, 100678. https://doi.org/10.1016/j.jbc.2021.100678

Ramakrishnan, V. M., & Boyd, N. L. (2018). The adipose stromal vascular fraction as a complex cellular source for tissue engineering applications. *Tissue Engineering Part B: Reviews*, *24*(4), 289–299. https://doi.org/10.1089/ten.teb.2017.0061

Ramsden, D. B., Ho, P. W. L., Ho, J. W. M., Liu, H. F., So, D. H. F., Tse, H. M., Chan, K. H., & Ho, S. L. (2012). Human neuronal uncoupling proteins 4 and 5 (UCP4 and UCP5): Structural properties, regulation, and physiological role in protection against oxidative stress and mitochondrial dysfunction. *Brain and Behavior*, *2*(4), 468–478. https://doi.org/10.1002/brb3.55

Ricquier, D., & Bouillaud, F. (2000). Mitochondrial uncoupling proteins: From mitochondria to the regulation of Energy Balance. *The Journal of Physiology*, *529*(1), 3–10. https://doi.org/10.1111/j.1469-7793.2000.00003.x

Sacks, H., & Symonds, M. E. (2013). Anatomical locations of human brown adipose tissue. *Diabetes*, *62*(6), 1783–1790. https://doi.org/10.2337/db12-1430

Said, S. I., & Mutt, V. (1970). Potent peripheral and splanchnic vasodilator peptide from normal gut. *Nature*, *225*(5235), 863–864. https://doi.org/10.1038/225863a0

Sanford, D., Luong, L., Vu, J. P., Oh, S., Gabalski, A., Lewis, M., Pisegna, J. R., & Germano, P. (2022). The VIP/VPAC1R pathway regulates energy and glucose homeostasis by modulating GLP-1, glucagon, leptin and PYY levels in mice. *Biology*, *11*(3), 431. https://doi.org/10.3390/biology11030431

Sherwood, N. M., Krueckl, S. L., & McRory, J. E. (2000). The origin and function of the pituitary adenylate cyclase-activating polypeptide (pacap)/glucagon superfamily*. *Endocrine Reviews*, *21*(6), 619–670. https://doi.org/10.1210/edrv.21.6.0414

Sherwood, N. M., Adams, B. A., Isaac, E. R., Wu, S., & Fradinger, E. A. (2007). Knocked Down and out: Pacap in development, reproduction and feeding. *Peptides*, *28*(9), 1680–1687. https://doi.org/10.1016/j.peptides.2007.03.008

Skurk, T., Alberti-Huber, C., Herder, C., & Hauner, H. (2007). Relationship between adipocyte size and Adipokine expression and secretion. *The Journal of Clinical Endocrinology & Metabolism*, *92*(3), 1023–1033. https://doi.org/10.1210/jc.2006-1055

Smith, G. I., Mittendorfer, B., & Klein, S. (2019). Metabolically healthy obesity: Facts and fantasies. *Journal of Clinical Investigation*, *129*(10), 3978–3989. https://doi.org/10.1172/jci129186

Spiegelman, B. M. (2013). Banting Lecture 2012. *Diabetes*, *62*(6), 1774–1782. https://doi.org/10.2337/db12-1665

Sureshkumar, K., Saenz, A., Ahmad, S. M., & Lutfy, K. (2021). The pacap/pac1 receptor system and feeding. *Brain Sciences*, *12*(1), 13. https://doi.org/10.3390/brainsci12010013

Tachibana, T., Oikawa, D., Adachi, N., Boswell, T., & Furuse, M. (2007). Central administration of vasoactive intestinal peptide and pituitary adenylate cyclase-activating polypeptide differentially regulates energy metabolism in chicks. *Comparative Biochemistry and Physiology Part A: Molecular & Integrative Physiology*, *147*(1), 156–164. https://doi.org/10.1016/j.cbpa.2006.12.043

Temmerman, L., Bogaerts, A., Meelkop, E., Cardoen, D., Boerjan, B., Janssen, T., & Schoofs, L. (2012). A proteomic approach to neuropeptide function elucidation. *Peptides*, *34*(1), 3–9. https://doi.org/10.1016/j.peptides.2011.08.025

Tomimoto, S., Ojika, T., Shintani, N., Hashimoto, H., Hamagami, K.-ichi, Ikeda, K., Nakata, M., Yada, T., Sakurai, Y., Shimada, T., Morita, Y., Ishida, C., & Baba, A. (2008). Markedly reduced white adipose tissue and increased insulin sensitivity in ADCYAP1-deficient mice. *Journal of Pharmacological Sciences*, *107*(1), 41–48. https://doi.org/10.1254/jphs.fp0072173

VIP Protein and RNA Expression Overview. Tissue expression of VIP - summary - The human protein atlas. (n.d.). Retrieved June 20, 2022, from https://www.proteinatlas.org/ENSG00000146469-VIP/tissue

Vu, J. P., Larauche, M., Flores, M., Luong, L., Norris, J., Oh, S., Liang, L.-J., Waschek, J., Pisegna, J. R., & Germano, P. M. (2015). Regulation of appetite, body composition, and metabolic hormones by vasoactive intestinal polypeptide (VIP). *Journal of Molecular Neuroscience*, *56*(2), 377–387. https://doi.org/10.1007/s12031-015-0556-z

Vu, J. P., Goyal, D., Luong, L., Oh, S., Sandhu, R., Norris, J., Parsons, W., Pisegna, J. R., & Germano, P. M. (2015). Pacap intraperitoneal treatment suppresses appetite and food intake via PAC1 receptor in mice by inhibiting ghrelin and increasing GLP-1 and leptin. *American Journal of Physiology-Gastrointestinal and Liver Physiology*, *309*(10). https://doi.org/10.1152/ajpgi.00190.2015

Wong, K., Isaac, D. M., & Wine, E. (2021). Growth delay in inflammatory bowel diseases: Significance, causes, and management. *Digestive Diseases and Sciences*, *66*(4), 954–964. https://doi.org/10.1007/s10620-020-06759-5

Yu, J., & Li, P. (2016). The size matters: Regulation of lipid storage by lipid droplet dynamics. *Science China Life Sciences*, *60*(1), 46–56. https://doi.org/10.1007/s11427-016-0322-x

2. ADIPOCYTE BIOLOGY AND FFA METABOLISM IS DISRUPTED IN MALE, BUT NOT FEMALE VIP DEFICIENT MICE

2.1. Abstract

Metabolic diseases associated with obesity contribute to an estimated 20.6% of U.S. national health care expenditures. Despite efforts to promote healthier lifestyles, the CDC reports that heart disease, T2D, and obesity rates continue to rise, posing a need for pharmaceuticals targeting adipose function. SNPs of the VIP pathway are most strongly correlated with human fat mass, suggesting that intervention of VIP signaling could offer new therapeutic strategies for mitigating human disease related to adipose expandability. Since VIP deficient mice maintain low body fat, we predicted their adipose tissue would display the biological parameters of healthy lean individuals. Surprisingly, we found an adipose tissue dysfunction characterized by decreased serum FFAs, hypertrophic adipocytes, and suppressed TMEM26+ beige preadipocyte markers in the iWAT of male but not female VIP deficient mice. In conclusion, although VIP deficient mice appear lean and healthy, their adipose characteristics suggest an increased risk for metabolic disease.

2.2. Introduction/Background

2.2.1. Adipose Quality Best Predicts Metabolic Disease

BMI is a parameter used by the World Health Organization (WHO) to identify correlations between disease and an individual's weight/height ratio (WHO, Obesity and overweight 2021); however, there are flaws in using this measurement. For instance, individuals with a high body mass index (BMI>30) are considered obese; however, this does not account for body composition and thus would classify a bodybuilder with low fat and high lean muscle tissue as 'obese' (CB, 2019). Another shortcoming to using BMI in metabolic disease assessment is the

inaccuracy of associating all obese individuals with poor health; however, 40% of patients with

fatty liver disease worldwide are not obese (Ye, 2020). Additionally, 10-20% of type II diabetes

(T2D) patients in the U.S. are non-obese and these numbers rise to 60-80% in some Asian

countries (Olaogun, 2020). The prevalence of metabolic disorders in lean individuals discredits

the associations made with obesity; however, adipose functions, irrespective of tissue amount,

are still crucial in metabolic homeostasis (Virtue, 2008).

It has been suggested that qualities mediating subcutaneous expansion, rather than the

total amount of adipose, drive metabolic disease (Virtue, 2008). For instance, "metabolically

healthy obese" individuals who store more subcutaneous than visceral fat are also protected from

heart disease (Smith, 2019). Consistently, women tend to deposit fat more subcutaneously

(Chang, 2018) and have a lower prevalence of heart disease than men, where heart disease is the

leading cause of death in the US (Men and heart disease, 2021).

2.2.2. Noninvasive Methods of Assessing Adipose Expandability in Humans

Current mechanisms of determining an individual's adipose expandability come from

comparing total adipose deposition in subcutaneous versus visceral locations. One method for

evaluating subcutaneous adipose expandability is measuring waist circumference (Ross, 2020);

however, this method cannot separate abdominal subcutaneous deposition from adipose inside

the visceral cavity (Bertoli, 2015). Body fat distribution can also be determined using computer

tomography (CT) scans and dual x-ray absorptiometry (DEXA) analysis; however, these

technologies are expensive and not always available (Chait, 2020).

Another tool for assessing risk for metabolic disease is genetic sequencing, which screens

individuals for gene variants associated with adipose dysfunction and metabolic disease,

allowing physicians to tailor lifestyle changes to a patient's genetics (McInnes, 2021). Genetic

variations also correlate with adipose expandability; for instance, PPARγ mutations associate with insulin resistance and abnormal lipid metabolism (Semple, 2006). Fat mass expandability is complex and can result from multiple gene polymorphisms (Ambele, 2020); thus, ongoing research to identify genes associated with impaired adipose expandability is imperative. Developing an effective method to predict underlying genetic predisposition to metabolic disease is a current goal of the scientific community, which will require more research that identifies genes important to metabolic health (Barosso, 2019). Genetically altered mouse models are often used to understand the necessity of a functioning gene for adipose function by directly assessing molecular characteristics influencing adipose function and expandability (Longo, 2019). Groups have correlated impaired adipocyte expansion with 1) adipocyte hypertrophy (Longo, 2019), 2) fatty acid metabolism (Slawik, 2007), and 3) beige adipogenesis (Zhang, 2021).

2.2.3. Adipocyte Hypertrophy is Linked to Metabolic Disease

Adipose tissue can grow and expand via two mechanisms: 1) individual cell growth (hypertrophy) and 2) the differentiation of new adipocytes (hyperplasia) (Jo, 2009). Hypertrophy is defined by individual cell growth to accommodate new lipids brought into adipose tissue (Jo, 2009). Excessively hypertrophic cells are problematic because they secrete adipokines such as IL-6, IL-8, and TNF-a, which can induce inflammation (Skurk, 2007). Additionally, hypertrophic adipocytes become insulin resistant and influence the development of T2D (Chait, 2020). Secretion of proinflammatory cytokines by hypertrophic adipocytes results in phosphorylation of insulin receptor substrate-1, a potential underlying mechanism of insulin resistance (Hirosumi, 2002). Interestingly, GLUT4 trafficking to the plasma membrane is also impaired in mice with hypertrophic adipocytes even in the absence of inflammation (Kim, 2015), demonstrating the complexity of adipocyte hypertrophy mediating insulin resistance.

The secretion of numerous inflammatory adipokines plays an important role in cardiovascular disease (Fuster, 2016). Hypertrophic adipocytes are also linked to heart failure (Anthony, 2019), a leading cause of death in the United States and responsible for the mortality of 1 in 4 men (Men and heart disease, 2021). Additionally, when adipocyte growth reaches its finite limit, excess circulating lipids are routed to storage in ectopic regions such as the heart and arteries (Serra, 2016). This phenomenon, described in the 'adipose tissue expandability hypothesis,' states that when subcutaneous adipose tissue reaches its limit of cellular expansion, lipids are undesirably stored in visceral regions that increase an individual's risk for metabolic diseases such as cardiomyopathy (Danforth, 2000).

2.2.4. Hypertrophic Adipocytes Arising from Impaired Adipogenesis

Hypertrophic adipocytes can arise from impaired adipogenesis or the differentiation of preadipocytes into new mature fat cells (Moseti, 2016). During adipogenesis, progenitors can differentiate into two types of adipocytes: white and beige (Ikeda, 2018). While white adipocytes mainly store fat into a single unilocular droplet, the beige adipocytes are multilocular and can 'burn' lipids to produce heat using uncoupling protein 1 (UCP1), which is embedded in the mitochondrial membrane and dissipates energy from proton gradients through thermogenesis (Ricquier, 2011). Beige adipocytes harness UCP1 action and upregulate mitochondrial biosynthesis only after being 'activated' by a stimulus such as norepinephrine (Spiegelman, 2013). Before activation, beige preadipocytes reside in the stromal vascular fraction and can be identified by molecular markers (Wu, 2012).

One such marker, transmembrane 26 (TMEM26), is a 41.5 kilodalton protein consisting of 5-8 transmembrane domains (Town, 2011). TMEM26 is a marker for beige preadipocytes rather than activated beige cells, making it a helpful gene for predicting 'beiging' potential

(Comas et al., 2019). To elaborate, TMEM26 decreases in the subcutaneous adipose of mice under beige adipogenic stimuli, followed by an upregulation in UCP1 (Lee et al., 2015).

Differentiation of adipocytes towards the beige, rather than white, lineage is primarily driven by the nuclear retinoid x receptor known as peroxisome proliferator-activated receptor-gamma (PPARγ) (Ma, 2018). PPARγ is necessary for adipogenesis as its depletion results in undifferentiated preadipocytes that cannot store lipids properly (Wafer et al., 2017). Adipose-specific PPARγ deficient mice have fat storage defects, hypoplasia, hypertrophic cells, and low-weight fat tissue (He, 2003), making them a prime example of how impaired adipogenesis can manifest adipocyte hypertrophy.

2.2.5. Fatty Acid Metabolism Influences Adipocyte Hypertrophy

Another mechanism influencing adipocyte hypertrophy is impaired fatty acid metabolism (Recazens et al., 2021). Adipocytes have the unique responsibility of storing lipids (lipogenesis) until needed during energy deficits, by which lipids are hydrolyzed (lipolysis) and transported to the extracellular space (Duncan, 2007). An impairment of lipolysis is present in mice lacking an enzyme known as hormone-sensitive lipase (HSL), resulting in adipocyte hypertrophy due to the inability of cells to release their lipid content (Shen, 2011). Other lipases assist in lipolysis, but HSL is the most functionally diverse, with the ability to hydrolyze acyl glycerides, cholesterol esters, and retinyl esters (Recazens, 2021). HSL also has a non-enzymatic influence on de novo lipogenesis and adipocyte lineage commitment mediated by PPARγ, a mechanism hypothesized to result from fatty acid ligands produced from lipolysis (Shen, 2011).

2.2.6. Importance of Considering VIP's Function in Adipose Expansion

In a genome-wide association study, the single nucleotide polymorphisms of genes in the VIP pathway most strongly correlated with human fat mass (Liu, 2010). VIP is a 28 amino acid

peptide first isolated from porcine intestinal tissue in 1970 (Said & Mutt, 1970). Neurons and immune cells that secrete VIP can induce the release of other hormones from tissues such as the pituitary gland and pancreas (Delgado, 2011). Some initial observations of VIP deficient mice were their stunted growth and impaired change in percent body fat, although this study only used male mice (Vu, 2015). Since mice lacking the VIP encoding gene exhibit impaired fat growth, they are potential models for obesity prevention and treatment; however, these mice display cardiomyopathy associated with the upregulation of genes related to heart failure (Szema, 2013), thus questioning the overall health of these lean mice.

Knowing that health risks can arise from an inability to expand adipose poses the question of whether the low body fat and cardiomyopathy profile of VIP deficient mice is rooted in cellular signals controlling their adipose expansion. It is interesting to see a mouse with low body fat display a risk for heart disease; however, this phenomenon also presents in lean caveolin-1 deficient mice displaying adipocyte hypertrophy and cardiomyopathy (Zhao, 2002). Assessing VIP deficient mice for adipocyte hypertrophy, FFA metabolism, and beiging capacity parameters will address the question of whether their low body fat profiles are desirable or a result of impaired adipose expandability, posing a risk for metabolic disease. Additionally, this information may help determine whether VIP inhibiting drugs might increase the risk for adipose dysfunction and present VIP as a candidate gene for metabolic disease rise.

2.3. Results

2.3.1. Hypertrophy Indicates Impaired Adipose Expansion in Male VIP Deficient Mice

To assess the subcutaneous adipose expandability of VIP deficient mice, we obtained cross-sections of a fat pad known as the posterior subcutaneous white adipose tissue (pscWAT) that can also be split into subdepots inguinal (iWAT) and dorsolumbar (dWAT) (**Figure 2.7**).

Under the histological analysis of the pscWAT at 25.2x, we observed larger cells in male VIP deficient mice (**Figure 2.1F**). Cell area was quantified using ImageJ and AdipoCount, showing larger mean adipocyte areas in male VIP deficient mice (**Figure 2.1G**), with a lower relative frequency of small cells between 20-120µm², higher frequency of large cells between 520-620µm² and 720-820µm² (**Figure 2.1D**). Interestingly, VIP deficiency in female mice did not manifest similar trends (**Figure 2.1A-C**). Further, male VIP deficient mice harbor the largest adipocyte areas (**Figure 2.1G**), which typically indicates cellular growth, but the smallest fat pad masses (**Figure 2.1H**), suggesting an impairment of adipogenesis. Since hypertrophic adipocytes are associated with larger fat pads in obese mice (Hammarstedt, 2018) or smaller pads of the HSL deficient mouse (Osuga, 2000) and Adipose-specific PPARγ deficient mice (He, 2003), the VIP deficient males may also be models for lean adipocyte hypertrophy. To determine whether these hypertrophic adipocytes manifested from impaired hydrolysis of cellular lipid content, similar to mechanisms seen in HSL KO mice (Shen, 2011), we measured serum FFAs glycerol (**Figure 2.2**).
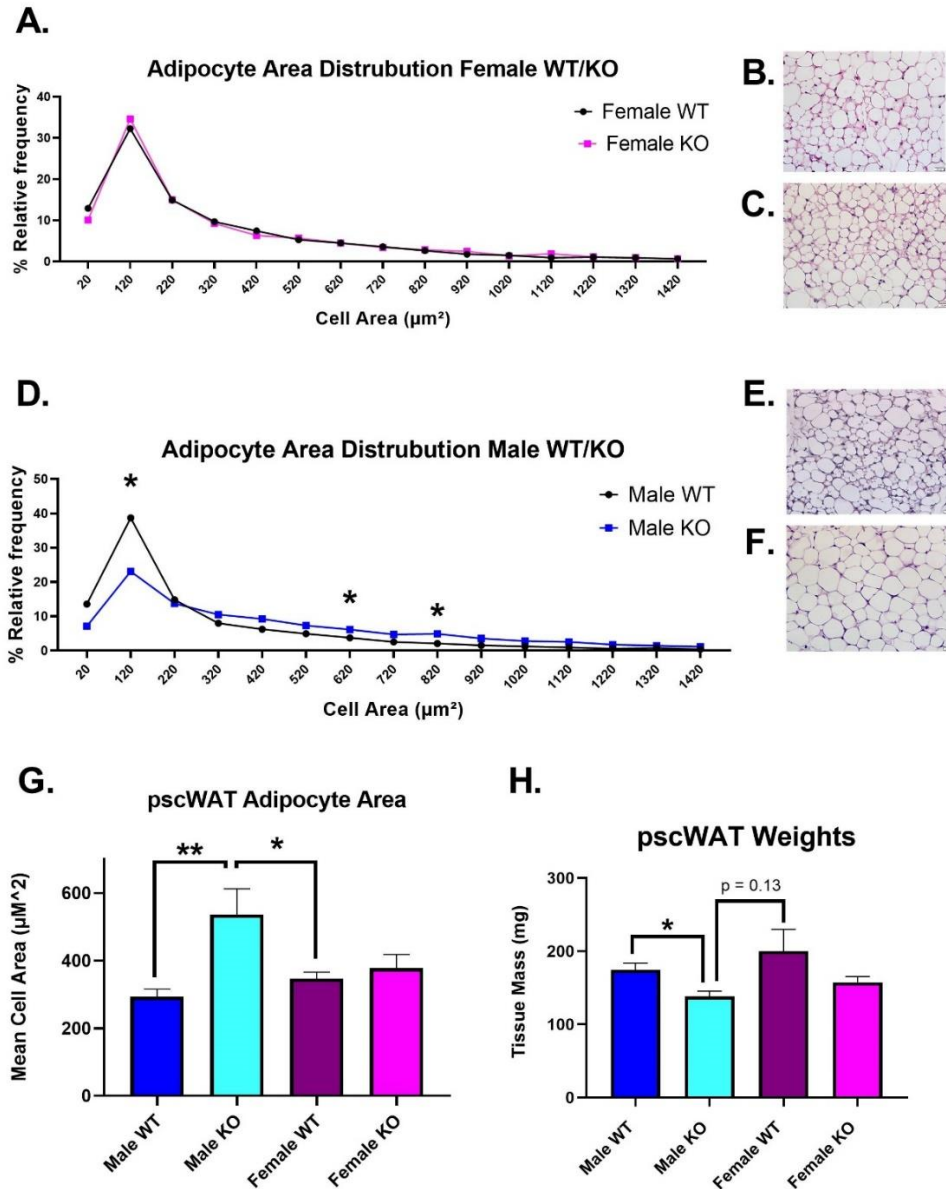
Figure 2.1. Hypertrophic Adipocytes Without Increased Fat Mass in Male VIP KO Mice. The frequency distribution of cells in random microscopy fields was enumerated in WT or KO groups in **A.** Female and **D**. Male. H&E-stained cross-sections of the pscWAT in **B.** Female WT, **C.** Female KO **E.** Male WT and **F.** Male KO. **G.** Mean cell area amongst groups. Male WT (n=4), Male KO (n=6), Female WT (n=4) ,and Female KO (n=4). **H**. pscWAT weight normalized to whole body weight at 8 weeks old. Female KO (n=4), all other groups (n=5). Bars represent mean +/- SEM * P<0.05 **P<0.01 *** P<0.001 ****P<0.0001. All images are magnified at 25.2x (scale bars = 20 µm).

2.3.2. Male VIP Deficient Mice Present Impaired Free Fatty Acid Metabolism

Impaired lipolysis can result in hypertrophic adipocytes (Osuga, 2000), and hypertrophic adipocytes resulting from hypoplasia can also experience higher levels of lipolysis (Li, 2022). To assess the state of fatty acid metabolism in VIP deficient mice, we measured serum FFAs and glycerol. Following similar trends to the hypertrophy data, sera FFAs were significantly lower in male, but not female, VIP deficient mice when compared to their WT littermates (**Figure 2.2A-B**). Male WT mice also had higher FFAs than female mice, although this sex difference is expected in C57B/L6 mice (Foryst-Ludwig, 2011). In contrast to finding decreased FFAs, glycerol content was independent of sex or genotype, with no statistically significant differences between groups (**Figure 2.2C-D**).

Additionally, glucose levels were unaffected by mouse genotype or sex (**Figure 2.2E**). There are inconsistencies in the literature regarding glucose homeostasis in VIP deficient mice, whereby one study found elevated glucose with a 3-fold increase in insulin (Martin et al., 2010). In stark contrast, another study saw no change in insulin levels but did not measure blood glucose (Vu et al., 2015). Here we report no change in glucose; however, it should be noted that serum was collected using the cheek puncture method, which is known to manifest higher glucose values in the range of 200-300 mg/dL (Fernández et al., 2010); thus there is a possibility that subtle changes in blood glucose would go unseen using this method of blood collection. A better analysis of glucose homeostasis would be to obtain blood from tail nicks, as this does not require the same level of mouse handling.

Glycerol may be utilized for glycerol-3-phosphatase oxidation or gluconeogenic pathways (Rotondo, 2017) and hiding the expected decrease in glycerol levels to match FFAs. In the fasted state, glycerol released by adipocytes can contribute 38-79% of circulating glucose,

causing hyperglycemia in obese individuals due to elevated lipolysis (Bortz, 1972). However, glucose levels were not different in the male VIP deficient group (Figure 2E), lending support to an impairment of FFA utilization only.

Analysis of blood metabolites shows a sex-specific disruption in fatty acid metabolism of VIP deficient male mice. Since serum FFAs are also disrupted in HSL and PPARγ deficient mice (Shen, 2011)(Semple, 2006), we suspected that VIP deficiency might impact the regulation of these genes to produce the same hypertrophic phenotype. Since HSL mediates lipolysis and PPARγ regulates adipogenesis, we hypothesized that they might play a role in the male VIP deficient mice developing hypertrophy and impaired FFA metabolism.
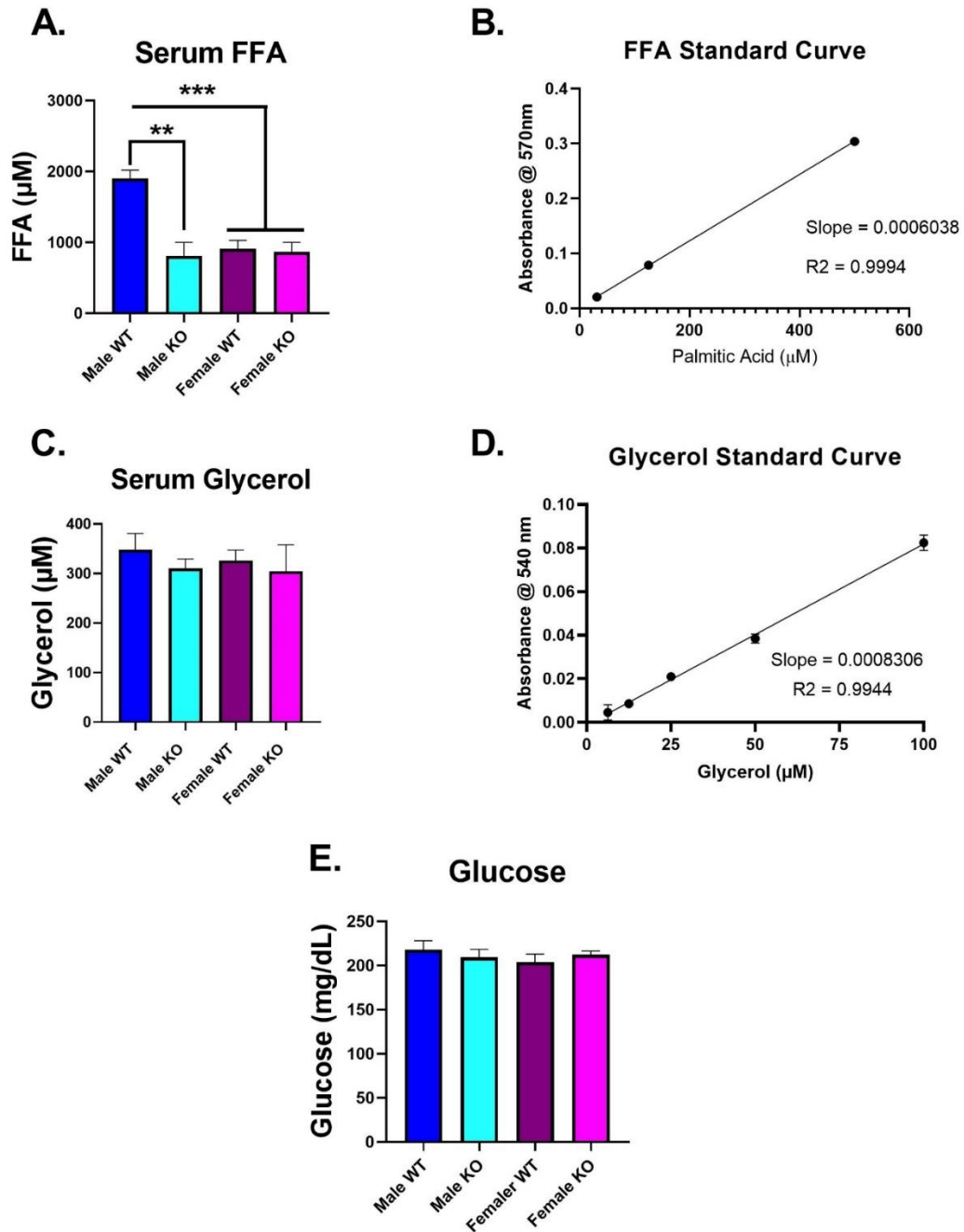
Figure 2.2. Reduced Serum FFAs, but not Glycerol or Glucose in Male VIP KO Mice.
A-B. FFA levels of male and female mice. Male KO (n=7) & all other groups (n=8). **C-D.**
Glycerol levels of male and female mice. Male WT (n=5), Male KO (n=4), Female WT (n=6)
and Female KO (n=4). **E.** Mean blood glucose concentration in male WT (n=7) & all other
groups (n=8). All mice are 8 weeks old. Bars represent mean +/- SEM. * P<0.05, **P<0.01, ***
P<0.001, ****P<0.0001.

2.3.3. Suppressed mRNA Expression of Adipogenic Markers, but not HSL Suggests Impaired Beige Adipogenesis in Male VIP KO

To assess the pscWAT for molecular expression patterns resembling impaired adipose expandability, we quantified the relative expression of PPARγ, TMEM26, and leptin to address adipogenesis; and HSL to investigate lipolysis. The pscWAT can also be sub-divided into the iWAT and dWAT, which can often reduce the heterogeneity of samples as the iWAT contains the inguinal lymph node and is more prone to UCP1 beige thermogenesis (Chi et al., 2018). The mRNA expression of the beige preadipocyte marker known as TMEM26 was significantly downregulated 3.8-fold in the iWAT of male VIP deficient mice (**Figure 2.3**), although measured values in KOs were below detectability and potentially underestimated. There was also a trending decrease in PPARγ expression within the iWAT(p=0.0635) and dWAT (p=0.1143) of male VIP deficient mice (**Figure 2.3**). While leptin expression was relatively similar between the iWAT and dWAT of WT mice, VIP KO males displayed a 3.27-fold decrease in the iWAT versus dWAT (**Figure 2.3**), which further supports an adipogenic defect in this region of the mice.

Interestingly, no statistically significant changes were observed in female mice, although the low expression of TMEM26 makes it hard to rule out any undetectable changes (**Figure 2.4**). There was no difference in the mRNA expression of HSL in the iWAT or dWAT of male and female VIP deficient mice (**Figures 2.3 and 2.4**). The pscWAT depot does not typically express brown adipocytes (Garcia, 2016); however, we were curious if VIP deficiency disrupted patterns of brown adipocyte recruitment. The BAT marker ZIC1 was close to or below the LOD for all groups (**Figures 2.3 and 2.4**); thus, the absence of brown adipocyte gene expression in the pscWAT appears unaffected by VIP at the mRNA level.
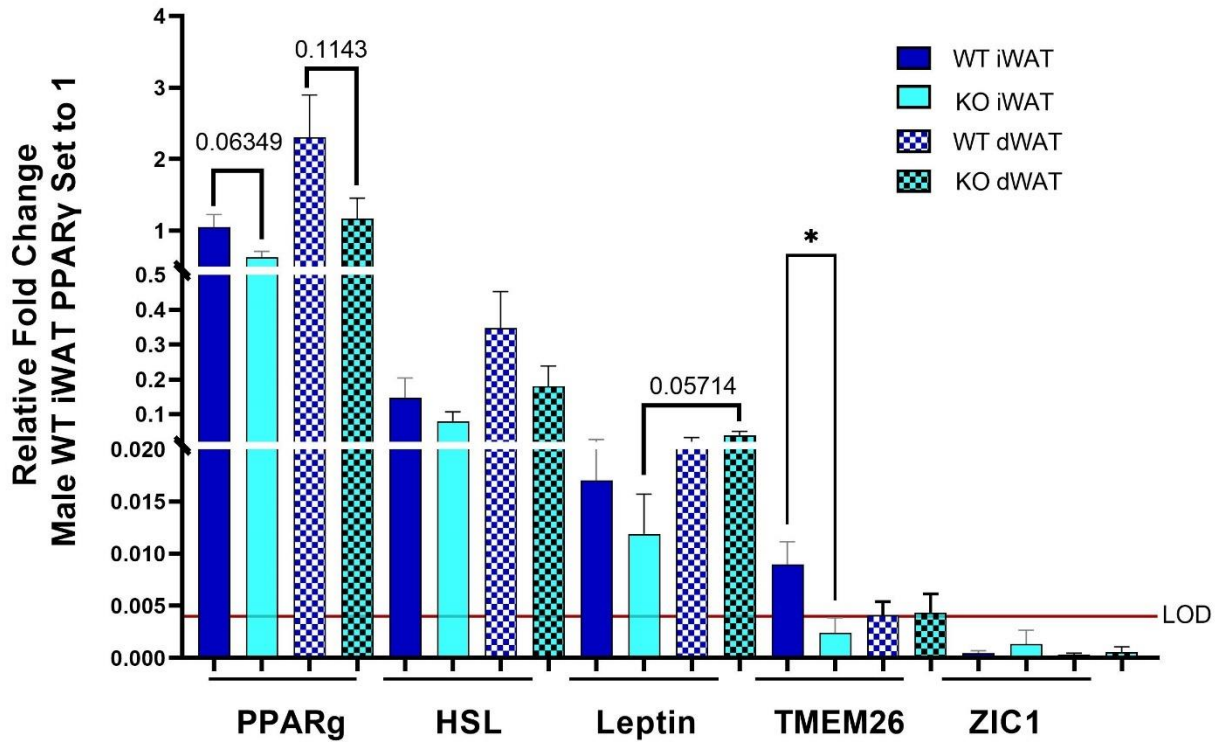
Figure 2.3. Decreased Relative mRNA Expression of TMEM26 in Male VIP KO iWAT. Male mice relative mRNA expression of PPARγ, HSL, Leptin, TMEM26, and ZIC1. Male WT iWAT PPARγ set to 1. Genes normalized to beta-actin, PPIA, and RPL19. All mice are eight weeks old. Values are represented as a fold change when WT is set to 1. WT iWAT (n=5). All other groups (n=4). Bars represent mean +/- SEM. * P<0.05 **P<0.01 *** P<0.001 ****P<0.0001. The Y-axis line represents the Limit of Detection (LOD).
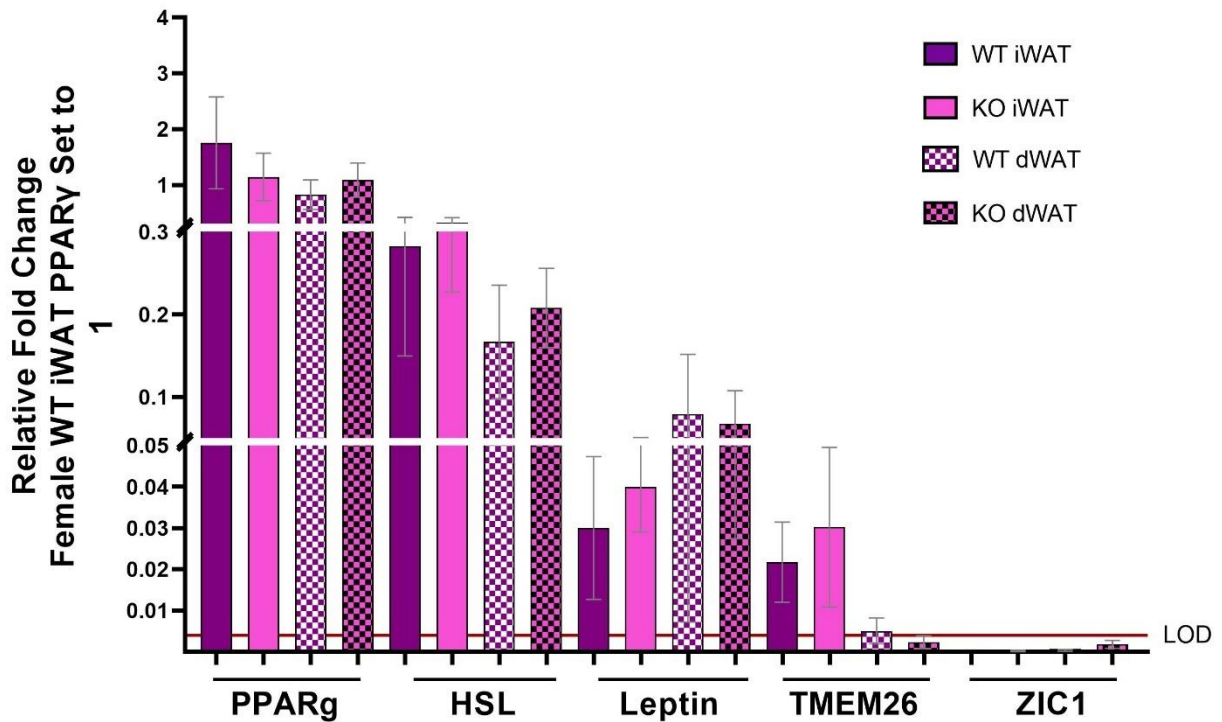
Figure 2.4. Trends in Relative mRNA Expression of Female VIP KO/WT iWAT and dWAT. Female mice relative mRNA Expression of PPARγ, HSL, Leptin, TMEM26, and ZIC1. Female WT iWAT PPARγ set to 1. Genes normalized to beta actin, PPIA, and RPL19. Female VIP KO and WT mice were separated by subdepots iWAT and dWAT. All mice are eight weeks old. Values are represented as a fold change with WT set to 1.WT groups (n=4) and KO groups (n=5). Bars represent mean +/- SEM. * P<0.05 **P<0.01 *** P<0.001 ****P<0.0001. The Y-axis line represents the Limit of Detection (LOD).

2.3.4. Sex Differences in mRNA Expression of TMEM26 in Subcutaneous Adipose

The sex differences in gene expression are interesting but expected as there are 708 genes differentially regulated in this depot based on sex in mice placed on a HFD (Grove, 2010). There was a 23.2-Fold decrease in the expression of TMEM26 in the dWAT of females compared to male WT mice and a similar trend in the iWAT (**Figure 2.5**). We suspect that estrogen could be driving these sex differences since it influences lipolysis in the subcutaneous depot (Chang, 2018). Additionally, estrogen treatment can inhibit PPARγ gene expression in subcutaneous

adipose tissue of human subjects (Lundholm, 2008), although this seems to contradict the notion

that females have a greater capacity for subcutaneous adipose expandability.
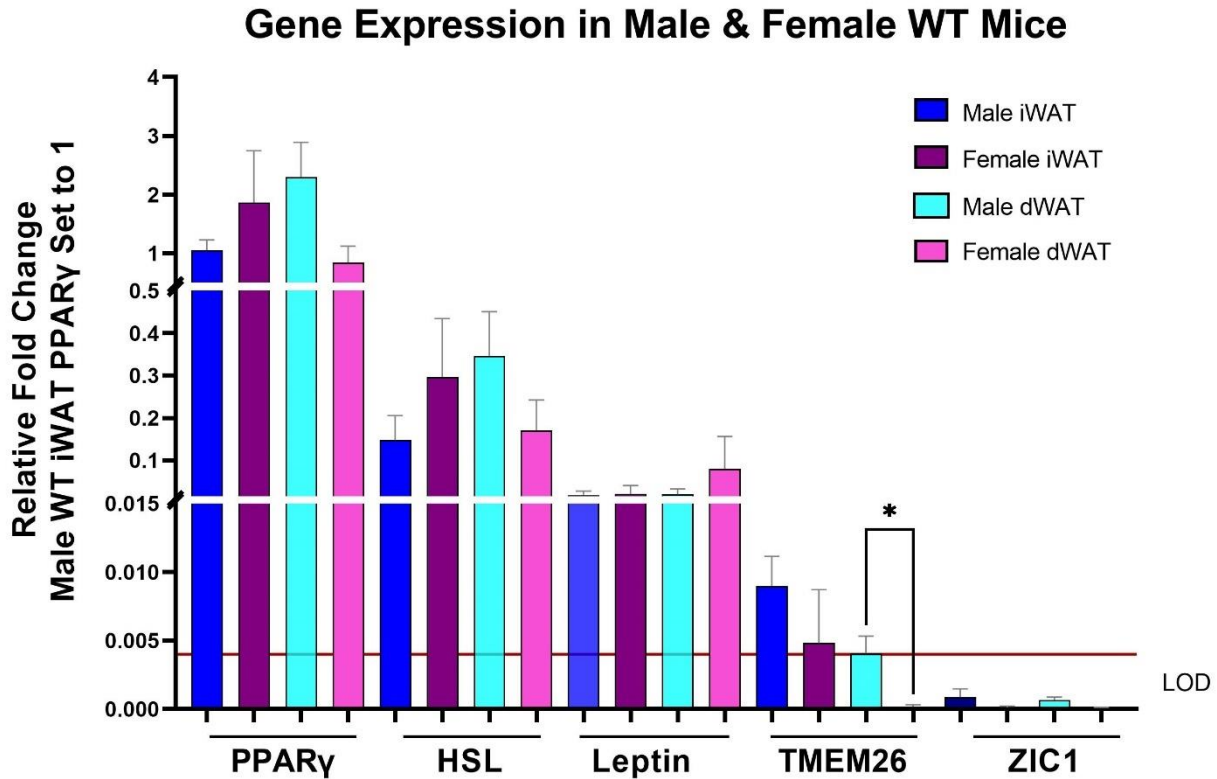
Figure 2.5. Sex Differences in dWAT TMEM26 Expression of WT Mice.
Male and Female wild-type mice relative mRNA Expression of ZIC1, Leptin, TMEM26, HSL,
and PPARγ. All mice are eight weeks old. Values are represented as a fold change with male
WT iWAT Leptin set to 1. Male WT iWAT (n=5) and all other groups (n=4). Bars represent
mean +/- SEM. * $P<0.05$ **$P<0.01$ *** $P<0.001$ ****$P<0.00$. The Y-axis line represents the
Limit of Detection (LOD).

2.3.5. A Potential Explanation for Sexual Dimorphisms in VIP KO Mouse Adipose

We are unsure why VIP deficiency induced changes in relative mRNA expression, serum

FFA levels, and adipocyte morphology in male but not female mice. Since we based our

investigation upon the observation that VIP deficient male mice have stunted body growth (Vu,

2015), we were curious whether females exhibited the same trend. To determine the necessity of

VIP for mouse body weight homeostasis, we measured body mass in both male and female VIP

WT/KO mice at 4, 8, and 12 weeks of age. Our results show that both male and female VIP deficient mice significantly decreased body weights at 4 and 8 weeks old **(Figure 2.6A-B)**. Interestingly, female KOs appeared to catch up in body weight at 12 weeks, whereas male VIP KOs maintained a lean phenotype. Although weights of the pscWAT would better show adipose expandability at 12 weeks, we suspect the female mice may catch up due to enhanced subcutaneous expandability.

A.   **B.**
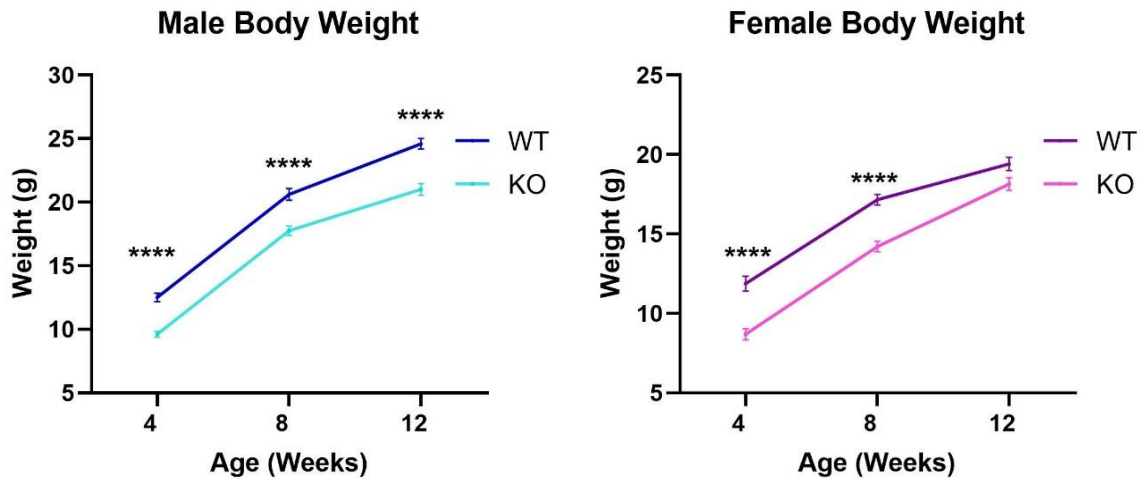
Figure 2.6. Female VIP Deficient Mice Catch up in Weight at 12 Weeks.
Two-way ANOVA of whole-body weights taken at 4, 8, and 12 weeks old in **A**. Male WT vs Male KO (n=12-29) and **B.** Female WT vs KO (n=16-25). Bars represent mean +/- SEM. Adjusted p-values: * $P<0.05$ **$P<0.01$ *** $P<0.001$ ****$P<0.00$.

2.4. Discussion

We have assessed the posterior subcutaneous fat pad of VIP deficient mice for adipose expandability by identifying 1) adipocyte hypertrophy, 2) impaired fatty acid metabolism, and 3) stunted capacity for tissue 'beiging.' Our results suggest these three characteristics are present in the male VIP deficient mice, but surprisingly absent in females, which contributes to the understanding of sex differences in adipose tissue function.

A larger mean cell area (**Figure 2.1G**) along with a decreased relative frequency of smaller adipocytes (**Figure 2.1D**) in male VIP deficient mice would predict the tissue is attempting to expand via hypertrophy. Interestingly, this form of cellular growth did not facilitate tissue growth (**Figure 2.1H**), a phenomenon denoted as 'impaired adipose expansion' and seen in HSL and PPARγ deficient mice (Osuga, 2000)(He, 2003). Hypertrophy is associated with impaired gene expression of adipogenic markers (Gustafson, 2019), whereby existing cells must store excessive lipids and cause larger adipocytes. We observed suppression of the adipogenic regulator PPARγ and white/beige adipocyte markers leptin and TMEM26, which further demonstrate impaired adipogenesis that may lead to hypertrophy of the iWAT. Because TMEM26 expression was suppressed below the detection limit, this fold change may be underestimated (**Figure 2.3**). An alternative explanation for the decrease in TMEM26+ beige preadipocytes could be enhanced thermogenesis, as this marker disappears after beige activation (Lee et al., 2015), although this is unlikely considering the histological findings (**Figure 2.1D**). Confirming TMEM26 dysregulation could be verified through mRNA sequencing or digital PCR, which can detect smaller quantities of expressed mRNA (Taylor, 2017).

Congruent with a study showing enhanced beiging capacity in the iWAT compared to dWAT (Chi et al., 2018), trends in the TMEM26 beige preadipocyte marker expression were higher in the iWAT than dWAT of both male and female WT mice (**Figure 2.5**). A lack of this beige marker in the iWAT of male VIP deficient mice suggests this depot will have impaired thermogenesis following cold exposure. We conducted our analyses in mice maintained at room temperature (20°C), which could serve as a baseline for a future cold exposure experiment with these mice. Challenging the VIP deficient mice to norepinephrine could also simulate the effect of cold-induced sympathetic activation of the pscWAT depot (Spiegelman, 2013).

We have shown that VIP deficient males have lower levels of FFAs in serum (**Figure 2.2A**). Interestingly, HSL deficient mice also present decreased circulating FFAs, but serum glycerol is also reduced (Shen, 2011), indicating HSL activity may not be the culprit of VIP deficient male adipocyte hypertrophy. HSL mRNA expression was also unchanged, which further decreased the likeliness of its dysregulation. Another potential explanation for the decreased FFAs is impaired intestinal absorption, which may not change the serum levels of glycerol. Further, a study describes VIP's ability to modify lipid absorption via the FAPB2 lipid transporter on epithelial enterocytes (Talbot, 2020).

Additionally, there is a link between intestinal FFA malabsorption and impaired adipogenesis in CD36 deficient mice (Christiaens, 2012)(Drover, 2005), thus warranting a connection between our detection of FFA and adipogenic gene defects in male KOs. The relationships between circulating FFAs and adipogenesis are developing; however, since FFA can function as ligands to PPARγ (Shen, 2011), decreased serum FFAs in VIP deficient males may drive impaired adipogenesis. Since PPARγ is a member of the retinoic acid receptor family (RXR), it is unsurprising that retinoid treatment potentiates PPARγ activity by increasing gene expression and lipid uptake (Szanto, 2005). Interestingly, there is blunted retinoic acid delivery by dendritic cells in VIP deficient intestinal tissue (Yu, 2021), which could impact the surrounding adipose tissue if also true in the inguinal lymph node. Treg recruitment to the inguinal lymph node is dysfunctional in female VIP deficient mice (Gallino, 2020), demonstrating a need to investigate the dendric cells and their function on inguinal adipogenesis.

We have shown that male, but not female, VIP deficient mice harbor hypertrophic adipocytes without tissue expansion, possibly attributed to decreased mRNA expression of the

adipogenic genes and impaired fatty acid metabolism. These findings suggest that VIP is necessary for sex-specific subcutaneous adipocyte function.

2.5. Conclusion

We have identified a subcutaneous depot of male VIP deficient mice exhibiting hypertrophic adipocytes without tissue growth and fewer beige TMEM26^{+} preadipocytes, both characteristics of impaired adipose expandability. These observations are typically associated with obesity when fat pads have overgrown; however, these mice are leaner and thus challenge that correlation. We conclude that VIP may play an underlying role in sex-specific functions that affect adipose expandability characteristics, which helps disentangle the metabolic pathways influencing sex differences in subcutaneous adipose biology. Additionally, we have shown that male, but not female VIP deficient mice manifest lower levels of circulating FFAs, which we suspect is a result of intestinal absorption, although sex-difference have yet to be explained. It is possible that the low availability of FFAs, which are precursors to the PPARγ ligands, are responsible for adipose dysfunction in males. We conclude that male VIP deficient mice are potential models of impaired subcutaneous adipose expansion and fatty acid metabolism. Additionally, we predict that their pscWAT will experience less growth during an energy surplus treatment such as HFD and experience tissue inflammation that may induce metabolic diseases such as T2D and heart disease.

2.6. Materials & Methods

2.6.1. Animals

VIP heterozygous breeders of C57BL/6 background were gifted by Professor James Waschek (Colwell et al. 2003) from the University of California, Los Angeles. Harem breeding of HET parents was conducted at North Dakota State University, and research was approved by

the NDSU Institutional Animal Care and Use Committee. Mice were cohoused with littermates

in polycarbonate cages (13.5" L x 11.5" W x 6.1" H; 75 square inches) with Alpha-Dri paper

bedding (Animal Care Systems, Centennial, CO), access to tap water and a 5001 LabDiet mouse

chow (St. Louis, MO, US) *ad libitum* with a 12-hour light/dark cycle. Mice were weaned at 4

weeks of age and placed in cages with same-sex littermates. Tail biopsies were collected during

weaning for PCR genotyping. Tissue harvest was taken at 8 weeks of age and mice were fasted

for 3 hours prior to carbon dioxide euthanasia and tissue collection. Tissues were always taken

between 1-3pm.

2.6.2. Genotyping by Polymerase Chain Reaction (PCR)

Tail biopsies obtained from mice at 4 weeks old were transported on ice and stored at -

20°C until assayed. Briefly, biopsies were submerged in 40 µL of DNA extraction solution

(Sigma Aldrich, Catalogue #E7526) and 10 µL of Tissue Prep (Sigma Aldrich, Catalogue

#T3073) for 20-120 minutes at RT. Samples were incubated at 95°C for 4 minutes, followed by

the addition of 40 µL neutralization buffer (Sigma Aldrich, Catalogue #N3910). Samples were

vortexed for 30 seconds and 1/20 dilutions were made using 1X TE buffer (100 mM Tris pH 7.4,

10 mM EDTA pH 8.0). PCR was carried out immediately or refrigerated at 4°C until DNA

extracts were assayed. Primers Sequences in **Table 2.1** were used in the making of a master mix

containing final concentrations in a 20 µL total volume: 312.5 nM forward and reverse VIP

primers (International DNA Technologies, Coralville, IA), 1X G2 GoTaq master mix (Promega,

Catalogue #M7823) and 2 µL of 1/20 diluted DNA extracts. Samples were placed into a 2720

Applied Biosystems thermocycler (Themo Fisher Scientific, Waltham, MA) under the following

parameters: 94°C for 5 min→ 94°C for 15min → 62°C for 45min→ 72°C for 45min→ Repeat a

total 40 cycles→ 72°C for 1min → 4°C indefinitely. PCR products were separated on a 1.5%

agarose gel and visualized with DNA EZ-Vision (VWR, Cat. # 97064-190) under UV light.

Table 2.1. Mouse Genotype Primer Sequences.

Allele	Primer Type	Primer Sequence
WT	Forward (V1)	5'- TTTCAAGGTGTGGGGCTAGAGACATACA - 3'
WT & KO	Common Reverse (V2)	5'- TTACCTGATTCGTTTGCCAATGAGTGAC - 3'
KO	Forward (N1)	5'- GCCCGGAGATGAGGAAGAGGAGAACAG - 3'

Primer Sequences were used to interrogate the presence of the WT and KO allele by PCR.

2.6.3. Tissue Isolation

The entire pscWAT and its subdepots, known as the inguinal white adipose tissue

(iWAT) and dorsolumbar white adipose tissue (dWAT), were isolated according to a universal

isolation protocol (Bagchi & MacDougald, 2019). Briefly, the skin was peeled back from the

peritoneal cavity behind the leg to locate the pscWAT, where the entire depot was excised. For

separation of the dorsolumbar subdepot (dWAT), the tissue was cut just above the lymph node

on the side proximal to the lumbar spine. The inguinal subdepot (iWAT) included the lymph

node and remaining tissue. A visual representation of this process is presented in **Figure 2.7**.
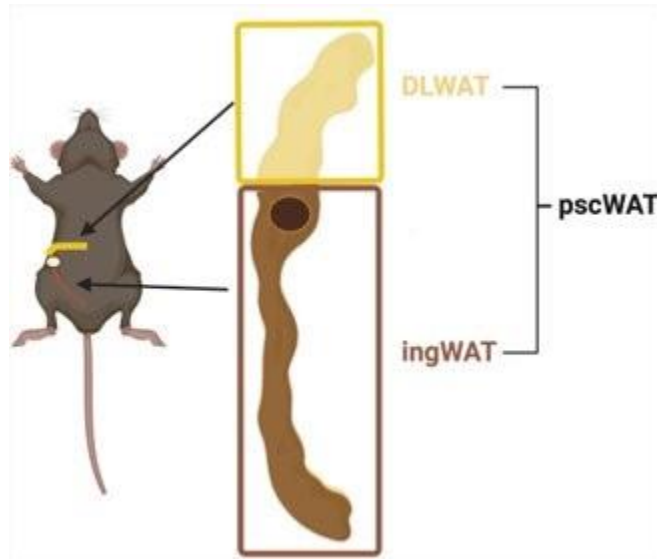
Figure 2.7. Anatomical Separation of the pscWAT and its Subdepots.
The pscWAT can be split into two regions: the dorsolumbar (dWAT) and the inguinal (iWAT) depots.

2.6.4. Microscopy Imaging

The entire pscWAT was fixed in 10% neutral buffered formalin for up to 48 hours and then placed in 70% ethanol until being embedded in paraffin. 5 μm thick slides were prepared for H&E staining. Random sections were viewed at 25.2x using an Olympus BX53 microscope (Tokyo, Japan), although care was taken to avoid blood vessels and damaged cells. Images were taken using an Olympus DP74 camera and CellSens Dimension Software (Tokyo, Japan). Multiple images (e.g. 6-10) were taken at random for each slide.

2.6.5. Adipocyte Cellular Area Measurements

The area of each cell was measured according to procedures previously described (Hu et al., 2021), and tutorial videos provided in the supplementary figures were followed. Images were segmented using AdipoCount 2.0 software, followed by calibration and cell area measurement using ImageJ 1.52a. Briefly, ImageJ was calibrated using an automated scale bar presented on the image by the microscope camera. Thresholds were set at max and 52. Cells on the border

46

were excluded. Cellular shapes were analyzed between 50-15000 μm^2 with circularity between 0-1.

2.6.6. Serum Collection

Food was removed from mouse cages, starting between 10-11 am, and mice were fasted for 2 hours with access to water ad libitum, followed by blood collection between 2-3 pm. Mice were restrained using a scruff holding technique and a submandibular cheek puncture was conducted using a sterile 5.5 mm lancet. Blood was collected in 1.5 ml vials and allowed to coagulate at room temperature for 30 min - 1 hour. Collection tubes were centrifuged at 2200 x g and the serum supernatants were removed and frozen at -80°C for up to 1 year before assaying.

2.6.7. Biochemical Assays

Glucose was directly measured from the cheek after puncture using a Clarity BG1000 blood glucose meter. Each mouse's glucose was tested once. Serum FFAs were measured using a colorimetric assay kit (Cell Biolabs; Catalogue # STA-618). Serum glycerol was measured using a colorimetric assay kit (Cell Biolabs; Catalogue # STA-398). Both the FFA & glycerol kit components were aliquoted and stored at -80°C for one week before use. All reagents were placed on ice during procedure and no aliquots underwent a freeze thaw. Samples were diluted using assay buffer provided in the kit and each sample dilution was optimized so that absorbance values fell within the standard curve for each kit. All measurements included in the analysis were conducted using the same master mix preparations. Biological replicates were initially tested in triplicate to assess replicability, after which they were only tested in duplicate. Reactions were carried out on a 96 well plate (Cole-Parmer Instrument Company; Catalogue #EW-01959-22) and colorimetric absorption was taken at 570 nm using Gen5 plate reader software (version 3.05) (Agilent Technologies. Santa Clara, CA).
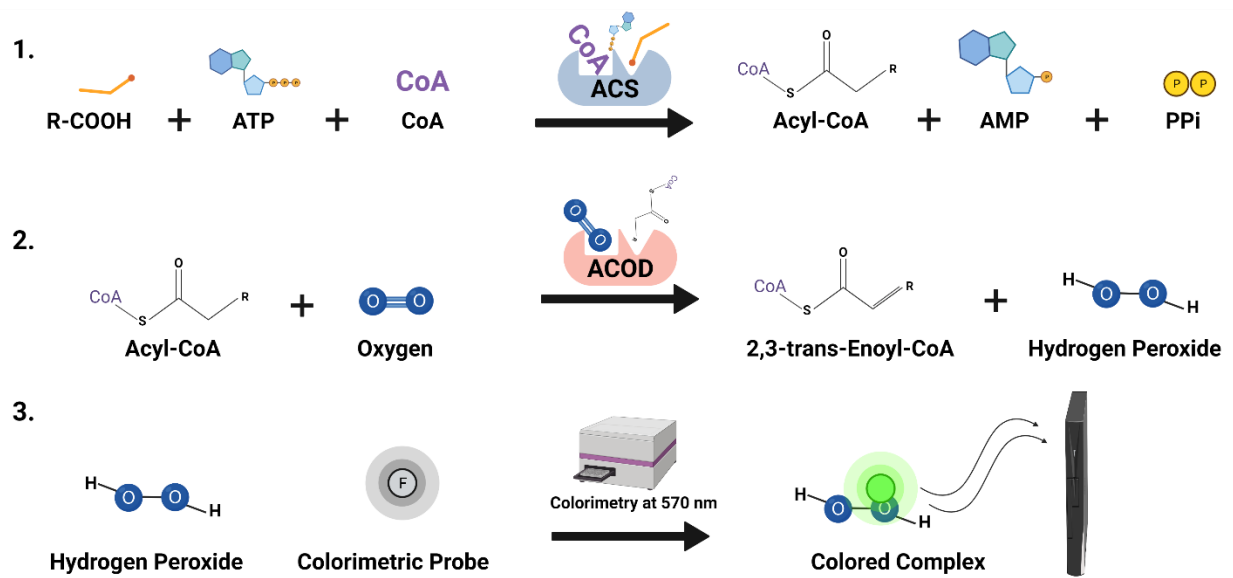
Figure 2.8. Three Step Reaction Conditions Within a Sample Tested on the Colorimetric FFA Assay.
Step 1: Substrates included sample free fatty acids (R-COOH), adenosine triphosphate (ATP) and Coenzyme A (CoA). The enzyme Acyl CoA Synthetase (ACS) produced the products acyl CoA, adenosine monophosphate (AMP), pyrophosphate (PPi). **Step 2:** Substrates Acyl CoA and atmospheric oxygen were processed by the enzyme Acyl CoA Oxidase (ACOS) to synthesize hydrogen peroxide and 2,3-trans-Enoyl-CoA. **Step 3:** Hydrogen peroxide was combined with a colorimetric probe and placed into a plate reader which absorbs light at 570 nm. Absorbance reading was directly proportional to starting FFA concentration of each sample.

2.6.8. RNA Extraction and cDNA Synthesis

The minimum information for publication of quantitative real time PCR experiments (MIQE) were adhered in the design of this study (Bustin et al., 2009). RNA was extracted using the Qiagen Universal mini-RNA extraction Kit (Catalogue #73404). The NanoDrop™ one-C was used for RNA quantification and purity assessment using 260/280, where all sample values fell between 1.99-2.17. RNA integrity was analyzed using a Qubit 4 fluorometer and samples with an IQ>6.2 considered acceptable. All samples were treated with DNase I & 10x Reaction Buffer with MgCl2 (Thermo Fischer Scientific: EN0521; B42). DNase parameters: 30-minute DNase I treatment at 37°C, 10 mn deactivation at 70°C with EDTA. A range between 0.75-1μg of template RNA was used for each sample, except for the synthesis of epididymal WAT cDNA,

where 2 µg were used during primer optimization. cDNA synthesis was carried out using the

Solis Biodyne FIREScript RT cDNA synthesis kit (#06-15-00050): FIREScript RT (200U/µl),

RiboGrip RNase inhibitor, dNTP MIX, 100µM Oligo dT and Random primers (1:1), Buffer (500

mM Tris-HCl pH 8.3, 500 mM KCl, 30 mM MgCl2, 100 mM DTT). Reverse transcription

temperature and time was carried out according to the manufacturer's protocol (DS-08-36 v3):

25°C for 5-10 min, 37-60°C for 15-30 min, 85°C for 5 min. All cDNA products were diluted

1:10 before use with 1X TE pH 8.0.

2.6.9. qPCR

Plate wells were prepared according to the manufacturer's protocol: 1X HOT FIREPol

Evagreen qPCR Supermix (08-36-0000S), ddH2O, F&R primers (200 nmols of each) and 5 µL

of sample. Primer specifics are summarized in **Table 2.2**. PCR conditions for all primers were

identical and carried out as follows: 12-minute Hot Start activation at 95°C → (15 s denaturation

at 95°C → 30s annealing @ 60°C) x 40 cycles. Melt curve with 5 second intervals from 65-95

°C. The value of Cq was determined using the regression determination method of BioRad

CFX96 Manager 3.1 software. Efficiency curves were created for each primer set (**Figure 2.9**).

The reference genes had an M score ranking < 1.5 (**Figure 2.10C**), which is a cutoff value that

has been previously reported (Van Acker, 2019). Cq values less than 36 were considered above

'noise' and used for relative quantification using the $2^{-\Delta\Delta Cq}$ Livak Method, although Cq values

greater than 36 were graphed but considered below the limit of detection. Assays were

performed in duplicate. The percent coefficient of variation of intraassay controls were below

2.45% (**Figure 2.11**). NRT of each sample and NTC of each primer was assessed, whereby

linearized NRT product contributed < 0.38% and linearized NTC < 0.41% of total fluorescence

to the RT+ sample (**Equation 2.1-2.2**).

$$(2\wedge(\text{-Cq NRT}/(\text{-}2\wedge(\text{-Cq RT+}))) * 100 \qquad \text{(Eq. 2.1)}$$

$$(2\wedge(\text{-Cq NTC}/(\text{-}2\wedge(\text{-Cq RT+}))) * 100 \qquad \text{(Eq. 2.2)}$$

Gene	Primer Pair Sequence 5'->3'	Target Sequence Accession #	Source	Product Length (bps)	Efficiency	Slope	R2	Product MT °C	Exon-Exon Boundary (nt)
Leptin	F: GAGACCCCTGTGTCGGTTC R: ATGAAGTCCAAGCCAGTGACC	NM_008493.3	IDT Prime Time	180	93.9%	-3.47	0.990	84.5	2-3 (203/204)
TMEM26	F: TCACCCTCAAGTTCAAGCG R: GTTTCCATGGTGCATTTCAAG	NM_177794.3	IDT Prime Time	113	100.8%	-3.30	0.996	82.0	1-2 (345/346)
ZIC1	F: GTTTTCGCGCGTTCAGAGAA R: CCCTCGAACTCGCACTTGAA	NM_009573.4	IDT Prime Time	80	95.3%	-3.44	0.989	89.0	2-3 (1733/1734)
PPARγ	F:CTGCTCCACACTATGAAGACAT R: ATGCAGGTTCTACTTTGATCGC	NM_011146	IDT Prime Time	113	92.3%	-3.52	0.998	80.5	2-3 (355/356)
HSL	F: GGCGAAAAGGCAAGATCAAAG R: CCATATTGTCTTCTGCGAGTGT	NM_010719.5	IDT Prime Time	96	93.0%	-3.49	0.980	83.5	1-2 (487/488)
RPL19	F: CCATGAGTATGCTCAGGCTACAG R: CTGATCTGCTGACGGGAGTTG	NM_009078.2	Gray 2020	127	93.1%	-3.50	0.997	84.5	1-2 (67/68) & 2-3 (144/145)
PPIA	F: CGTCTCCTTCGAGCTGTTTGCAG R: GTCACCACCCTGGCACATG	NM_008907.2	Gray 2020	143	103.0%	-3.25	0.990	82.5	1-2 (113/114) & 3-4 (223/224)
Beta Actin	F: GCTCTGGCTCCTAGCACCAT R: GCCACCGATCCACACAGAGT	NM_007393.5	Gray 2020	75	96.1%	-3.42	0.990	83.0	5-6 (1093/1094)

Figure 2.9. *Mus musculus* Primer Specifics.
All primers were designed using NCBI Primer Design (Ye, 2012). Each row denotes a specific gene, F&R primer sequences (5'>3'), targeted sequence accession #, source of primer design, product length in base pairs (BP), percent efficiency, slope, R^2, MT in RT+ samples, and exon-exon boundary information.

A.

***Mus musculus* WT Primer Efficiency Curves**
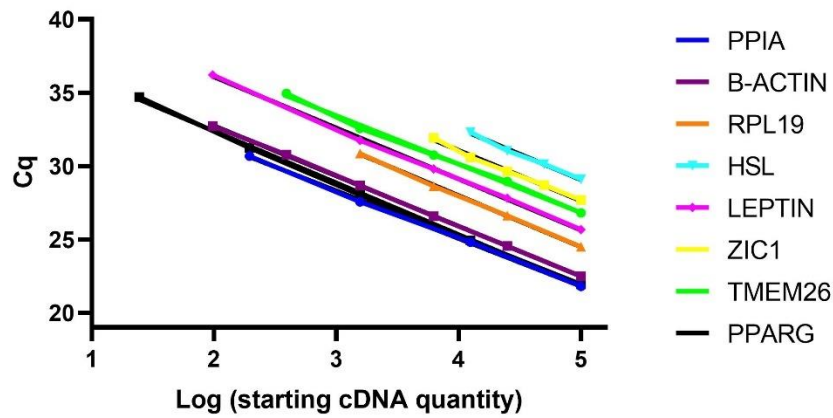
B.

***Mus musculus* KO vs WT Primer Efficiency Curves**
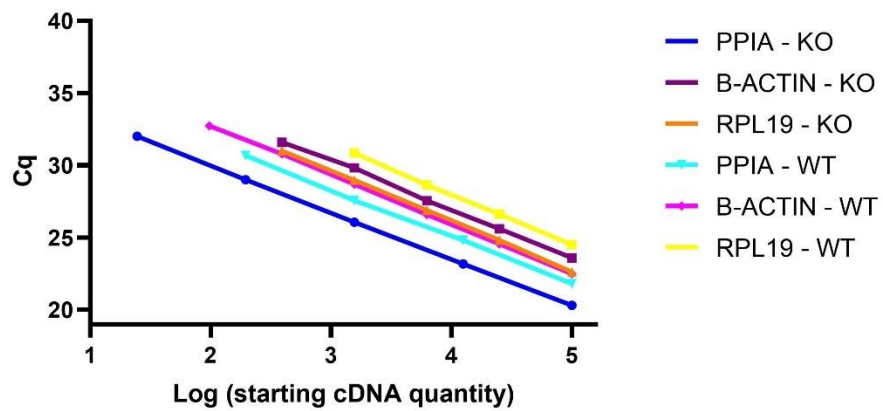
Figure 2.10. *Mus musculus* Primer Efficiency Curves.
Primer curves were made using **A.** WT mice and **B.** WT vs KO mice. Efficiencies were between 92-103%.
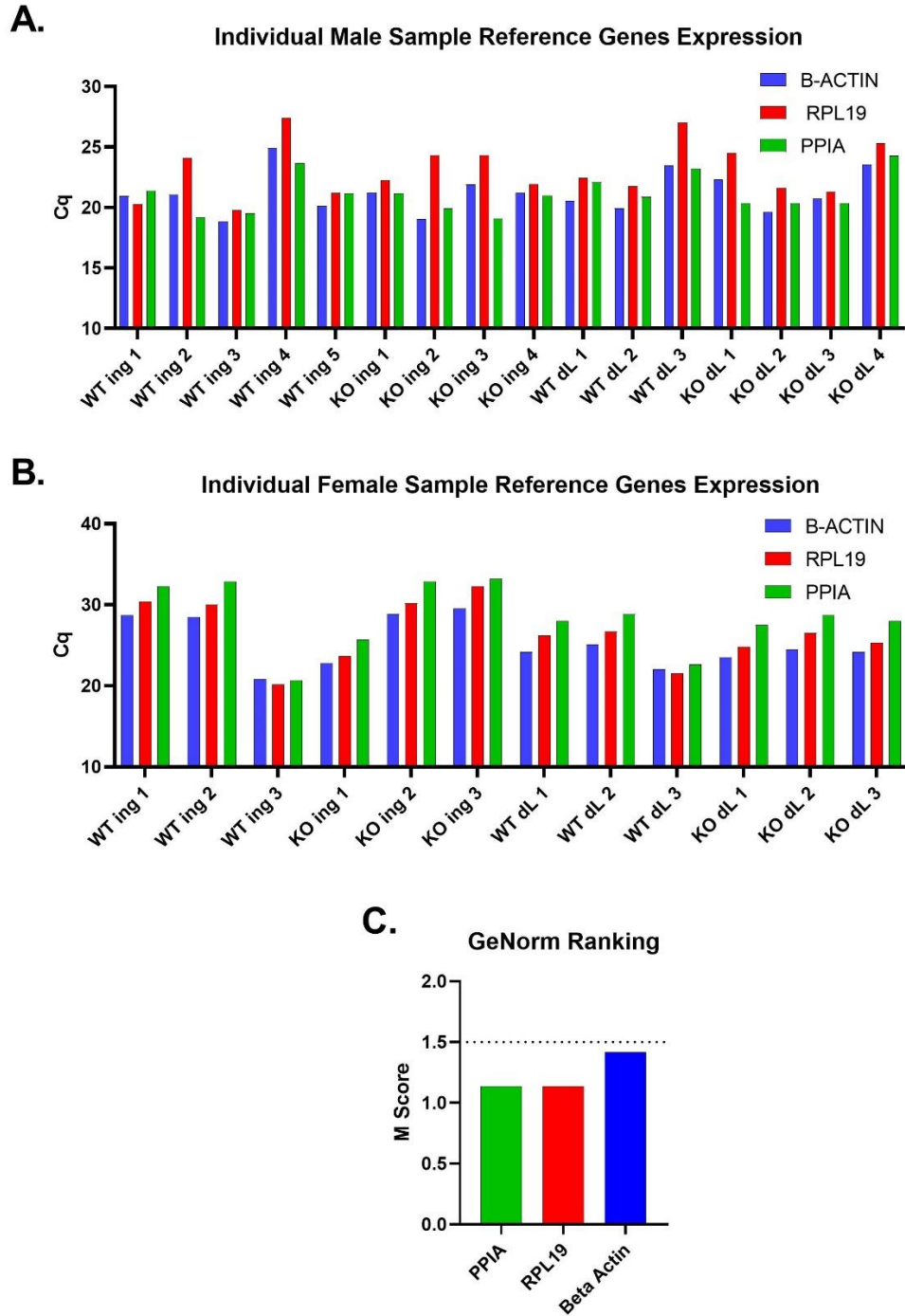
Figure 2.11. Reference Gene Stability Assessment Across Mouse Samples.
Average of technical replicates for each mouse in **A.** Males and **B.** Females. **C.** GeNorm ranking
M Score of reference genes PPIA, RPL19, and beta-actin in both male and female mice. Max
acceptable score of 1.5 is denoted by a dotted line.
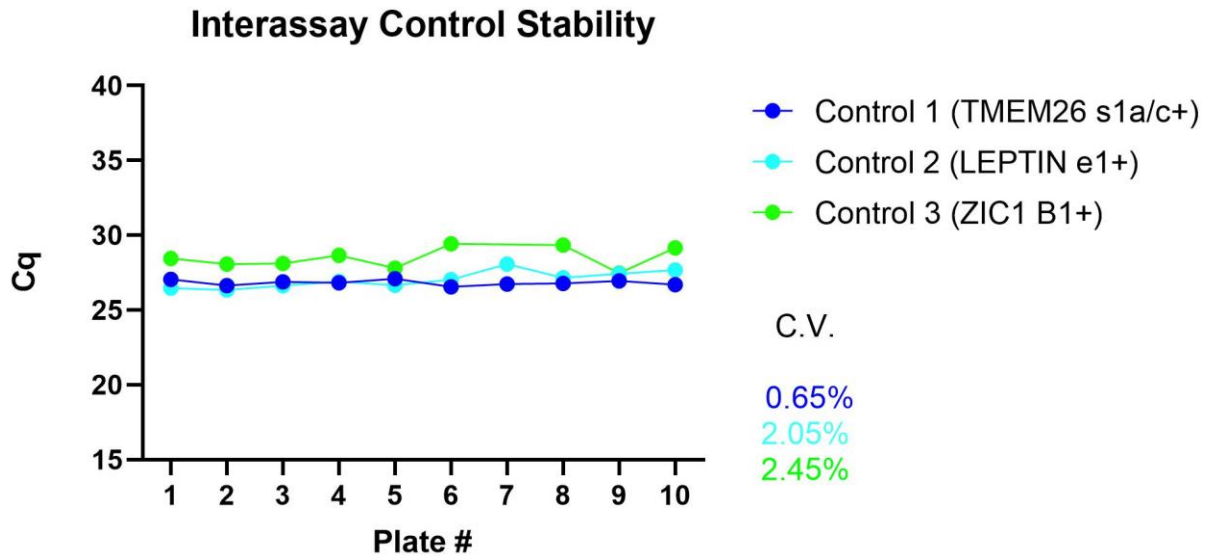
Figure 2.12. Coefficient of Variation Between Plates on Separate qPCR Runs. Inter-assay plate control trends with associated coefficient of variation (C.V.). Datapoints represent mean of technical replicates for each plate.

2.6.10. Statistical Analysis

Relative quantification was made using the Livak method (Livak & Schmittgen, 2001) and Bio-Rad qPCR data analysis (BioRadLifeScience, 2019). We first assessed each group for normal or lognormal (non-gaussian) distribution using graph pad normality testing. To correct for the reported lognormal distribution, we preformed Mann-Whitney tests (CI = 95%) on all cell morphological and tissue weight analyses. Weekly body weights were analyzed using a two-way ANOVA. All analyses were conducted using GraphPad Prism version 9.3.1 for Mac OS (GraphPad Software, San Diego, California USA, www.graphpad.com). Data are presented at a bar graph of the mean ± SEM. Only statistically significant values are indicated on bar graphs, such that: * $P<0.05$, **$P<0.01$, *** $P<0.001$ ****$P<0.0001$. Comparisons where $P>0.05$ contain no symbol.

2.7. References

Abad, C., & Tan, Y.-V. (2018). Immunomodulatory roles of pacap and VIP: Lessons from knockout mice. *Journal of Molecular Neuroscience*, *66*(1), 102–113. https://doi.org/10.1007/s12031-018-1150-y

Adams, B. A., Gray, S. L., Isaac, E. R., Bianco, A. C., Vidal-Puig, A. J., & Sherwood, N. M. (2007). Feeding and metabolism in mice lacking pituitary adenylate cyclase-activating polypeptide. *Endocrinology*, *149*(4), 1571–1580. https://doi.org/10.1210/en.2007-0515

Ambele, M. A., Dhanraj, P., Giles, R., & Pepper, M. S. (2020). Adipogenesis: A complex interplay of multiple molecular determinants and pathways. *International Journal of Molecular Sciences*, *21*(12), 4283. https://doi.org/10.3390/ijms21124283

Anthony, S. R., Guarnieri, A. R., Gozdiff, A., Helsley, R. N., Phillip Owens, A., & Tranter, M. (2019). Mechanisms linking adipose tissue inflammation to cardiac hypertrophy and fibrosis. *Clinical Science*, *133*(22), 2329–2344. https://doi.org/10.1042/cs20190578

Bagchi, D. P., & MacDougald, O. A. (2019). Identification and dissection of diverse mouse adipose depots. *Journal of Visualized Experiments*, (149). https://doi.org/10.3791/59499

Bains, M., Laney, C., Wolfe, A. E., Orr, M., Waschek, J. A., Ericsson, A. C., & Dorsam, G. P. (2019). Vasoactive intestinal peptide deficiency is associated with altered gut microbiota communities in male and female C57BL/6 mice. *Frontiers in Microbiology*, *10*. https://doi.org/10.3389/fmicb.2019.02689

Bali, S., & Utaal, M. S. (2019). Serum lipids and lipoproteins: A brief review of the composition, transport and physiological functions. *International Journal of Scientific Reports*, *5*(10), 309. https://doi.org/10.18203/issn.2454-2156.intjscirep20194253

Bateman, A., Martin, M.-J., Orchard, S., Magrane, M., Agivetova, R., Ahmad, S., Alpi, E., Bowler-Barnett, E. H., Britto, R., Bursteinas, B., Bye-A-Jee, H., Coetzee, R., Cukura, A., Da Silva, A., Denny, P., Dogan, T., Ebenezer, T. G., Fan, J., Castro, L. G., … Teodoro, D. (2020). Uniprot: The Universal Protein Knowledgebase in 2021. *Nucleic Acids Research*, *49*(D1). https://doi.org/10.1093/nar/gkaa1100

Bennett, V., & Cuatrecasas, P. (1975). Mechanism of activation of adenylate cyclase byVibrio cholerae enterotoxin. *The Journal of Membrane Biology*, *22*(1), 29–52. https://doi.org/10.1007/bf01868162

Bertoli, S., Leone, A., Vignati, L., Spadafranca, A., Bedogni, G., Vanzulli, A., Rodeschini, E., & Battezzati, A. (2015). Metabolic correlates of subcutaneous and visceral abdominal fat measured by ultrasonography: A comparison with waist circumference. *Nutrition Journal*, *15*(1). https://doi.org/10.1186/s12937-015-0120-2

BioRadLifeSciences. (2019). *Https://www.youtube.com/watch?v=TWmu7lXrvIE*. *YouTube*. Retrieved June 22, 2022, from https://www.youtube.com/watch?v=TWmu7lXrvIE.

Bortz, W. M., Paul, P., Haff, A. C., & Holmes, W. L. (1972). Glycerol turnover and oxidation in man. *Journal of Clinical Investigation*, *51*(6), 1537–1546. https://doi.org/10.1172/jci106950

Bustin, S. A., Benes, V., Garson, J. A., Hellemans, J., Huggett, J., Kubista, M., Mueller, R., Nolan, T., Pfaffl, M. W., Shipley, G. L., Vandesompele, J., & Wittwer, C. T. (2009). The MIQE guidelines: Minimum information for publication of quantitative real-time PCR experiments. *Clinical Chemistry*, *55*(4), 611–622. https://doi.org/10.1373/clinchem.2008.112797

Cawley, J., & Meyerhoefer, C. (2012). The medical care costs of obesity: An instrumental variables approach. Journal of Health Economics, 31(1), 219–230. https://doi.org/10.1016/j.jhealeco.2011.10.003

CB, W., & A., J. (2019). *BMI classification percentile and cut off points*. National Center for Biotechnology Information. Retrieved June 3, 2022, from https://pubmed.ncbi.nlm.nih.gov/31082114/

Centers for Disease Control and Prevention. (2021, February 3). *Men and heart disease*. Centers for Disease Control and Prevention. Retrieved June 3, 2022, from https://www.cdc.gov/heartdisease/men.htm#how

Chait, A., & den Hartigh, L. J. (2020). Adipose tissue distribution, inflammation and its metabolic consequences, including diabetes and cardiovascular disease. *Frontiers in Cardiovascular Medicine*, *7*. https://doi.org/10.3389/fcvm.2020.00022

Chang, E., Varghese, M., & Singer, K. (2018). Gender and sex differences in adipose tissue. *Current Diabetes Reports*, *18*(9). https://doi.org/10.1007/s11892-018-1031-3

Chi, J., Wu, Z., Choi, C. H. J., Nguyen, L., Tegegne, S., Ackerman, S. E., Crane, A., Marchildon, F., Tessier-Lavigne, M., & Cohen, P. (2018). Three-dimensional adipose tissue imaging reveals regional variation in beige fat biogenesis and PRDM16-dependent sympathetic neurite density. *Yearbook of Paediatric Endocrinology*. https://doi.org/10.1530/ey.15.11.15

Chooi, Y. C., Ding, C., & Magkos, F. (2019). The epidemiology of Obesity. *Metabolism*, *92*, 6–10. https://doi.org/10.1016/j.metabol.2018.09.005

Christiaens, V., Van Hul, M., Lijnen, H. R., & Scroyen, I. (2012). CD36 promotes adipocyte differentiation and adipogenesis. *Biochimica Et Biophysica Acta (BBA) - General Subjects*, *1820*(7), 949–956. https://doi.org/10.1016/j.bbagen.2012.04.001

Chung, J. Y., Ain, Q. U., Song, Y., Yong, S.-B., & Kim, Y.-H. (2019). Targeted delivery of CRISPR interference system against *fabp4* to white adipocytes ameliorates obesity, inflammation, hepatic steatosis, and insulin resistance. *Genome Research*, *29*(9), 1442–1452. https://doi.org/10.1101/gr.246900.118

Colwell, C. S., Michel, S., Itri, J., Rodriguez, W., Tam, J., Lelievre, V., Hu, Z., Liu, X., & Waschek, J. A. (2003). Disrupted circadian rhythms in VIP- and phi-deficient mice. *American Journal of Physiology-Regulatory, Integrative and Comparative Physiology*, *285*(5). https://doi.org/10.1152/ajpregu.00200.2003

Comas, F., Martínez, C., Sabater, M., Ortega, F., Latorre, J., Díaz-Sáez, F., Aragonés, J., Camps, M., Gumà, A., Ricart, W., Fernández-Real, J. M., & Moreno-Navarrete, J. M. (2019). Neuregulin 4 is a novel marker of beige adipocyte precursor cells in human adipose tissue. *Frontiers in Physiology*, *10*. https://doi.org/10.3389/fphys.2019.00039

Costa, V., Gallo, M. A., Letizia, F., Aprile, M., Casamassimi, A., & Ciccodicola, A. (2010). PPARG: Gene expression regulation and next-generation sequencing for unsolved issues. *PPAR Research*, *2010*, 1–17. https://doi.org/10.1155/2010/409168

Danforth, E. (2000). Failure of adipocyte differentiation causes type II diabetes mellitus? *Nature Genetics*, *26*(1), 13–13. https://doi.org/10.1038/79111

Delgado, M., & Ganea, D. (2011). Vasoactive intestinal peptide: A neuropeptide with pleiotropic immune functions. *Amino Acids*, *45*(1), 25–39. https://doi.org/10.1007/s00726-011-1184-8

Dixon, J. B. (2010). Lymphatic lipid transport: Sewer or subway? *Trends in Endocrinology & Metabolism*, *21*(8), 480–487. https://doi.org/10.1016/j.tem.2010.04.003

Drover, V. A., Ajmal, M., Nassir, F., Davidson, N. O., Nauli, A. M., Sahoo, D., Tso, P., & Abumrad, N. A. (2005). CD36 deficiency impairs intestinal lipid secretion and clearance of chylomicrons from the blood. *Journal of Clinical Investigation*, *115*(5), 1290–1297. https://doi.org/10.1172/jci21514

Duff, M. O., Olson, S., Wei, X., Osman, A., Plocik, A., Bolisetty, M., Celniker, S., & Graveley, B. (2014). Genome-wide identification of zero nucleotide recursive splicing in *drosophila*. https://doi.org/10.1101/006163

Duncan, R. E., Ahmadian, M., Jaworski, K., Sarkadi-Nagy, E., & Sul, H. S. (2007). Regulation of lipolysis in adipocytes. *Annual Review of Nutrition*, *27*(1), 79–101. https://doi.org/10.1146/annurev.nutr.27.061406.093734

Edvinsson, L. (2016). Pituitary adenylate cyclase activating polypeptide (PACAP) in migraine pathophysiology. *Current Topics in Neurotoxicity*, 609–615. https://doi.org/10.1007/978-3-319-35135-3_35

Erendor, F., Sahin, E. O., Sanlioglu, A. D., Balci, M. K., Griffith, T. S., & Sanlioglu, S. (2020). Lentiviral gene therapy vectors encoding VIP suppressed diabetes-related inflammation and augmented pancreatic beta-cell proliferation. *Gene Therapy*, *28*(3-4), 130–141. https://doi.org/10.1038/s41434-020-0183-3

Ericsson, A. C., Bains, M., McAdams, Z., Daniels, J., Busi, S. B., Waschek, J. A., & Dorsam, G. P. (2022). The G protein-coupled receptor, VPAC1, mediates vasoactive intestinal peptide-dependent functional homeostasis of the gut microbiota. *Gastro Hep Advances*, 1(2), 253–264. https://doi.org/10.1016/j.gastha.2021.11.005

Fernández, I., Peña, A., Del Teso, N., Pérez, V., & Rodríguez-Cuesta, J. (2010). Clinical biochemistry parameters in C57BL/6J mice after blood collection from the submandibular vein and retroorbital plexus. Journal of the American Association for Laboratory Animal Science, 49(2), 202-206.Filatov, E. et al., 2021. Contribution of thermogenic mechanisms by male and female mice lacking pituitary adenylate cyclase-activating polypeptide in response to cold acclimation. American Journal of Physiology-Endocrinology and Metabolism, 320(3).

Foryst-Ludwig, A., Kreissl, M. C., Sprang, C., Thalke, B., Böhm, C., Benz, V., Gürgen, D., Dragun, D., Schubert, C., Mai, K., Stawowy, P., Spranger, J., Regitz-Zagrosek, V., Unger, T., & Kintscher, U. (2011). Sex differences in physiological cardiac hypertrophy are associated with exercise-mediated changes in energy substrate availability. *American Journal of Physiology-Heart and Circulatory Physiology*, *301*(1). https://doi.org/10.1152/ajpheart.01222.2010

Fryk, E., Olausson, J., Mossberg, K., Strindberg, L., Schmelz, M., Brogren, H., Gan, L.-M., Piazza, S., Provenzani, A., Becattini, B., Lind, L., Solinas, G., & Jansson, P.-A. (2021). Hyperinsulinemia and insulin resistance in the obese may develop as part of a homeostatic response to elevated free fatty acids: A mechanistic case-control and a population-based cohort study. *EBioMedicine*, *65*, 103264. https://doi.org/10.1016/j.ebiom.2021.103264

Fuente-Martín, E., Argente-Arizón, P., Ros, P., Argente, J., & Chowen, J. A. (2013). Sex differences in adipose tissue. *Adipocyte*, *2*(3), 128–134. https://doi.org/10.4161/adip.24075

Fungfuang, W., Terada, M., Komatsu, N., Moon, C., & Saito, T. R. (2013). Effects of estrogen on food intake, serum leptin levels and leptin mrna expression in adipose tissue of female rats. *Laboratory Animal Research*, *29*(3), 168. https://doi.org/10.5625/lar.2013.29.3.168

Fuster, J. J., Ouchi, N., Gokce, N., & Walsh, K. (2016). Obesity-induced changes in adipose tissue microenvironment and their impact on cardiovascular disease. *Circulation Research*, *118*(11), 1786–1807. https://doi.org/10.1161/circresaha.115.306885

Gallino, L., Hauk, V., Fernández, L., Soczewski, E., Gori, S., Grasso, E., Calo, G., Saraco, N., Berensztein, E., Waschek, J. A., Pérez Leirós, C., & Ramhorst, R. (2020). VIP promotes recruitment of Tregs to the uterine–placental interface during the peri-implantation period to sustain a tolerogenic microenvironment. *Frontiers in Immunology*, *10*. https://doi.org/10.3389/fimmu.2019.02907

Garcia, R. A., Roemmich, J. N., & Claycombe, K. J. (2016). Evaluation of markers of beige adipocytes in white adipose tissue of the mouse. *Nutrition & Metabolism*, *13*(1). https://doi.org/10.1186/s12986-016-0081-2

Gray, S. L., & Vidal-Puig, A. J. (2008). Adipose tissue expandability in the maintenance of metabolic homeostasis. *Nutrition Reviews*, *65*. https://doi.org/10.1111/j.1753-4887.2007.tb00331.x

Gray, S. L., Nora, E. D., Grosse, J., Manieri, M., Stoeger, T., Medina-Gomez, G., Burling, K., Wattler, S., Russ, A., Yeo, G. S. H., Chatterjee, V. K., O'Rahilly, S., Voshol, P. J., Cinti, S., & Vidal-Puig, A. (2006). Leptin deficiency unmasks the deleterious effects of impaired peroxisome proliferator–activated receptor γ function (P465L PPARΓ) in mice. *Diabetes*, *55*(10), 2669–2677. https://doi.org/10.2337/db06-0389

Grove, K. L., Fried, S. K., Greenberg, A. S., Xiao, X. Q., & Clegg, D. J. (2010). A microarray analysis of sexual dimorphism of adipose tissues in high-fat-diet-induced obese mice. *International Journal of Obesity*, *34*(6), 989–1000. https://doi.org/10.1038/ijo.2010.12

Gui, Y., Cai, Z., Silha, J. V., & Murphy, L. J. (2006). Variations in parametrial white adipose tissue mass during the mouse estrous cycle: Relationship with the expression of peroxisome proliferator-activated receptor-γ and retinoic acid receptor-α. *Canadian Journal of Physiology and Pharmacology*, *84*(8-9), 887–892. https://doi.org/10.1139/y06-032

Gustafson, B., Nerstedt, A., & Smith, U. (2019). Reduced subcutaneous adipogenesis in human hypertrophic obesity is linked to senescent precursor cells. *Nature Communications*, *10*(1). https://doi.org/10.1038/s41467-019-10688-x

Hammarstedt, A., Gogg, S., Hedjazifar, S., Nerstedt, A., & Smith, U. (2018). Impaired adipogenesis and dysfunctional adipose tissue in human hypertrophic obesity. *Physiological Reviews*, *98*(4), 1911–1941. https://doi.org/10.1152/physrev.00034.2017

Han, J., Meng, Q., Shen, L., & Wu, G. (2018). Interleukin-6 induces fat loss in cancer cachexia by promoting white adipose tissue lipolysis and browning. *Lipids in Health and Disease*, *17*(1). https://doi.org/10.1186/s12944-018-0657-0

Havel, R. J. (1987). Lipid transport function of lipoproteins in blood plasma. *American Journal of Physiology-Endocrinology and Metabolism*, *253*(1). https://doi.org/10.1152/ajpendo.1987.253.1.e1

He, W., Barak, Y., Hevener, A., Olson, P., Liao, D., Le, J., Nelson, M., Ong, E., Olefsky, J. M., & Evans, R. M. (2003). Adipose-specific peroxisome proliferator-activated receptor γ knockout causes insulin resistance in fat and liver but not in muscle. *Proceedings of the National Academy of Sciences*, *100*(26), 15712–15717. https://doi.org/10.1073/pnas.2536828100

Hirosumi, J., Tuncman, G., Chang, L., Görgün, C. Z., Uysal, K. T., Maeda, K., Karin, M., & Hotamisligil, G. S. (2002). A central role for JNK in obesity and insulin resistance. *Nature*, *420*(6913), 333–336. https://doi.org/10.1038/nature01137

Hu, Y., Yu, J., Cui, X., Zhang, Z., Li, Q., Guo, W., Zhao, C., Chen, X., Meng, M., Li, Y., Guo, M., Qiu, J., Shen, F., Wang, D., Ma, X., Xu, L., Shen, F., & Gu, X. (2021). Combination usage of AdipoCount and image-pro plus/imagej software for quantification of adipocyte sizes. *Frontiers in Endocrinology*, *12*. https://doi.org/10.3389/fendo.2021.642000

Ikeda, K., Maretich, P., & Kajimura, S. (2018). The common and distinct features of brown and beige adipocytes. *Trends in Endocrinology & Metabolism*, *29*(3), 191–200. https://doi.org/10.1016/j.tem.2018.01.001

Jo, J., Gavrilova, O., Pack, S., Jou, W., Mullen, S., Sumner, A. E., Cushman, S. W., & Periwal, V. (2009). Hypertrophy and/or hyperplasia: Dynamics of Adipose Tissue Growth. *PLoS Computational Biology*, *5*(3). https://doi.org/10.1371/journal.pcbi.1000324

Kamble, P. G., Hetty, S., Vranic, M., Almby, K., Castillejo-López, C., Abalo, X. M., Pereira, M. J., & Eriksson, J. W. (2020). Proof-of-concept for CRISPR/Cas9 gene editing in human preadipocytes: Deletion of FKBP5 and PPARG and effects on adipocyte differentiation and metabolism. *Scientific Reports*, *10*(1). https://doi.org/10.1038/s41598-020-67293-y

Karastergiou, K., Smith, S. R., Greenberg, A. S., & Fried, S. K. (2012). Sex differences in human adipose tissues – the biology of Pear Shape. *Biology of Sex Differences*, *3*(1). https://doi.org/10.1186/2042-6410-3-13

Kim, J. I., Huh, J. Y., Sohn, J. H., Choe, S. S., Lee, Y. S., Lim, C. Y., Jo, A., Park, S. B., Han, W., & Kim, J. B. (2015). Lipid-overloaded enlarged adipocytes provoke insulin resistance independent of inflammation. *Molecular and Cellular Biology*, *35*(10), 1686–1699. https://doi.org/10.1128/mcb.01321-14

Kim, S.-N., Jung, Y.-S., Kwon, H.-J., Seong, J. K., Granneman, J. G., & Lee, Y.-H. (2016). Sex differences in sympathetic innervation and browning of white adipose tissue of Mice. *Biology of Sex Differences*, *7*(1). https://doi.org/10.1186/s13293-016-0121-7

Kliewer, S. A., Lenhard, J. M., Willson, T. M., Patel, I., Morris, D. C., & Lehmann, J. M. (1995). A prostaglandin J2 metabolite binds peroxisome proliferator-activated receptor γ and promotes adipocyte differentiation. *Cell*, *83*(5), 813–819. https://doi.org/10.1016/0092-8674(95)90194-9

Lee, M.-W., Odegaard, J. I., Mukundan, L., Qiu, Y., Molofsky, A. B., Nussbaum, J. C., Yun, K., Locksley, R. M., & Chawla, A. (2015). Activated type 2 innate lymphoid cells regulate beige fat biogenesis. *Cell*, *160*(1-2), 74–87. https://doi.org/10.1016/j.cell.2014.12.011

Li, Y., Li, Z., Ngandiri, D. A., Llerins Perez, M., Wolf, A., & Wang, Y. (2022). The molecular brakes of adipose tissue lipolysis. *Frontiers in Physiology*, *13*. https://doi.org/10.3389/fphys.2022.826314

Liu, Y.-J., Guo, Y.-F., Zhang, L.-S., Pei, Y.-F., Yu, N., Yu, P., Papasian, C. J., & Deng, H.-W. (2010). Biological pathway-based genome-wide association analysis identified the

vasoactive intestinal peptide (VIP) pathway important for obesity. *Obesity*, *18*(12), 2339–2346. https://doi.org/10.1038/oby.2010.83

Livak, K. J., & Schmittgen, T. D. (2001). Analysis of relative gene expression data using real-time quantitative PCR and the 2−ΔΔCT method. *Methods*, *25*(4), 402–408. https://doi.org/10.1006/meth.2001.1262

Longo, M., Zatterale, F., Naderi, J., Parrillo, L., Formisano, P., Raciti, G. A., Beguinot, F., & Miele, C. (2019). Adipose tissue dysfunction as determinant of obesity-associated metabolic complications. *International Journal of Molecular Sciences*, *20*(9), 2358. https://doi.org/10.3390/ijms20092358

Loos, R. J., & Yeo, G. S. (2021). The genetics of obesity: From Discovery to Biology. *Nature Reviews Genetics*, *23*(2), 120–133. https://doi.org/10.1038/s41576-021-00414-z

Lundholm, L., Zang, H., Hirschberg, A. L., Gustafsson, J.-Å., Arner, P., & Dahlman-Wright, K. (2008). Key lipogenic gene expression can be decreased by estrogen in human adipose tissue. *Fertility and Sterility*, *90*(1), 44–48. https://doi.org/10.1016/j.fertnstert.2007.06.011

Ma, X., Wang, D., Zhao, W., & Xu, L. (2018). Deciphering the roles of PPARΓ in adipocytes via dynamic change of transcription complex. *Frontiers in Endocrinology*, *9*. https://doi.org/10.3389/fendo.2018.00473

MacCannell, A. D., Futers, T. S., Whitehead, A., Moran, A., Witte, K. K., & Roberts, L. D. (2021). Sexual dimorphism in adipose tissue mitochondrial function and metabolic flexibility in obesity. *International Journal of Obesity*, *45*(8), 1773–1781. https://doi.org/10.1038/s41366-021-00843-0

Martin, B., Shin, Y.-K., White, C. M., Ji, S., Kim, W., Carlson, O. D., Napora, J. K., Chadwick, W., Chapter, M., Waschek, J. A., Mattson, M. P., Maudsley, S., & Egan, J. M. (2010). Vasoactive intestinal peptide–null mice demonstrate enhanced sweet taste preference, dysglycemia, and reduced taste bud leptin receptor expression. *Diabetes*, *59*(5), 1143–1152. https://doi.org/10.2337/db09-0807

Martino, A., Cabiati, M., Campan, M., Prescimone, T., Minocci, D., Caselli, C., Rossi, A. M., Giannessi, D., & Del Ry, S. (2011). Selection of reference genes for normalization of real-time PCR data in minipig heart failure model and evaluation of TNF-α mrna expression. *Journal of Biotechnology*, *153*(3-4), 92–99. https://doi.org/10.1016/j.jbiotec.2011.04.002

Masuo, Y., Noguchi, J., Morita, S., & Matsumoto, Y. (1995). Effects of intracerebroventricular administration of pituitary adenylate cyclase-activating polypeptide (PACAP) on the motor activity and reserpine-induced hypothermia in murines. *Brain Research*, *700*(1-2), 219–226. https://doi.org/10.1016/0006-8993(95)00978-y

McInnes, G., Sharo, A. G., Koleske, M. L., Brown, J. E. H., Norstad, M., Adhikari, A. N., Wang, S., Brenner, S. E., Halpern, J., Koenig, B. A., Magnus, D. C., Gallagher, R. C., Giacomini, K. M., & Altman, R. B. (2021). Opportunities and challenges for the computational interpretation of rare variation in clinically important genes. *The American Journal of Human Genetics*, *108*(4), 535–548. https://doi.org/10.1016/j.ajhg.2021.03.003

Moreno-Indias, I., & Tinahones, F. J. (2015). Impaired adipose tissue expandability and lipogenic capacities as ones of the main causes of metabolic disorders. *Journal of Diabetes Research*, *2015*, 1–12. https://doi.org/10.1155/2015/970375

Morris, D. L., & Rui, L. (2009). Recent advances in understanding leptin signaling and leptin resistance. *American Journal of Physiology-Endocrinology and Metabolism*, *297*(6). https://doi.org/10.1152/ajpendo.00274.2009

Moseti, D., Regassa, A., & Kim, W.-K. (2016). Molecular regulation of adipogenesis and potential anti-adipogenic bioactive molecules. *International Journal of Molecular Sciences*, *17*(1), 124. https://doi.org/10.3390/ijms17010124

Nascimento-Sales, M., Fredo-da-Costa, I., Borges Mendes, A. C., Melo, S., Ravache, T. T., Gomez, T. G., Gaisler-Silva, F., Ribeiro, M. O., Santos, A. R., Carneiro-Ramos, M. S., & Christoffolete, M. A. (2017). Is the FVB/n mouse strain truly resistant to diet-induced obesity? *Physiological Reports*, *5*(9). https://doi.org/10.14814/phy2.13271

Olaogun, I., Farag, M., & Hamid, P. (2020). The pathophysiology of type 2 diabetes mellitus in non-obese individuals: An overview of the current understanding. *Cureus*. https://doi.org/10.7759/cureus.7614

Osuga, J.-ichi, Ishibashi, S., Oka, T., Yagyu, H., Tozawa, R., Fujimoto, A., Shionoiri, F., Yahagi, N., Kraemer, F. B., Tsutsumi, O., & Yamada, N. (2000). Targeted disruption of hormone-sensitive lipase results in male sterility and adipocyte hypertrophy, but not in obesity. *Proceedings of the National Academy of Sciences*, *97*(2), 787–792. https://doi.org/10.1073/pnas.97.2.787

Paladini, F., Adinolfi, V., Cocco, E., Ciociola, E., Tamburrano, G., Cascino, I., Lucantoni, F., Morano, S., & Sorrentino, R. (2012). Gender-dependent association of type 2 diabetes with the vasoactive intestinal peptide receptor 1. *Gene*, *493*(2), 278–281. https://doi.org/10.1016/j.gene.2011.11.055

Pilkington, A.-C., Paz, H. A., & Wankhade, U. D. (2021). Beige adipose tissue identification and marker specificity—overview. *Frontiers in Endocrinology*, *12*. https://doi.org/10.3389/fendo.2021.599134

Recazens, E., Mouisel, E., & Langin, D. (2021). Hormone-sensitive lipase: Sixty years later. *Progress in Lipid Research*, *82*, 101084. https://doi.org/10.1016/j.plipres.2020.101084

Resch, J. M., Boisvert, J. P., Hourigan, A. E., Mueller, C. R., Yi, S. S., & Choi, S. J. (2011). Stimulation of the hypothalamic ventromedial nuclei by pituitary adenylate cyclase-activating polypeptide induces hypophagia and thermogenesis. *American Journal of Physiology-Regulatory, Integrative and Comparative Physiology*, *301*(6).

Ricquier, D. (2011). Uncoupling protein 1 of brown adipocytes, the only uncoupler: A historical perspective. *Frontiers in Endocrinology*, *2*. https://doi.org/10.3389/fendo.2011.00085 https://doi.org/10.1152/ajpregu.00334.2011

Rotondo, F., Ho-Palma, A. C., Remesar, X., Fernández-López, J. A., Romero, M. del, & Alemany, M. (2017). Glycerol is synthesized and secreted by adipocytes to dispose of excess glucose, via glycerogenesis and increased acyl-glycerol turnover. *Scientific Reports*, *7*(1). https://doi.org/10.1038/s41598-017-09450-4

Ross, R., Neeland, I. J., Yamashita, S., Shai, I., Seidell, J., Magni, P., Santos, R. D., Arsenault, B., Cuevas, A., Hu, F. B., Griffin, B. A., Zambon, A., Barter, P., Fruchart, J.-C., Eckel, R. H., Matsuzawa, Y., & Després, J.-P. (2020). Waist circumference as a vital sign in clinical practice: A consensus statement from the IAS and ICCR Working Group on visceral obesity. *Nature Reviews Endocrinology*, *16*(3), 177–189. https://doi.org/10.1038/s41574-019-0310-7

Said, S. I., & Mutt, V. (1970). Potent peripheral and splanchnic vasodilator peptide from normal gut. *Nature*, *225*(5235), 863–864. https://doi.org/10.1038/225863a0

Semple, R. K. (2006). PPAR and human metabolic disease. *Journal of Clinical Investigation*, *116*(3), 581–589. https://doi.org/10.1172/jci28003

Serra, M. C., Ryan, A. S., & Goldberg, A. P. (2016). Reduced LPL and subcutaneous lipid storage capacity are associated with metabolic syndrome in postmenopausal women with obesity. *Obesity Science & Practice*, *3*(1), 106–114. https://doi.org/10.1002/osp4.86

Shen, W.-J., Yu, Z., Patel, S., Jue, D., Liu, L.-F., & Kraemer, F. B. (2011). Hormone-sensitive lipase modulates adipose metabolism through PPARГ. *Biochimica Et Biophysica Acta (BBA) - Molecular and Cell Biology of Lipids*, *1811*(1), 9–16. https://doi.org/10.1016/j.bbalip.2010.10.001

Shen, W. J., Liu, L. F., Patel, S., & Kraemer, F. B. (2011). Hormone-sensitive lipase-knockout mice maintain high bone density during aging. *The FASEB Journal*, *25*(8), 2722–2730. https://doi.org/10.1096/fj.11-181016

Skurk, T., Alberti-Huber, C., Herder, C., & Hauner, H. (2007). Relationship between adipocyte size and Adipokine expression and secretion. *The Journal of Clinical Endocrinology & Metabolism*, *92*(3), 1023–1033. https://doi.org/10.1210/jc.2006-1055

Slawik, M., & Vidal-Puig, A. J. (2007). Adipose tissue expandability and the metabolic syndrome. *Genes & Nutrition*, *2*(1), 41–45. https://doi.org/10.1007/s12263-007-0014-9

Smith, G. I., Mittendorfer, B., & Klein, S. (2019). Metabolically healthy obesity: Facts and fantasies. *Journal of Clinical Investigation*, *129*(10), 3978–3989. https://doi.org/10.1172/jci129186

Smith, U., & Kahn, B. B. (2016). Adipose tissue regulates insulin sensitivity: Role of adipogenesis, *de novo* lipogenesis and novel lipids. *Journal of Internal Medicine*, *280*(5), 465–475. https://doi.org/10.1111/joim.12540

Spiegelman, B. M. (2013). Banting Lecture 2012. *Diabetes*, *62*(6), 1774–1782. https://doi.org/10.2337/db12-1665

Szanto, A., & Nagy, L. (2005). Retinoids potentiate peroxisome proliferator-activated receptor γ action in differentiation, gene expression, and lipid metabolic processes in developing myeloid cells. *Molecular Pharmacology*, *67*(6), 1935–1943. https://doi.org/10.1124/mol.104.006445

Szema, A. M., Hamidi, S. A., Smith, S. D., & Benveniste, H. (2013). VIP gene deletion in mice causes cardiomyopathy associated with upregulation of heart failure genes. *PLoS ONE*, *8*(5). https://doi.org/10.1371/journal.pone.0061449

Talbot, J., Hahn, P., Kroehling, L., Nguyen, H., Li, D., & Littman, D. R. (2020). Feeding-dependent VIP neuron–ilc3 circuit regulates the intestinal barrier. *Nature*, *579*(7800), 575–580. https://doi.org/10.1038/s41586-020-2039-9

Taylor, S. C., Laperriere, G., & Germain, H. (2017). Droplet digital PCR versus qPCR for gene expression analysis with low abundant targets: From variable nonsense to publication Quality Data. *Scientific Reports*, *7*(1). https://doi.org/10.1038/s41598-017-02217-x

Thompson, B. R., Lobo, S., & Bernlohr, D. A. (2010). Fatty acid flux in adipocytes: The in's and out's of fat cell lipid trafficking. *Molecular and Cellular Endocrinology*, *318*(1-2), 24–33. https://doi.org/10.1016/j.mce.2009.08.015

Town, L., McGlinn, E., Davidson, T.-L., Browne, C. M., Chawengsaksophak, K., Koopman, P., Richman, J. M., & Wicking, C. (2011). TMEM26 is dynamically expressed during palate and limb development but is not required for embryonic survival. *PLoS ONE*, *6*(9). https://doi.org/10.1371/journal.pone.0025228

Tsutsumi, M., Claus, T. H., Liang, Y., Li, Y., Yang, L., Zhu, J., Dela Cruz, F., Peng, X., Chen, H., Yung, S. L., Hamren, S., Livingston, J. N., & Pan, C. Q. (2002). A potent and highly selective VPAC2 agonist enhances glucose-induced insulin release and glucose disposal. *Diabetes*, *51*(5), 1453–1460. https://doi.org/10.2337/diabetes.51.5.1453

Van Acker, S. I., Van Acker, Z. P., Haagdorens, M., Pintelon, I., Koppen, C., & Zakaria, N. (2019). Selecting appropriate reference genes for quantitative real-time polymerase chain reaction studies in isolated and cultured ocular surface epithelia. *Scientific Reports*, *9*(1). https://doi.org/10.1038/s41598-019-56054-1

Velle, K. B., & Fritz-Laylin, L. K. (2019). Diversity and evolution of actin-dependent phenotypes. *Current Opinion in Genetics & Development*, *58-59*, 40–48. https://doi.org/10.1016/j.gde.2019.07.016

Virtue, S., & Vidal-Puig, A. (2008). It's not how fat you are, it's what you do with it that counts. *PLoS Biology*, *6*(9). https://doi.org/10.1371/journal.pbio.0060237

Vogt, N. M., Kerby, R. L., Dill-McFarland, K. A., Harding, S. J., Merluzzi, A. P., Johnson, S. C., Carlsson, C. M., Asthana, S., Zetterberg, H., Blennow, K., Bendlin, B. B., & Rey, F. E. (2017). Gut microbiome alterations in alzheimer's disease. *Scientific Reports*, *7*(1). https://doi.org/10.1038/s41598-017-13601-y

Vu, J. P., Larauche, M., Flores, M., Luong, L., Norris, J., Oh, S., Liang, L.-J., Waschek, J., Pisegna, J. R., & Germano, P. M. (2015). Regulation of appetite, body composition, and metabolic hormones by vasoactive intestinal polypeptide (VIP). *Journal of Molecular Neuroscience*, *56*(2), 377–387. https://doi.org/10.1007/s12031-015-0556-z

Vu, J. P., Goyal, D., Luong, L., Oh, S., Sandhu, R., Norris, J., Parsons, W., Pisegna, J. R., & Germano, P. M. (2015). Pacap intraperitoneal treatment suppresses appetite and food intake via PAC1 receptor in mice by inhibiting ghrelin and increasing GLP-1 and leptin. *American Journal of Physiology-Gastrointestinal and Liver Physiology*, *309*(10). https://doi.org/10.1152/ajpgi.00190.2015

Wafer, R., Tandon, P., & Minchin, J. E. (2017). The role of peroxisome proliferator-activated receptor gamma (PPARG) in adipogenesis: Applying knowledge from the fish aquaculture industry to biomedical research. *Frontiers in Endocrinology*, *8*. https://doi.org/10.3389/fendo.2017.00102

WHO, 2021. Obesity and overweight. *World Health Organization*. Available at: https://www.who.int/news-room/fact-sheets/detail/obesity-and-overweight [Accessed April 13, 2022].

Wu, J., Boström, P., Sparks, L. M., Ye, L., Choi, J. H., Giang, A.-H., Khandekar, M., Virtanen, K. A., Nuutila, P., Schaart, G., Huang, K., Tu, H., van Marken Lichtenbelt, W. D., Hoeks, J., Enerbäck, S., Schrauwen, P., & Spiegelman, B. M. (2012). Beige adipocytes are a distinct type of thermogenic fat cell in mouse and human. *Cell*, *150*(2), 366–376. https://doi.org/10.1016/j.cell.2012.05.016

Xia, B., Cai, G. H., Yang, H., Wang, S. P., Mitchell, G. A., & Wu, J. W. (2017). Adipose tissue deficiency of hormone-sensitive lipase causes fatty liver in mice. *PLOS Genetics*, *13*(12). https://doi.org/10.1371/journal.pgen.1007110

Xie, X., Guo, P., Yu, H., Wang, Y., & Chen, G. (2017). Ribosomal proteins: Insight into molecular roles and functions in hepatocellular carcinoma. *Oncogene*, *37*(3), 277–285. https://doi.org/10.1038/onc.2017.343

Xiong, W., Zhao, X., Villacorta, L., Rom, O., Garcia-Barrio, M. T., Guo, Y., Fan, Y., Zhu, T., Zhang, J., Zeng, R., Chen, Y. E., Jiang, Z., & Chang, L. (2018). Brown adipocyte-specific PPARΓ (peroxisome proliferator-activated receptor γ) deletion impairs perivascular adipose tissue development and enhances atherosclerosis in mice. *Arteriosclerosis, Thrombosis, and Vascular Biology*, *38*(8), 1738–1747. https://doi.org/10.1161/atvbaha.118.311367

Yamashita, J., Nishiike, Y., Fleming, T., Kayo, D., & Okubo, K. (2021). Estrogen mediates sex differences in preoptic neuropeptide and pituitary hormone production in medaka. *Communications Biology*, *4*(1). https://doi.org/10.1038/s42003-021-02476-5

Ye, Q., Zou, B., Yeo, Y. H., Li, J., Huang, D. Q., Wu, Y., Yang, H., Liu, C., Kam, L. Y., Tan, X. X., Chien, N., Trinh, S., Henry, L., Stave, C. D., Hosaka, T., Cheung, R. C., & Nguyen, M. H. (2020). Global prevalence, incidence, and outcomes of non-obese or lean non-alcoholic fatty liver disease: A systematic review and meta-analysis. *The Lancet Gastroenterology & Hepatology*, *5*(8), 739–752. https://doi.org/10.1016/s2468-1253(20)30077-7

Yue, F., Cheng, Y., Breschi, A., Vierstra, J., Wu, W., Ryba, T., ... & Ren, B. (2014). A comparative encyclopedia of DNA elements in the mouse genome. Nature, 515(7527), 355-364.

Zammouri, J., Vatier, C., Capel, E., Auclair, M., Storey-London, C., Bismuth, E., Mosbah, H., Donadille, B., Janmaat, S., Fève, B., Jéru, I., & Vigouroux, C. (2022). Molecular and cellular bases of lipodystrophy syndromes. *Frontiers in Endocrinology*, *12*. https://doi.org/10.3389/fendo.2021.803189

Zhang, Y., Dallner, O. S., Nakadai, T., Fayzikhodjaeva, G., Lu, Y. H., Lazar, M. A., ... & Friedman, J. M. (2018). A noncanonical PPARγ/RXRα-binding sequence regulates leptin expression in response to changes in adipose tissue mass. Proceedings of the National Academy of Sciences, 115(26), E6039-E6047.

Zhang, Y., Hao, J., Tarrago, M. G., Warner, G. M., Giorgadze, N., Wei, Q., Huang, Y., He, K., Chen, C., Peclat, T. R., White, T. A., Ling, K., Tchkonia, T., Kirkland, J. L., Chini, E. N., & Hu, J. (2021). FBF1 deficiency promotes beiging and healthy expansion of white adipose tissue. *Cell Reports*, *36*(5), 109481. https://doi.org/10.1016/j.celrep.2021.109481

Zhao, Y.-Y., Liu, Y., Stan, R.-V., Fan, L., Gu, Y., Dalton, N., Chu, P.-H., Peterson, K., Ross, J., & Chien, K. R. (2002). Defects in *caveolin-1* cause dilated cardiomyopathy and pulmonary hypertension in knockout mice. *Proceedings of the National Academy of Sciences*, *99*(17), 11375–11380. https://doi.org/10.1073/pnas.172360799

Zhou, Z., Neupane, M., Zhou, H. R., Wu, D., Chang, C. C., Moustaid-Moussa, N., & Claycombe, K. J. (2012). Leptin differentially regulate STAT3 activation in ob/ob mouse adipose mesenchymal stem cells. Nutrition & metabolism, 9(1), 1-13.

3. MESSENGER RNA GENE EXPRESSION SCREENING OF VIP AND PACAP NEUROPEPTIDES AND THEIR ENDOGENOUS RECEPTORS IN RUMINANTS; IMPLICATIONS INTO THE EVOLUTIONARY DIVERGENCE OF THIS SIGNALING AXIS

3.1. Abstract

Mammalian VIP and PACAP are highly conserved neuropeptides that share 100% amino acid identity in humans, mice, sheep, and cattle. Interestingly, their endogenous G protein-coupled receptors VPAC1, VPAC2, and PAC1 have a more divergent sequence homology. The widespread tissue distribution of these peptides and their receptors is necessary for promoting anti-inflammatory actions, a well-studied function in mice and humans; however, their expression profile, which may shed light on biological roles, in ruminant tissues is unknown. To this end, we have screened for the distribution of these neuropeptides and their endogenous receptors in 15 different tissues using RT-qPCR. Results find similar expression of both VIP and PACAP in the brain and colon of steers and wethers. Additionally, VIP was detected in the cecum of both species. Interestingly, the receptors' expression profiles were more variable between steers and wethers. These findings suggest that VIP and PACAP mRNA expression profiles have conserved expression distribution between cattle and sheep, whereas their receptors display divergent patterns; an observation that is congruent with these peptides' amino acid sequence identity amongst *Homo sapiens*, *Mus musculus*, *Bos taurus*, and *Ovis aries*. Verifying the presence of VIP/PACAP and their receptors in ruminants warrants supplementing these peptides to decrease inflammation and bolster feed efficiency in livestock placed on a high concentrate diet.

3.2. Introduction

Feeding ruminants is an essential step in livestock production. Cattle and sheep are utilized for food, labor, and other commodities by the human population, making it necessary to optimize livestock production practices. In the past decade, prices of grain, corn, and other feed ingredients have been rising, causing farmers to look for alternative ways to increase nutritional efficiency (Wu, 2021). The rumen microbiome is of great interest for increasing nutrient availability because it ferments feedstuffs to produce energy-rich metabolites such as the short chain fatty acids propionate and butyrate (Matthews, 2019). High-concentrate diets can increase energy availability in livestock by diverting rumen-fermented hydrogen towards propionate production instead of methanogenesis (Moss, 2000). During high-concentrate feeding, up to 40% of dietary starch escapes ruminal fermentation (Ørskov, 1986), thus putting pressure on digestive enzymes to aid small intestine absorption (Swanson, 2002). It has also been demonstrated that there is a limit to the secretion of α-amylase, which becomes a limiting factor to glucose absorption in ruminants on finishing diets (Swanson, 2002). Before animal harvest, farmers will often administer a high-concentrate diet to maximize animal weight; however, this feeding style can induce subacute ruminal acidosis (SARA) along with a proinflammatory tone and compromise digestibility, feed intake, and milk production (Zhang et al., 2016). An ideal supplement would decrease ruminal acidosis and bolster intestinal nutrient absorption, thus increasing feed efficiency and allowing farmers to administer lower amounts of feed to see similar weight gain in their animals.

PACAP and VIP, two anti-inflammatory peptides that have recently been shown to regulate gut microbiota homeostasis in mice (Bains, 2019)(Heimesaat, 2017), can protect against inflammatory disorders by inhibiting pro-inflammatory pathways (Abad, 2018). VIP and PACAP

are thought to have emerged from an exon duplication and two tetraploidization events of a common PACAP-like ancestor gene (Cardoso, 2020), explaining why these peptides share 68% amino acid identity and bind to their endogenous receptors VPAC1 and VPAC2 with equal affinity (Arimura, 1992). PACAP also binds to a third receptor, PAC1, with 1000 times greater affinity than VIP, deeming functions of PAC1 to be mainly PACAP driven (Ramos-Álvarez, 2015). The peptide sequences of both VIP and PACAP are highly conserved among vertebrates, tunicates, and invertebrates, but PACAP is more structurally conserved, thus supporting a common "PACAP-like" ancestor gene (Ng, 2012). Vasoactive Intestinal Peptide (VIP) was first isolated from porcine intestinal tissue and identified as a 28 amino acid peptide (Said & Mutt, 1970). VIP has pleiotropic functions including anti-inflammatory mediation of the cytokines TNF- α, IL-6, IL-12, nitric oxide, and chemokines (Delgado, 2004). Interestingly, VIP has also been shown to stimulate the release of pancreatic juices including cholecystokinin and α-amylase (Tanaka, 1995), making it a strong therapeutic candidate for starch digestion in ruminants. VIP's 'sister peptide', PACAP, was derived from the ovine hypothalamus in two isoforms: a 27 and 38 amino acid peptide (Miyata, 1990). Both isoforms have comparable binding affinities to their PAC1 receptor; however, an intravenous supply of PACAP-38, but not PACAP-27, can enter the CNS via soluble transporters on the blood-brain barrier, thus making it more helpful in treating nervous system disorders (Ramos-Álvarez, 2015). Both PACAP and VIP regulate the transcription of TNF-a (Delgado, 2001), likely via a mechanism involving their shared receptors; however, PAC1-PACAP interactions regulate inflammation via multiple receptor subtypes and targets (Van, 2018).

To date, there is a paucity of expression studies for the VIP/PACAP signaling axis in ruminants. Since peritoneal injections of VIP can alleviate dextran sulfate sodium-induced colitis

in mice (Jayawardena, 2017)(Wu, 2015), we hypothesize that manipulating VIP and its downstream signaling would reduce ruminal SARA and inflammation and increase nutrient uptake that would result in weight gain when on finishing diets; however, this prediction is based on the assumption that VIP's receptors are similarly distributed between mice and ruminants. Species divergence of VIP receptors has been previously observed. For instance, VPAC2 is differently expressed in the thyroid, pancreatic tissue, and lungs of mice and humans, questioning the efficacy of VPAC2 targeting treatments validated in mice (Harmar, 2004). Before researching VIP or PACAP administration in ruminants, the first phase of this research is to establish a mRNA expression profile defining the distribution of VIP and PACAP ligands and their cognate GPCRs in ruminants that will help predict tissue-specific effects. In the present study, we measured relative mRNA expression of VIP, PACAP, and their endogenous receptors across 15 different tissues in wethers and steers.

3.3. Results

Investigations into the VIP/PACAP signaling axis has been performed in rodents and humans for the past 30 years. In ruminants, there is a paucity of research reporting on the biological actions in a cellular, physiological or pathophysiological manner, let alone gene expression profiles. We set out to accomplish a singular objective that encompassed measuring the relative quantitative expression levels for both neuropeptides, VIP and PACAP, along with their cognate G protein-coupled receptors, VPAC1, VPAC2 and PAC1. To this end, we collected brain, duodenum, jejunum, colon, cecum, rumen, muscle, fat, spleen, kidney, liver, reticulum, omasum, and abomasum tissues from 4 biologically identical steers and 4 wethers. RNA was extracted and cDNA synthesized for all individual tissues before pooling by species tissue (**Figure 3.3**). Each pool was assayed using qPCR for two technical replicates using VIP,

PACAP, VPAC1, VPAC2, PAC1, and two reference gene primers (GAPDH and SDHA in steers) (PPIA and B2M in wethers). VIP was detected in the brain, colon and cecum of both species, whereas PACAP was only present in the brain and colon (**Figure 3.1-3.2**). Interestingly, different screening profiles were detected for all three receptors. VPAC1 was detectable in the jejunum, colon, ilium, cecum, duodenum, brain, and muscle of both steers and sheep; however, it was also detected in the kidney of steers and liver, spleen, and fat of wethers. VPAC2 mRNA expression was detected in the spleen and omasum of steers, whereas it was undetectable in any of the wether tissues. PAC1 was detected in the brain and colon of both species which are the same tissues PACAP was detected in; but, PAC1 was also detected in the rumen, spleen, fat, and omasum of steers as well as the muscle of wethers. Tissue expressions rankings are summarized in **Table 3.1**. These observations demonstrate a strikingly similar profile of VIP and PACAP mRNA expression in the tissues of cow and sheep, whereas there is divergence in receptor distribution between these two ruminant species. The same trends are reflected in amino acid identity, where VIP and PACAP sequences are 100% identical, but VPAC1, VPAC2, and PAC1 are between 78.9-90.7% in *Mus musculus*, *Bos taurus*, and *Ovis aries* compared to *Homo sapiens* (**Table 3.2**).

Figure 3.1. Relative expression of VIP, PACAP, VPAC1,VPAC2 & PACAP normalized to GPADH & SDHA in Steer Tissue Pools.
Mean fold change of two technical replicates in 15 steer tissue pools represented as fold change when VIP in the brain was set to 1.
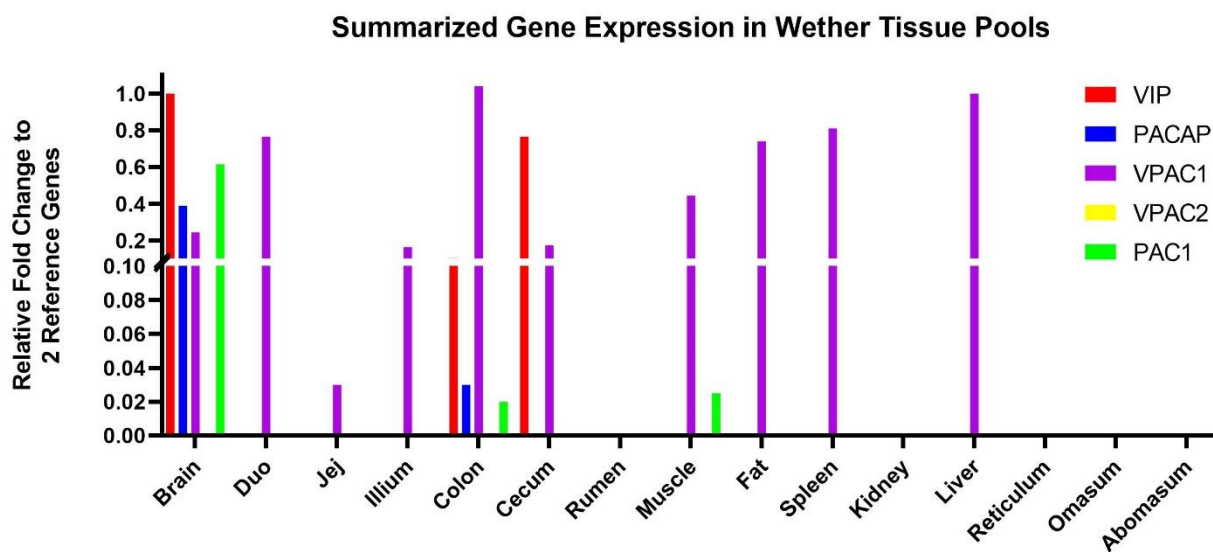

Figure 3.2. Relative expression of VIP, PACAP, VPAC1,VPAC2 & PACAP normalized to PPIA & B2M in Wether Tissue Pools.
Mean fold change of two technical replicates in 15 wether tissue pools represented as fold change when VIP in the brain was set to 1.

Table 3.1. Relative mRNA Expression Ranking in Ruminant Tissues.

Gene	Ruminant	Expression Ranking
VIP	Steers	1. Cecum 2. Brain 3. Colon
	Wethers	1. Brain 2. Cecum 3. Colon
PACAP	Steers	1. Brain 2. Colon
	Wethers	1. Brain 2. Colon
VPAC1	Steers	1. Jejunum 2. **Kidney** 3. Colon 4. Ilium 5. Cecum 6. Duodenum 7. Brain 8. Muscle
	Wethers	1. **Liver** 2. Colon 3. **Spleen** 4. Duodenum 5. **Fat** 6. Muscle 7. Brain 8. Cecum 9. Ilium 10. Jejunum
VPAC2	Steers	1. **Spleen** 2. **Omasum**
	Wethers	Not Detected
PAC1	Steers	1. Brain 2**. Spleen** 3. **Fat** 4. Colon 5. **Omasum** 6. **Rumen**
	Wethers	1. Brain 2. **Muscle** 3. Colon

Ranking order of mRNA expression in steers and wethers. Organs with **BOLD** font have mRNA expression undetected in the opposing species.

Table 3.2. Superfamily Member Identities.

Peptide	AA Sequence or REF #	% Identity to *Homo Sapiens*
VIP		
Homo sapiens	HSDAVFTDNYTRLRKQMAVKKYLNSILN	100%
Mus musculus	HSDAVFTDNYTRLRKQMAVKKYLNSILN	100%
Bos taurus	HSDAVFTDNYTRLRKQMAVKKYLNSILN	100%
Ovis aries	HSDAVFTDNYTRLRKQMAVKKYLNSILN	100%
PACAP-38		
Homo sapiens	HSDGIFTDSYSRYRKQMAVKKYLAAVLGKRYKQRVKNK	100%
Mus musculus	HSDGIFTDSYSRYRKQMAVKKYLAAVLGKRYKQRVKNK	100%
Bos taurus	HSDGIFTDSYSRYRKQMAVKKYLAAVLGKRYKQRVKNK	100%
Ovis aries	HSDGIFTDSYSRYRKQMAVKKYLAAVLGKRYKQRVKNK	100%
VPAC1		
Homo sapiens	sp|P32241|31-457	100%
Mus musculus	sp|P97751|31-459	84.3%
Bos taurus	tr|F1MF07|31-457	89.9%
Ovis aries	tr|W5NZL6|31-492	78.9%
VPAC2		
Homo sapiens	sp|P41587|24-438	100%
Mus musculus	sp|P41588|23-437	87.7%
Bos taurus	tr|F1MIT6|25-442	86.3%
Ovis aries	*tr|W5PKZ4|20-96,109-363,369-424	79.8%
PAC1		
Homo sapiens	sp|P41586|21-468	100%
Mus musculus	sp|P70205|21-496	88.4%
Bos taurus	sp|Q29627|38-513	90.7%
Ovis aries	tr|W5PCC2|21-520	81.8%

Amino acid sequence of PACAP, VIP and their endogenous receptors in *Homo sapiens, Mus musculus, Ovis aries, Bos taurus*. Identity aligned with NCBI multiple alignment tool: Identity = # of similar amino acids/ total number of amino acids. *Compositional Bias.

3.4. Discussion

This study aimed to screen 15 tissues from two different ruminant species for the mRNA

expression of VIP, PACAP, and their endogenous GPCRs. We screened each tissue for three

candidate reference genes. Results from this screening show a consistent ranking of the neuropeptide mRNA expression across both steer and wether tissues. Additionally, we report the successful generation of 9 primer pairs for quantifying mRNA in ruminants, some of which are suitable for analyzing their target cDNA products in both Bos and Ovis.

The relative mRNA expression of VIP and PACAP followed a similar tissue distribution between steers and wethers, whereby both peptides were highly expressed in the brain and colon. Similarly, mice display the highest mRNA expression of VIP in large intestine and cortex/frontal lobe regions (Yue, 2014) and humans express VIP mostly in the appendix, colon, small intestine, and brain (Fagerberg, 2014). VIP was also detected in the cecum pool of our steers and wethers, which could be related to VIP's necessity for maintaining appendix size and fecal microbiota (Lelievre, 2007) (Bains, 2019). PACAP was detected in the Brain and Colon of both ruminant species (**Table 3.1**), congruent with its high mRNA expression in the central nervous system and colon of humans and mice (Yue, 2014) (Fagerberg, 2014). These 'sister peptides' have been described as important brain-gut axis communicators in mice and humans (Wei, 2020), likely due to their high expression in respective tissues and disturbance of both systems in knock-out mice (Heimesaat, 2017)(Bains, 2019)(Lelievre, 2007). We have identified similar expression profiles in ruminant species, suggesting these peptides also maintain homeostasis between the gastrointestinal tract and nervous system in steers and wethers. Supplementation of these peptides could further identify the functional roles of VIP and PACAP in ruminants, which one of our future research goals.

There were differences in the detectability of receptors in steers and wethers. VPAC1, which can bind both ligands with equal affinity, is highly expressed in the GI track, brain, fat, liver and spleen of mice and humans (Yue, 2014) (Fagerberg et al., 2014). Consistent with this

74

profile, we observed high expression of VPAC1 in gastrointestinal and brain tissues of steers and wether. Interestingly, there were some differences in the detection of this receptor between ruminants. First, there was no detectable expression of VPAC1 in the spleen or fat pads of steers, suggesting a divergence from mice, humans, and wethers. Second, skeletal muscle tissue showed VPAC1 expression in both ruminants, whereas this tissue does not show the same expression profile in mice or humans (Yue, 2014) (Duff et al., 2014). Additionally, we identified high VPAC2 expression in the skeletal and cardiac muscles of the steers, whereas there was no VPAC2 expression in any wethers tissues; however, we suspected this might happen as a previous report showed very low RPKM (Reads Per Kilobase Million) of VPAC2 amongst sheep tissues (Jiang, 2014). As more tissues showed detection of VPAC1 than VPAC2, we could postulate that ruminants utilize VPAC1 for similar physiological functions across many tissues. It is also interesting that the steers showed VPAC2 and PAC1 expression in the spleen, but wethers showed VPAC1 expression in the spleen, prompting questions regarding the immunological utilization of these receptors in both species. There is an agreed high expression of PAC1 mRNA in the brain and colon of these ruminants and mammals. Additionally, PAC1 was detected in steer, but not wether, omasum, rumen, and fat tissues. Future protein expression and functionality must expand upon these results and is an exciting major goal for our research effort.

This study has some limitations, for instance, the pooling of all four samples into a specific tissue pool. Pooling removed the biological replication of this experiment; however, we decided this was an efficient strategy when the detectability of each gene is unknown. Our results have provided biologically significant data reporting the differences in mRNA expression

amongst tissues in steers and wethers, which we have compared to reported distributions of these genes in human and mouse tissues.

We conclude that the neuropeptides VIP and PACAP show similar tissue mRNA expression between ruminants and mammals, whereas their endogenous receptors show a divergence in tissue expression and amino acid identity between ruminant species. The variation of receptor tissue distribution between wethers and steers may facilitate different functions for each ruminant. The presence of VPAC1 on the spleen of wethers suggests that these animals may immunologically respond better to VIP than PACAP supplementation; however, the detection of PAC1 on rumen tissue implies that PACAP may have a specific effect on ruminal acidosis.

3.5. Conclusion

We conclude that the neuropeptides VIP and PACAP show similar tissue mRNA expression between ruminants and mammals, whereas their endogenous receptors show a divergence in tissue expression and amino acid identity between ruminant species. The variation of receptor tissue distribution between wethers and steers may facilitate different functions for each ruminant. The presence of VPAC1 on the spleen of wethers suggests that these animals may immunologically respond better to VIP than PACAP supplementation; however, the detection of PAC1 on rumen tissue implies that PACAP may have a specific effect on ruminal acidosis.

3.6. Materials and Methods

3.6.1. Tissue Harvest

Tissues were graciously provided by the Animal Science Department at NDSU. Tissues were collected from four steers 455-621 days old and 486-808 kgs total body weight. Wethers were 252-276 days old and 72-88 kgs total body weight. The brain, duodenum, jejunum, ileum,

cecum, colon, rumen, reticulum, omasum, abomasum, muscle, omental fat, liver, spleen, and kidney were harvested from each animal and frozen at -80°C until assayed.

3.6.2. RNA Extraction & cDNA Synthesis

The minimum information for publication of quantitative real-time PCR experiments (MIQE) was adhered to in the design of this study (Bustin et al., 2009). RNA was extracted using the Qiagen Universal mini-RNA extraction Kit (Catalogue #73404). The NanoDrop™ one-C was used for RNA quantification and purity assessment using 260/280, where all sample ratios fell between 1.9-2.3. RNA integrity was measured using a Qubit 4 fluorometer and samples with an IQ>6.4 were considered acceptable (ThermoFischer Scienfic, 2018). All total RNA samples were treated with DNase I & 10x Reaction Buffer with $MgCl_2$ (Thermo Fischer Scientific: EN0521; B42) by incubating with DNase I for 30-minutes at 37°C, followed by a 10 min 70°C deactivation step with EDTA (final concentration 4.5 mM). A range of 0.75-1 µg of template total RNA was used for each sample. cDNA synthesis was conducted using the Solis BioDyne FIREScript RT cDNA synthesis kit (#06-15-00050). Briefly, cDNA reactions had a volume of 20 µl and final concentrations of FIREScript RT (10 U/µl), RiboGrip™ RNase Inhibitor (1 U/µl), dNTP MIX (500 µM of each), Oligo dT (5 µM), Random primers (5 µM) and 1x RT Reaction Buffer with DTT (50 mM Tris-HCl pH 8.3, 50 mM KCl, 3 mM MgCl2, 10 mM DTT). Reverse transcription temperature and time was carried out according to the manufacturer's protocol (**DS-08-36 v3**), which was 25°C for 5-10 min, 37-60°C for 15-30 min, 85°C for 5 min. Biological replicates of tissue samples were pooled as described in **Figure 3.3**. Briefly, an n=3-4 of each tissue was pooled into a single cDNA sample prior to diluting 1:10 followed by PCR analysis.
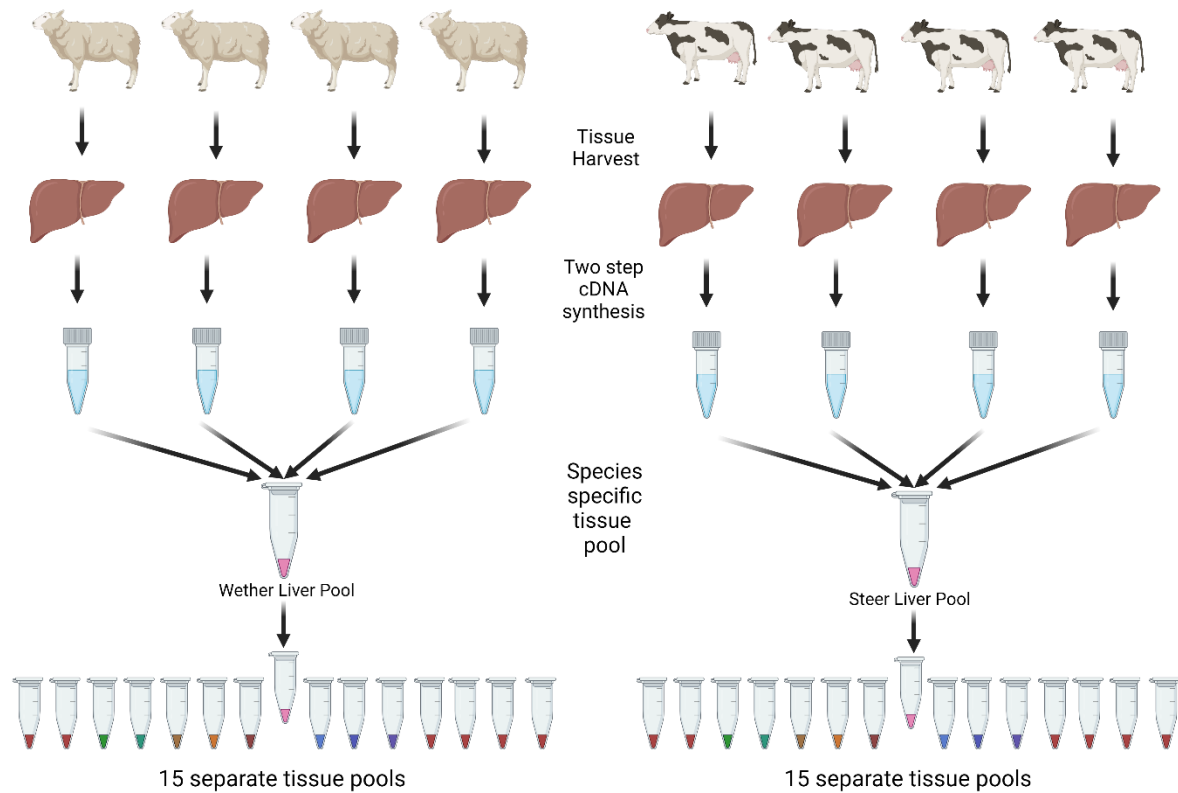
Figure 3.3. Pooling strategy used for species specific tissues prior to qPCR screening of VIP, PACAP, VPAC1,VPAC2, PAC1 & reference genes.

3.6.3. RT-qPCR

Reverse transcriptase quantitative PCR was conducted using the BioRad CFX96 thermocylcer. Plates (96-wells) were prepared according to the manufacturer's protocol. Each reaction contained a of final concentrations of 1X HOT FIREPol Evagreen qPCR Supermix (08-36-0000S), ddH2O, F&R primers (200 nmols of each) and 5 µL of diluted cDNA samples. PCR conditions began with a 12-minute hot start activation at 95°C followed by 40 cycles of 15 s denaturation at 95°C and 30 s annealing at 60°C x 40 cycles. A melt curve with 5 second intervals from 65-95 °C followed all PCR experiments. Primers (final concentration 200nM) were optimized using the same reaction conditions with efficiencies between 91-108% (**Figure 3.4**). Primer specifics can be found in **Figure 3.5**. The value of Cq was determined using the regression determination method of BioRad Manager 3.1 software. Cq values less than 36 were

78

used for relative quantification using the $2^{-\Delta\Delta Cq}$ Livak Method (Livak & Schittgen, 2001). PCR

cDNA samples were performed in duplicate. The percent coefficient of variation of intraassay

controls were below 1.278% (**Figure 3.7**). No reverse transcriptase (NRT) and no template

controls (NTC) were assessed for each sample to ensure the elimination of genomic DNA,

whereby linearized NRT product contributed <7.72% and NTC<5.63% of total fluorescence t o
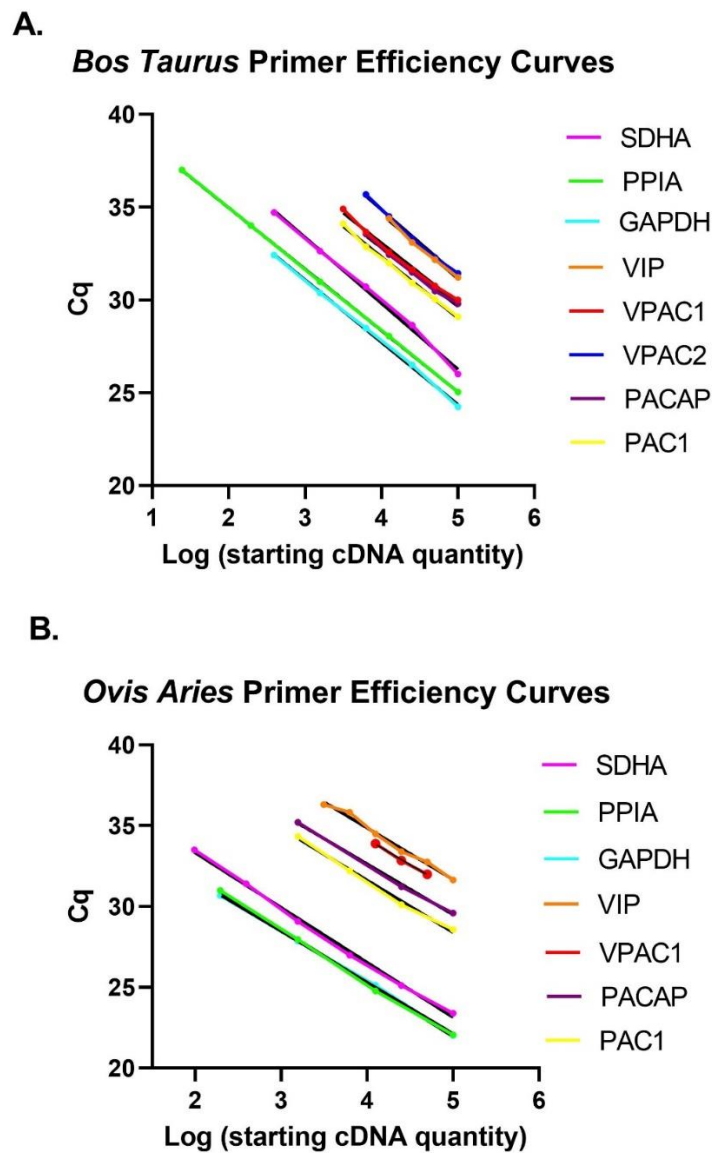
the RT+ sample (**Equations 2.1-2.2**).

Figure 3.4. *Bos Taurus/Ovis Aries* Primer Efficiency Curves.
Primer curves made using **A.** *Bos Taurus* and **B**. *Ovis Aries*. Efficiencies were between 91-108%.

Gene	Species	Primer Pair Sequence (5'->3')	Target Sequence Accession #	Product length (bps)	Efficiency	Slope	R2	Product MT °C	Exon-Exon Boundary (nt)
VIP	B	F: CCACTCAGATGCTGTCTTCACT R: TTCACTGCTTCGCTTTCCATTTAG	NM_173970.3	103	94.1%	-3.47	0.99	80.0	5-6 (642/643)
	O	F: CACTGACAACTACACACGCC R: GACTCTCCTTCGCTGCTTCTC	NM_001126368.1	93	105.6%	-3.1	0.99	79.0	4-5 (467/468)
PACAP	B	F: TGTACGACGAGGACGGAAAC R: GTGGGCGACATCTCTTTCCT	NM_001046555.1	131	107.4%	-3.12	0.99	90.5	2-3 (242/243)
	O		NM_001009776.1	131	108.6%	-3.13	0.99	90.5	N/A
VPAC1	B	F: ATCCTTGCCTCCATCTTGGTG R: GCTGTCACTCTTCCCGACAT	NM_001081607.1	99	103.1%	-3.25	0.99	81.5	9-10 (1029/1030)
	O		XM_042235879.1	99	107.5%	-3.15	0.96	81.5	N/A
VPAC2	B	F: CATCCGCATCTCCTCCAAGTA R: TCTGCACCTCGCTGTTGA	NM_001206781.1	107	90.9%	-3.56	0.99	84.5	12-13 (1287/1288)
PAC1	B	F: ATCATCATTGGCTGGGGGAC R: ATGATGCCGATGAAGAGCACA	NM_175715.2	176	101.4%	-3.29	0.99	85.5	10-11 (1371/1372)
	O		XM_027968637.2	176	104.3%	-3.22	0.99	85.5	N/A
GAPDH	B	F: TCGGAGTGAACGGATTCGGC R: TGATGACGAGCTTCCCGTTC	NM_001034034.2	192	98.5%	-3.36	0.99	80.5	2-3 (94/95)
	O		NM_001190390.1	192	106.4%	-3.18	0.99	80.5	2-3 (62/63)
PPIA	B	F: GCCAAGACTGAGTGGTTGGAT R: TTGCTGGTCTTGCCATTCCT	NM_178320.2	113	100.6%	-3.31	1.00	84.5	4-5 (373/374)
	O		NM_001308578.1	113	100.3%	-3.31	0.99	84.5	4-5 (363/364)
SDHA	B	F: TCCTGCAGACCCGGAGATAA R: TCTGCATGTTGAGTCGCAGT	NM_174178.2	130	91.2%	-3.55	0.99	81.0	10-11 (1446/1447)
B2M	O	F: CTGCTGCAAGGATGGCTGTCT R: GGACCTCTGGAATACGCTGGAT	NM_001009284.2	93	96.9%	-3.39	0.99	87.5	1-2 (79/80)

Figure 3.5. *Bos Taurus/Ovis* Aries Primer Specifics.
All primers were designed using NCBI Primer Design (Ye, 2012). Each row denotes a specific gene, optimized species, F&R primer sequences (5'>3'), targeted sequence accession #, product length in base pairs (BP), percent efficiency, slope, R^2, MT in RT$^+$ samples, and exon-exon boundary information. O = *Ovis*, B = *Bos Taurus*.
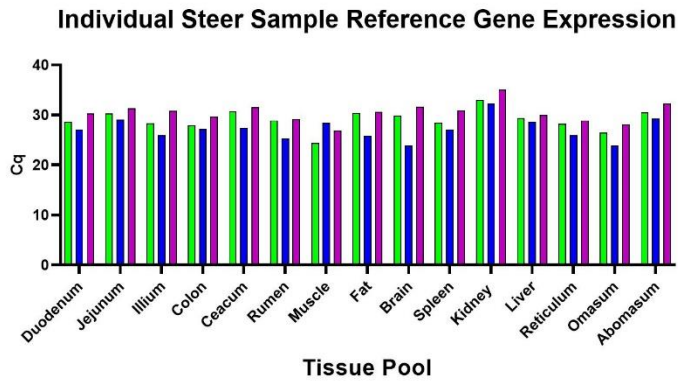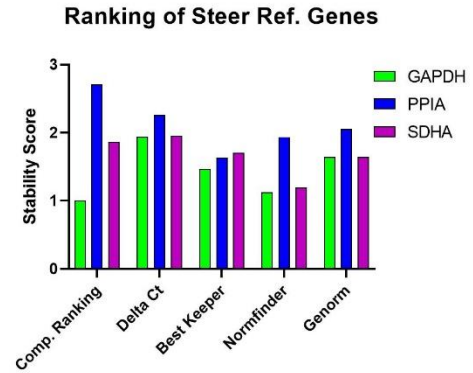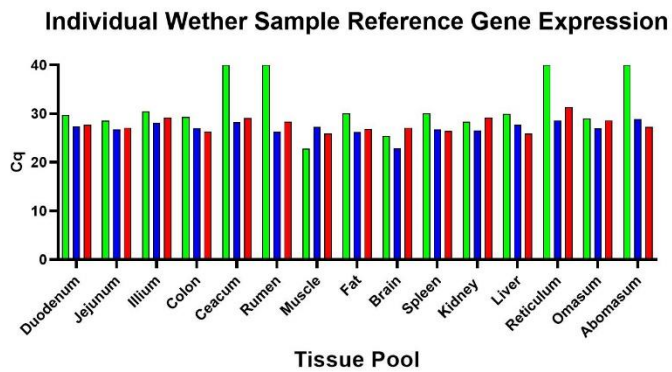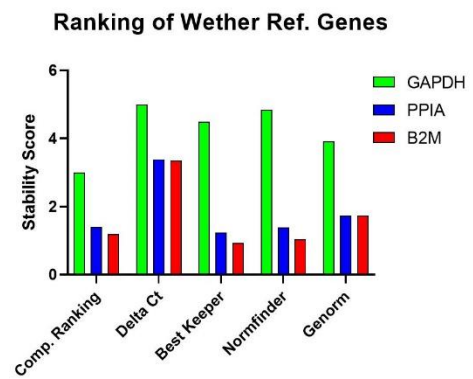
Figure 3.6. Reference Gene Stability Assessment Across Steer and Whether Samples. Average of technical replicates and stability score ranking of reference genes GAPDH, PPIA, B2M and SDHA in **A-B.** Steers and **C-D.** Wethers.
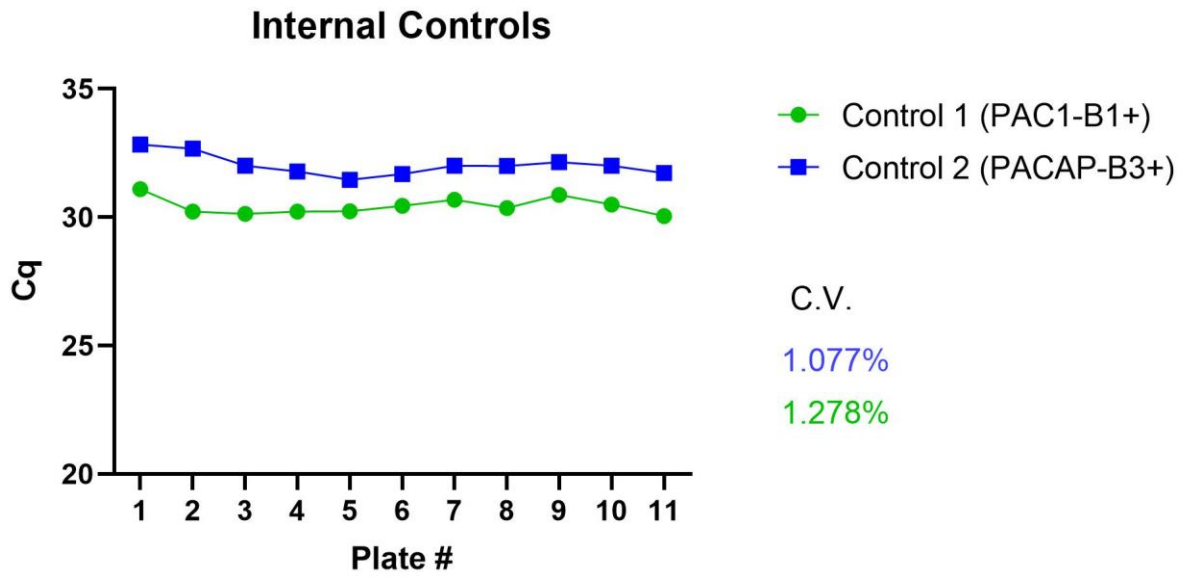
Figure 3.7. Coefficient of Variation Between Plates on Separate qPCR Runs. Inter-assay plate control trends with associated coefficient of variation (C.V.). Data points represent mean of technical replicates for each plate.

3.6.4. Data Analysis

Relative quantification was made using the Livak method (Livak & Schmittgen, 2001) and Bio-Rad qPCR data analysis (BioRadLifeScience, 2019). Fold change was calculated for each GOI by setting the measurement of VIP in the brain of steers or wethers arbitrary to 1. Relative mRNA expression levels were calculated for VIP, PACAP, VPAC1, VPAC2 and PACAP genes. The highest expressing tissue had the largest fold-change and was ranked number 1- and lower fold-changes were ranked with higher numbers.

3.7. References

Abad, C., & Tan, Y.-V. (2018). Immunomodulatory roles of pacap and VIP: Lessons from knockout mice. *Journal of Molecular Neuroscience*, *66*(1), 102–113. https://doi.org/10.1007/s12031-018-1150-y

Arimura, A. (1992). Pituitary adenylate cyclase activating polypeptide (PACAP): Discovery and current status of research. *Regulatory Peptides*, *37*(3), 285–303. https://doi.org/10.1016/0167-0115(92)90621-z

Bains, M., Laney, C., Wolfe, A. E., Orr, M., Waschek, J. A., Ericsson, A. C., & Dorsam, G. P. (2019). Vasoactive intestinal peptide deficiency is associated with altered gut microbiota communities in male and female C57BL/6 mice. *Frontiers in Microbiology*, *10*. https://doi.org/10.3389/fmicb.2019.02689

BioRadLifeSciences. (2019). *Https://www.youtube.com/watch?v=TWmu7lXrvIE. YouTube*. Retrieved June 22, 2022, from https://www.youtube.com/watch?v=TWmu7lXrvIE.

Delgado, M., & Ganea, D. (2001). Inhibition of endotoxin-induced macrophage chemokine production by vasoactive intestinal peptide and pituitary adenylate cyclase-activating polypeptide in vitro and in vivo. *The Journal of Immunology*, *167*(2), 966–975. https://doi.org/10.4049/jimmunol.167.2.966

Delgado, M., Gonzalez-Rey, E., & Ganea, D. (2004). VIP/pacap preferentially attract th2 effectors through differential regulation of chemokine production by dendritic cells. *The FASEB Journal*, *18*(12), 1453–1455. https://doi.org/10.1096/fj.04-1548fje

Duff, M. O., Olson, S., Wei, X., Osman, A., Plocik, A., Bolisetty, M., Celniker, S., & Graveley, B. (2014). Genome-wide identification of zero nucleotide recursive splicing in*drosophila*. https://doi.org/10.1101/006163

Fagerberg, L., Hallström, B. M., Oksvold, P., Kampf, C., Djureinovic, D., Odeberg, J., Habuka, M., Tahmasebpoor, S., Danielsson, A., Edlund, K., Asplund, A., Sjöstedt, E., Lundberg, E., Szigyarto, C. A.-K., Skogs, M., Takanen, J. O., Berling, H., Tegel, H., Mulder, J., … Uhlén, M. (2014). Analysis of the human tissue-specific expression by genome-wide integration of transcriptomics and antibody-based proteomics. *Molecular & Cellular Proteomics*, *13*(2), 397–406. https://doi.org/10.1074/mcp.m113.035600

Harmar, A. J., Sheward, W. J., Morrison, C. F., Waser, B., Gugger, M., & Reubi, J. C. (2004). Distribution of the VPAC2 receptor in peripheral tissues of the mouse. *Endocrinology*, *145*(3), 1203–1210. https://doi.org/10.1210/en.2003-1058

Heimesaat, M. M., Reifenberger, G., Vicena, V., Illes, A., Horvath, G., Tamas, A., Fulop, B. D., Bereswill, S., & Reglodi, D. (2017). Intestinal microbiota changes in mice lacking pituitary adenylate cyclase activating polypeptide (PACAP) — bifidobacteria make the difference. *European Journal of Microbiology and Immunology*, *7*(3), 187–199. https://doi.org/10.1556/1886.2017.00021

Jayawardena, D., Anbazhagan, A. N., Guzman, G., Dudeja, P. K., & Onyuksel, H. (2017). Vasoactive intestinal peptide nanomedicine for the management of inflammatory bowel disease. *Molecular Pharmaceutics*, *14*(11), 3698–3708. https://doi.org/10.1021/acs.molpharmaceut.7b00452

Jiang, Y., Xie, M., Chen, W., Talbot, R., Maddox, J. F., Faraut, T., ... & Dalrymple, B. P. (2014). The sheep genome illuminates biology of the rumen and lipid metabolism. Science, 344(6188), 1168-1173.

Lelievre, V., Favrais, G., Abad, C., Adle-Biassette, H., Lu, Y., Germano, P. M., Cheung-Lau, G., Pisegna, J. R., Gressens, P., Lawson, G., & Waschek, J. A. (2007). Gastrointestinal dysfunction in mice with a targeted mutation in the gene encoding vasoactive intestinal polypeptide: A model for the study of intestinal ileus and Hirschsprung's disease. *Peptides*, *28*(9), 1688–1699. https://doi.org/10.1016/j.peptides.2007.05.006

Matthews, C., Crispie, F., Lewis, E., Reid, M., O'Toole, P. W., & Cotter, P. D. (2018). The rumen microbiome: A crucial consideration when optimising milk and meat production and Nitrogen Utilisation Efficiency. *Gut Microbes*, *10*(2), 115–132. https://doi.org/10.1080/19490976.2018.1505176

Miyata, A., Jiang, L., Dahl, R. D., Kitada, C., Kubo, K., Fujino, M., ... & Arimura, A. (1990). Isolation of a neuropeptide corresponding to the N-terminal 27 residues of the pituitary adenylate cyclase activating polypeptide with 38 residues (PACAP38). Biochemical and biophysical research communications, 170(2), 643-648. Moss, A. R., Jouany, J.-P., & Newbold, J. (2000). Methane production by ruminants:Its contribution to Global Warming. Annales De Zootechnie, 49(3), 231–253. https://doi.org/10.1051/animres:2000119

Ng, S. Y., Chow, B. K., Kasamatsu, J., Kasahara, M., & Lee, L. T. (2012). Agnathan VIP, pacap and their receptors: Ancestral origins of today's highly diversified forms. *PLoS ONE*, *7*(9). https://doi.org/10.1371/journal.pone.0044691

Ørskov, E. R. (1986). Starch digestion and utilization in ruminants. *Journal of Animal Science*, *63*(5), 1624–1633. https://doi.org/10.2527/jas1986.6351624x

Ramos-Álvarez, I., Mantey, S. A., Nakamura, T., Nuche-Berenguer, B., Moreno, P., Moody, T. W., Maderdrut, J. L., Coy, D. H., & Jensen, R. T. (2015). A structure–function study of pacap using conformationally restricted analogs: Identification of PAC1 receptor-selective PACAP agonists. *Peptides*, *66*, 26–42. https://doi.org/10.1016/j.peptides.2015.01.009

Said, S. I., & Mutt, V. (1970). Potent peripheral and splanchnic vasodilator peptide from normal gut. Nature, 225(5235), 863-864.Swanson, K. C., Richards, C. J., & Harmon, D. L. (2002). Influence of abomasal infusion of glucose or partially hydrolyzed starch on pancreatic exocrine secretion in beef steers. Journal of Animal Science, 80(4), 1112–1116. https://doi.org/10.2527/2002.8041112x

Swanson, K. C., Richards, C. J., & Harmon, D. L. (2002). Influence of abomasal infusion of glucose or partially hydrolyzed starch on pancreatic exocrine secretion in beef steers. *Journal of Animal Science*, *80*(4), 1112–1116. https://doi.org/10.2527/2002.8041112x

Swanson, K. C. (2019). Small intestinal anatomy, physiology, and digestion in ruminants. *Reference Module in Food Science*. https://doi.org/10.1016/b978-0-08-100596-5.22638-3

Tanaka, K., Shibuya, I., & Kanno, T. (1995). Potentiation of cholecystokinin-induced amylase release by peptide VIP in Guinea pig pancreatic acini. *The Japanese Journal of Physiology*, *45*(2), 241–256. https://doi.org/10.2170/jjphysiol.45.241

ThermoFischer Scientific. (2018). *Qubit RNA IQ Assay: a fast and easy fluorometric RNA quality assessment*. Document connect. Retrieved June 22, 2022, from https://www.thermofisher.com/document-connect/document-connect.html?url=https%3A%2F%2Fassets.thermofisher.com%2FTFS-Assets%2FBID%2Fposters%2Fqubit-rna-iq-assay-fluorometric-rna-quality-assessment-poster.pdf

Van, C., Condro, M. C., Lov, K., Zhu, R., Ricaflanca, P. T., Ko, H. H., Diep, A. L., Hoang, A. Q., Pisegna, J., Rohrer, H., & Waschek, J. A. (2018). Pacap/PAC1 regulation of inflammation via catecholaminergic neurons in a model of multiple sclerosis. Journal of Molecular Neuroscience, 68(3), 439–451. https://doi.org/10.1007/s12031-018-1137-8

Wei, P., Keller, C., & Li, L. (2020). Neuropeptides in gut-brain axis and their influence on host immunity and stress. *Computational and Structural Biotechnology Journal*, *18*, 843–851. https://doi.org/10.1016/j.csbj.2020.02.018

Wu, X., Conlin, V. S., Morampudi, V., Ryz, N. R., Nasser, Y., Bhinder, G., Bergstrom, K. S., Yu, H. B., Waterhouse, C. C., Buchan, A. M., Popescu, O. E., Gibson, W. T., Waschek, J. A., Vallance, B. A., & Jacobson, K. (2015). Vasoactive intestinal polypeptide promotes intestinal barrier homeostasis and protection against colitis in mice. *PLOS ONE*, *10*(5). https://doi.org/10.1371/journal.pone.0125225

Wu, Z., Weersink, A., & Maynard, A. (2021). Fuel-feed-livestock price linkages under structural changes. *Applied Economics*, *54*(2), 206–223. https://doi.org/10.1080/00036846.2021.1965082

Ye, J., Coulouris, G., Zaretskaya, I., Cutcutache, I., Rozen, S., & Madden, T. L. (2012). Primer-Blast: A tool to design target-specific primers for polymerase chain reaction. *BMC Bioinformatics*, *13*(1). https://doi.org/10.1186/1471-2105-13-134

Yue, F., Cheng, Y., Breschi, A., Vierstra, J., Wu, W., Ryba, T., ... & Ren, B. (2014). A comparative encyclopedia of DNA elements in the mouse genome. Nature, 515(7527), 355-364.